PB87-101770

Boiler Simulator Studies on Sorbent Utilization for SO2 Control

Energy and Environmental Research Corp.
Irvine, CA

Prepared for

Environmental Protection Agency
Research Triangle Park, NC

Sep 86

U.S. Department of Commerce
National Technical Information Service
NTIS

PB87-101770

EPA/600/7-86/028
September 1986

BOILER SIMULATOR STUDIES ON SORBENT UTILIZATION FOR SO_2 CONTROL

By

B. J. Overmoe, L. Ho, S. L. Chen,
W. R. Seeker, D. W. Pershing, and M. P. Heap

Energy and Environmental Research Corporation
18 Mason
Irvine, California 92718

EPA Contract 68-02-3633

EPA Project Officer: Dennis C. Drehmel

Air and Energy Engineering Research Laboratory
U.S. Environmental Protection Agency
Research Triangle Park, NC 27711

AIR AND ENERGY ENGINEERING RESEARCH LABORATORY
OFFICE OF RESEARCH AND DEVELOPMENT
U.S. ENVIRONMENTAL PROTECTION AGENCY
RESEARCH TRIANGLE PARK, NC 27711

REPRODUCED BY
U.S. DEPARTMENT OF COMMERCE
NATIONAL TECHNICAL
INFORMATION SERVICE
SPRINGFIELD, VA. 22161

TECHNICAL REPORT DATA

(Please read Instructions on the reverse before completing)

1. REPORT NO. EPA/600/7-86/028	2.	3. RECIPIENT'S ACCESSION NO. PB87 101770/AS

4. TITLE AND SUBTITLE Boiler Simulator Studies on Sorbent Utilization for SO_2 Control	5. REPORT DATE September 1986 6. PERFORMING ORGANIZATION CODE
7. AUTHOR(S) B. J. Overmoe, L. Ho, S. L. Chen, W. R. Seeker, D. W. Pershing, and M. P. Heap	8. PERFORMING ORGANIZATION REPORT NO.
9. PERFORMING ORGANIZATION NAME AND ADDRESS Energy and Environmental Research Corporation 18 Mason Irvine, California 92718	10. PROGRAM ELEMENT NO. 11. CONTRACT/GRANT NO. 68-02-3633
12. SPONSORING AGENCY NAME AND ADDRESS EPA, Office of Research and Development Air and Energy Engineering Research Laboratory Research Triangle Park, NC 27711	13. TYPE OF REPORT AND PERIOD COVERED Final; 3/84 - 9/84 14. SPONSORING AGENCY CODE EPA/600/13

15. SUPPLEMENTARY NOTES AEERL project officer is Dennis C. Drehmel, Mail Drop 4, 919/541-7505.

16. ABSTRACT The report gives results of a program to provide process design information for sorbent utilization as applied to EPA's LIMB process. Specifically, the program was designed to investigate the role of boiler thermal history, sorbent injection location, Ca/S molar ratio, and SO2 partial pressure on capture effectiveness with limestones, dolomites, and slaked limes with and without metallic promoters. The experimental studies were supported by theoretical calculations using grain and pore models that considered both the heterogeneous chemical reaction and the relevant diffusional processes. The experimental results and the sulfation model calculations indicate that the sorbent injection locations and the residence time within the sulfation temperature window can significantly influence overall sulfur capture for any sorbent. Unless the sorbent is promoted with a metal additive, downstream injection at about 1500 K results in optimum sorbent utilization. Increasing the gas-phase SO2 concentration improves sorbent utilization, but the dependence is non-linear due to the combined effects of intrinsic chemistry and diffusion. In general, dolomitic sorbents perform better than calcitic sorbents, and hydroxides are superior to carbonates. The true influence of pressure slaking is unclear; however, the best sorbents tested were the pressure-slaked dolomites.

17. KEY WORDS AND DOCUMENT ANALYSIS

a. DESCRIPTORS		b. IDENTIFIERS/OPEN ENDED TERMS	c. COSATI Field/Group	
Pollution	Boilers	Pollution Control	13B	13A
Sulfur Dioxide		Stationary Sources	07B	
Sorbents		LIMB	11G	
Limestone		Limestone Injection Multistage Burners	08G	
Dolomite (Mineral)				
Calcium Hydroxides				

18. DISTRIBUTION STATEMENT Release to Public	19. SECURITY CLASS *(This Report)* Unclassified	21. NO. OF PAGES 172
	20. SECURITY CLASS *(This page)* Unclassified	22. PRICE

NOTICE

This document has been reviewed in accordance with U.S. Environmental Protection Agency policy and approved for publication. Mention of trade names or commercial products does not constitute endorsement or recommendation for use.

ABSTRACT

The objective of this program was to provide process design information for sorbent utilization as applied to the LIMB process. Specifically, this program was designed to yield information as to the optimum methods of sorbent injection and to study mineral matter interactions. All of the experiments were performed on the 1.0 MBtu/hr Boiler Simulator Furnace (BSF).

The results of the optimization studies indicated that the best overall captures were achieved with the pressure slaked dolomitic sorbents followed by dolomite, the hydroxides, and the carbonates. Pressure slaking enhanced capture and the presence of magnesium also enhanced capture though Mg did not react to form $MgSO_4$. Downstream injection gave consistently higher captures than burner injection, and as quench rate increased, capture decreased for downstream injection.

The results of the mineral matter interaction studies indicated that the sorbent ranking was about the same with coal as with gas and similar captures were achieved with the two fuels. The effects of quench rate and injection location were also the same with coal as with gas. The additive screening studies suggested that chromium was the best promoter, followed by sodium and molybdenum. Na and Cr were capable of enhancing capture independent of sorbent type, however, sodium became nearly ineffective in coal flames. Surface area measurements indicated that Cr promoted particle sintering even though high captures were attained.

TABLE OF CONTENTS

Section Page

Abstract.. iii
List of Figures... viii
List of Tables.. xiv

1.0 INTRODUCTION.. 1-1

1.1 Background.. 1-1
1.2 Purpose and Scope..................................... 1-6
1.2.1 Task 1 - Facility Characterization.................. 1-7
1.2.2 Task 2 - Definition of Optimum Injection Conditions.............................. 1-7
1.2.3 Task 3 - Characterization of Ash Interactions............................. 1-7
1.2.4 Task 4 - Data Analysis and Reporting................ 1-8

2.0 EXPERIMENTAL FACILITY................................. 2-1

2.1 Furnace... 2-1
2.2 Distributed Mixing Burner............................. 2-1
2.3 Support Facilities.................................... 2-6
2.3.1 Ash Handling and ID Fan............................. 2-6
2.3.2 Water Recirculation System.......................... 2-6
2.3.3 Coal/Sorbent Delivery Systems....................... 2-6
2.3.4 Air Delivery System................................. 2-7
2.4 Measurements.. 2-7
2.4.1 Gas Samples... 2-9
2.4.2 Solid Samples....................................... 2-13
2.4.3 Temperature Measurements............................ 2-13
2.5 Data Acquisition...................................... 2-18

Preceding page blank

TABLE OF CONTENTS (continued)

Section Page

3.0 SORBENTS AND FUELS.................................. 3-1

3.1 Sorbent Properties.................................. 3-1
3.2 Fuel Properties.................................. 3-1

4.0 FURNACE CHARACTERIZATION.................................. 4-1

4.1 Thermal History Data.................................. 4-1
4.2 Initial Capture Data.................................. 4-1
4.3 Model Predictions.................................. 4-5
4.4 Preliminary Mineral Matter Interactions............ 4-5

5.0 OPTIMIZATION OF SULFUR CAPTURE.......................... 5-1

5.1 Sorbent Screening.................................. 5-1
  5.1.1 Sorbent Comparison.......................... 5-4
  5.1.2 Influence of Slaking.......................... 5-7
  5.1.3 The Role of Magnesium.......................... 5-11
  5.1.4 Low Temperature Capture.......................... 5-15
5.2 Thermal Parameters.................................. 5-19
  5.2.1 Influence of Peak Temperature/Quench Rate.... 5-19
  5.2.2 Model Predictions.......................... 5-24
  5.2.3 Influence of Injection Location.,............ 5-24
5.3 Summary.................................. 5-29

6.0 EVALUATION OF MINERAL INTERACTIONS...................... 6-1

6.1 Capture with Coal.................................. 6-1
  6.1.1 Sorbent Comparison.......................... 6-1
  6.1.2 Influence of Injection Location.............. 6-4
  6.1.3 Influence of Thermal History................ 6-4

TABLE OF CONTENTS (continued)

Section Page

6.0 (continued)

6.2 Capture Comparison Between Coal and Gas............. 6-8
6.2.1 Burner Injection.............................. 6-8
6.2.2 Downstream Injection.......................... 6-8
6.3 Mineral Interactions................................ 6-15
6.3.1 Additive Screening............................ 6-15
6.3.2 Na and Cr Enhancement with Gas................ 6-21
6.3.3 Na and Cr Enhancement with Coal............... 6-25
6.4 Mechanistic Parameters.............................. 6-34
6.5 Summary... 6-38

7.0 SULFUR CAPTURE MODEL.................................. 7-1

8.0 CONCLUSIONS... 8-1

8.1 Conclusions-Capture Optimization Studies............ 8-1
8.2 Conclusions-Mineral Matter Interaction Studies...... 8-2

9.0 REFERENCES.. 9-1

APPENDIX A -- Quality Assurance.............................. A-1

LIST OF FIGURES

Figure Page

1-1 Range of SO_2 Removal Reported for Plant-, Pilot-, and Bench-Scale Studies with Sorbent Addition............ 1-5

2-1 Boiler Simulator Furnace (BSF).......................... 2-3

2-2 BSF Tower Module.. 2-4

2-3 Distributed Mixing Burner (DMB)......................... 2-5

2-4 Phase Discrimination Profile............................ 2-10

2-5 Sample Conditioning for Gas Streams..................... 2-11

2-6 Analytical Systems...................................... 2-12

2-7 IFRF Solids Loading Probe............................... 2-14

2-8 Grab Sample... 2-15

2-9 Surface Area Sample Train............................... 2-16

2-10 Suction Pyrometer Schematic............................ 2-17

4-1 Comparison of Furnaces With Natural Gas................. 4-2

4-2 Comparison of Furnaces with Coal........................ 4-3

4-3 Capture Comparison for Downstream Injection............. 4-4

4-4 Comparison of Model predictions and Measurements for New BSF... 4-6

LIST OF FIGURES (continued)

Figure Page

4-5 Comparison of Low and Normal Load Temperature Profiles.... 4-7

4-6 Influence of Thermal History on Capture and Model Predictions.. 4-8

4-7 Coal vs Gas Capture at Low Load.......................... 4-10

4-8 Coal vs Gas Capture at Normal Load....................... 4-11

4-9 Ash Deactivation in Old BSF.............................. 4-12

4-10 Overview of Mineral Matter Effects....................... 4-13

4-11 Combined Mineral Matter Effects.......................... 4-15

5-1 Thermal History Comparison............................... 5-2

5-2 Thermal History in the Sulfation Zone.................... 5-3

5-3 Sorbent Comparison at Reduced Load....................... 5-5

5-4 Sorbent Comparison at Reduced Load on a Mass Basis........ 5-6

5-5 Sorbent Comparison for American Boiler Profile........... 5-8

5-6 Influence of Slaking for Calcitic Sorbents at Reduced Load... 5-9

5-7 Influence of Slaking for Calcitic Materials with American Boiler Profile................................... 5-10

LIST OF FIGURES (continued)

Figure Page

5-8 Influence of Pressure Slaking for Dolomitic Materials..... 5-12

5-9 Influence of Magnesium Content.......................... 5-13

5-10 Sulfur Capture with Magnesium.......................... 5-14

5-11 Low Temperature Capture for Carbonates.................. 5-16

5-12 Low Temperature Capture for Hydroxides.................. 5-17

5-13 Low Temperature Sorbent Injection....................... 5-18

5-14 Thermal History Comparison.............................. 5-20

5-15 Influence of Quench Rate for Downstream Injection........ 5-21

5-16 Influence of Peak Temperature/Quench Rate for Burner Injection.................................. 5-22

5-17 Available Surface Area Data............................. 5-23

5-18 Model predictions for Variable Quench Rate.............. 5-25

5-19 Model Predictions for Burner Injection.................. 5-26

5-20 Influence of Injection Location at Reduced Load......... 5-27

5-21 Influence of Injection Location at American Boiler Profile.. 5-28

6-1 Sorbent Comparison with Coal at Reduced Load............ 6-2

LIST OF FIGURES (continued)

Figure		Page
6-2	Sorbent Comparison with Coal for American Boiler Profile..	6-3
6-3	Influence of Injection Location at Reduced Load.........	6-5
6-4	Influence of Injection Location for American Boiler Profile..	6-6
6-5	Influence of Thermal History on Capture in Coal Flames...	6-7
6-6	Thermal History Comparison Between Coal and Gas..........	6-9
6-7	Reduced Load Mineral Matter Effect Effect for Burner Injection..	6-10
6-8	AB Profile Mineral Matter Effect for Burner Injection....	6-11
6-9	Reduced Load Mineral Matter Effect for Downstream Injection..	6-12
6-10	AB Profile Mineral Matter Effect for Downstream Injection..	6-13
6-11	Influence of Fly Ash - Premixed with Sorbent.............	6-14
6-12	Transition Metals Additive Screening.....................	6-16
6-13	Alkali Metal Promoters...................................	6-18

LIST OF FIGURES (continued)

Figure Page

6-14 Additives with American Boiler Profile.................... 6-19

6-15 Influence of Additive Concentration....................... 6-20

6-16 Chromium Enhancement with Different Sorbent Types......... 6-22

6-17 Influence of Injection Location with Cr_2O_3................ 6-23

6-18 Influence of Injection Location with Na_2CO_3.............. 6-24

6-19 Impact of Thermal History on Enhancement with Cr_2O_3....... 6-26

6-20 Impact of Thermal History on Enhancement with Na_2CO_3...... 6-27

6-21 Enhancement with Cr and Na in Coal Flames................ 6-28

6-22 Impact of Fuel Type on Enhancement with Cr_2O_3............ 6-30

6-23 Impact of Fuel Type on Enhancement with Na_2CO_3........... 6-31

6-24 Impact of Injection Location on Enhancement in Coal Flames.. 6-32

6-25 Impact of Thermal History on Enhancement in Coal Flames.. 6-33

6-26 Influence of SO_2 Partial Pressure........................ 6-35

6-27 Influence of SO_2 partial Pressure with Cr_2O_3............. 6-36

6-28 Dependence on O_2 Concentration.......................... 6-37

LIST OF FIGURES (continued)

Figure Page

6-29 Zone Capture for Burner Injection........................ 6-39

6-30 Zone Capture for Downstream Injection................... 6-40

7-1 The Basic Features of the Grain Model................... 7-2

LIST OF TABLES

Table		Page
2-1	RADIANT TOWER DESIGN SPECIFICATIONS	2-2
2-2	MEASUREMENTS	2-8
3-1	PHYSICAL AND CHEMICAL PROPERTIES OF SORBENTS	3-2
3-2	FUEL ANALYSES	3-3
6-1	MEASURED SURFACE AREAS	6-41
7-1	NOMENCLATURE FOR SULFATION CALCULATIONS	7-4

1.0 INTRODUCTION

This report summarizes the experimental and analytical efforts performed under EPA Contract No. 68-02-3633. The report, entitled "Bench-Scale Studies on Sorbent Utilization for SO_2 Control", was in part a continuation of earlier Boiler Simulator Furnace (BSF) programs in that the existing data base was compared with data generated on the new tower BSF. The previous program focused on combined NO_x/SO_x control with calcium based sorbents injected through a distributed mixing burner (DMB). In this program, emphasis was placed on SO_x control and methods for improving sorbent utilization and reactivity. The research effort was also extended to the use of additive to promote sulfur capture with a variety of sorbents.

This chapter gives a brief description of the sorbent injection process and an overview of the EPA Limestone Injection in Multistaged Burners (LIMB) program. In addition, the purpose and scope of the contract effort is presented.

1.1 Background

Sulfur capture by calcium based sorbents has been the subject of much research over the last two decades (1-4). Furnace injection was tried and abandoned because of poor sulfur capture performance. The failure was attributed (1) to decreased sorbent activity due to dead burning at furnace temperatures, inadequate dispersion of the sorbent throughout the combustion products, and operational problems due to air heater plugging. Interest in the technique was reviewed when recent pilot scale studies at EER indicated that higher sulfur captures could be achieved under low NO_x combustion conditions. The need to develop a low cost, retrofittable SO_x control technology and reduced performance goals have caused additional interest in the limestone injection concept. LIMB, Limestone Injection in Multistaged Burners, was initially coined when it was thought that simultaneous NO_x/SO_x control could be developed using limestone injection through a distributing mixing burner. It now appears that the optimum sorbent injection location will be above the primary combustion zone and that other sorbents are considerably more attractive than limestone; however, the acronym remains.

The basic concept of the process is to inject pulverized sorbent into the combustion chamber of a boiler where a number of reactions can occur. Typical sorbents are limestone ($CaCO_3$), calcium hydroxide ($Ca(OH)_2$), and dolomite ($CaCO_3 \cdot MgCO_3$). When the sorbent is initially injected into the high temperature combustion zone, calcination occurs and CO_2 or H_2O is evolved according to the following reactions:

$$CaCO_3 \xrightarrow[500\text{-}900^oC]{} CaO(s) + CO_2(g) \quad (1.1)$$

$$MgCO_3 \xrightarrow[300\text{-}700^oC]{} MgO(s) + CO_2(g) \quad (1.2)$$

$$Ca(OH)_2 \xrightarrow[200\text{-}550^oC]{} CaO(s) + H_2O(g) \quad (1.3)$$

In the case of limestones, structural rearrangement takes place as the CO_2 is being evolved because the crystal structure of the carbonate (rhombohedral) differs from that of the oxide (cubic). Since the calcination process is homogeneous, sites for recrystalization of the oxide are well dispersed so that localized crystallites, or grains, are formed with a pore structure between them. Overall calcination rates have been well documented by Hyatt et al.(5), Borgwardt(6,7), and Coutant et al(2). Particle heat up appears to occur very rapidly (c.a. 50 ms) after the particle is mixed with the hot gas stream and at typical combustion temperatures the overall calcination process appears to be essentially complete in less than 200 ms. The calcination conditions, particularly temperature and CO_2 partial pressure, influence the ultimate porosity and grain size. Extended exposure to high temperature often causes the grains to coalesce (sinter) because the highly mobile oxide units quickly fill in the gaps where grain boundaries, or contact points occur. This results in larger grains, with lower surface area.

Once the sorbent particle is oxidized to CaO, it can react with the available sulfur species to form calcium sulfate. The overall reaction for sulfation is:

$$SO_2 + 1/2O_2 + CaO = CaSO_4$$

but the exact mechanism for this reaction is not known. It may involve an initial formation of calcium sulfite or result from a reaction of sulfate ions with CaO. The overall reaction system has been studied extensively by Borgwardt(6), Ishihara(8), and others(9,10).

The sorbent injection process has been studied in pilot- and plant-scale studies in Germany, Japan, Poland, and the United States. Figure 1-1 shows the range of SO_2 removal reported in some early studies (after Gartrell(11)). The type of sorbent was either hydrated lime or hydrated dolomitic lime and the range of conditions were indicative of several boilers, injection locations, etc. The parameters that were found to affect the absorption efficiency of injected limestone in these studies were:

- those properties of the limestone that affected the degree of porosity after calcination;
- particle size and surface area;
- temperature at the point of injection;
- retention time;
- limestone distribution;
- mass transfer between SO_2 in the flue gas and sorbent particles;

- SO_2 concentration;

- furnace operating conditions;

- limestone feed rate.

Figure 1-1 highlights data from three different operating boilers. The Shawnee steam plant was the site of the EPA demonstration conducted by TVA. The Wisconsin Electric Company plant is an arch-fired unit and the Detroit Edison plant is a corner-fired unit. Point 4 represents captures obtained in a brown coal boiler operated by RWE in West Germany. The sorbent was mixed with the fuel in the Wisconsin, Detroit Edison, and RWE tests. SO_2 removal was significantly better when the sorbents were injected at higher furnace elevations where the gas temperatures were lower. Long-term testing could not be carried out because of reheater plugging, which caused excessive pressure drop in the reheater.

The data for the arch-fired boiler shows better capture than that obtained in the TVA unit, which is a front wall fired boiler. In an arch-fired boiler, the heat release zone is spread out by reducing the rate of fuel-air mixing and the primary stream has a lower fraction of air than is normally used in wall-fired units. In these tests, the additive was injected with the coal. Improved SO_2 removal in this particular boiler design could be attributed to reduced combustion intensities, or to the longer residence time experienced by the sorbent under fuel rich conditions. Corner-fired units, such as that tested at Detroit Edison, have some of these characteristics, and the data reported in these tests are better than those obtained in the TVA study.

Hein and co-workers(12) of RWE in West Germany have conducted an extensive research program on the use of calcium-based sorbents to reduce sulfur oxide emissions from power plants burning Rhinish brown coals. Tests carried out in a 175-ton-of-steam/hr boiler indicated that the natural sulfur retention ability could be improved by blending the sorbent with the fuel prior to the grinding system.

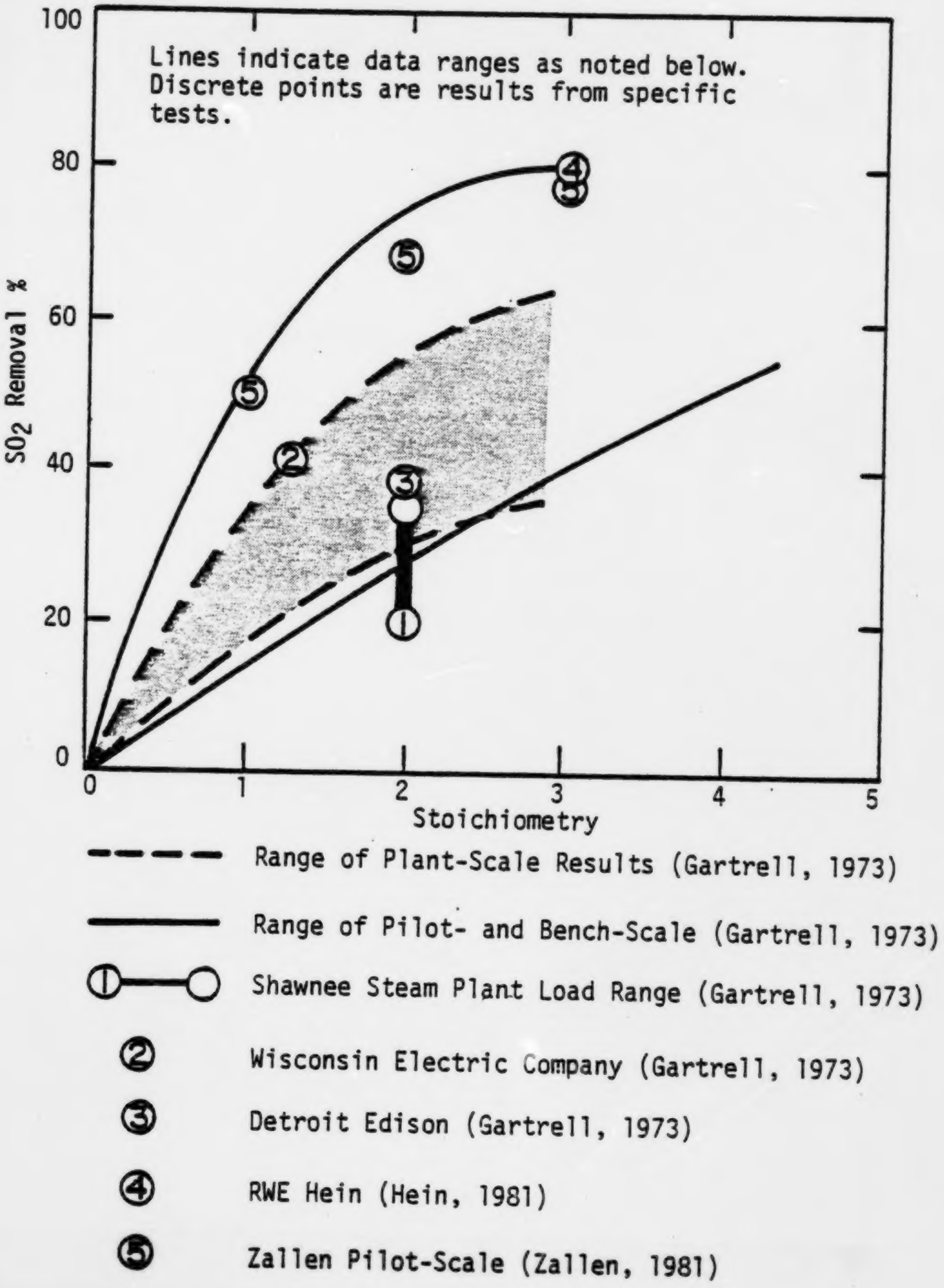

Figure 1-1. Range of SO_2 removal reported for plant-, pilot-, and bench-scale studies with sorbent addition.

Zallen, et al(13) conducted a series of pilot-scale tests with an EPA distributed mixing burner. These tests were carried out in a test furnace which was partially refractory and at loads ranging from 50 to 75 percent of full capacity. The sorbent was batch-mixed with the coal prior to the pulverizer and injected into the furnace with the coal. In this instance, the sorbent experienced the maximum temperature within the furnace, since it passed through the flame zone. However, the sulfur captures reported by Zallen were extremely good which introduced the conjecture that SO_2 removal efficiency was improved under fuel rich conditions typical of those encountered in low NO_x burners.

Much of the work for this program was based on work done by Case, et al(14,15) for previous bench-scale BSF programs. They investigated a wide range of parameters in terms of their impact on sulfur capture. Among these were the influence of fuel type, sorbent type, injection location, and operational parameters such as peak flame temperature, furnace load, and burner zone stoichiometry. The results from these programs created a valuable data base and gave direction for initial testing on the new BSF used for this program.

1.2 Purpose and Scope

The overall objective of this program was to provide process design information for sorbent utilization as applied to the LIMB process. Specific objectives of the program included: the determination of operating conditions which would yield high sorbent reactivity, clarification of sorbent/ash interactions and guidelines for avoiding them, and a search for additives that would enhance sulfur capture.

In order to accomplish these objectives, the program was divided into four tasks which are described below.

1.2.1 Task 1 - Facility Characterization

Since the radiant portion of the furnace was new for this program, it was required that the facility be characterized before the subsequent tasks could begin. Initially, temperature profiles were required for several load and cooling configurations. It was of interest to match the old BSF temperature profile in order to compare capture data. The next steps required that a mass loading profile be taken followed by the initial capture data with vicron sorbent. All of these tests were carried out in natural gas flames.

1.2.2 Task 2 - Definition of Optimum Injection Conditions

After the facility had been completely characterized, the Task 2 studies were initiated. The major goal of Task 2 was to determine the conditions necessary to achieve optimum sulfur capture. The test plan called for these tests to be carried out in natural gas flames so that mineral matter interactions could be avoided. Parameters that were studied in this task included sorbent type, injection location, sulfation zone quench rate and peak flame temperature. In addition, most of the additive testing was to be done under this task in conjunction with the other parameters just listed.

1.2.3 Task 3 - Characterization of Ash Interactions

After completion of the Task 2 studies, testing was to focus on capture with coal. The purpose of this task was to determine what impact coal mineral matter had on sulfur capture with a variety of sorbents, operational parameters, and thermal considerations as outlined in Task 2. The additives chosen in the second task were also to be tested with coal in this task to determine what effect, if any, coal mineral matter had on the enhancement process.

1.2.4 Task 4 - Data Analysis and Reporting

The objective of this task was to review the data generated in the other three tasks in order to provide recommendations and direction for the test matrix. This task was to be ongoing throughout the course of the project resulting in data reduction and assimilation, monthly progress reports, and finally this report.

2.0 EXPERIMENTAL FACILITY

2.1 Furnace

All of the data presented in this report were obtained with the 1.0 MBtu/hr Boiler Simulator Furnace which is illustrated in Figure 2-1. The facility consisted of two main section; a refractory-lined vertical radiant tower and a horizontal convective section containing air-cooled heat exchangers. The radiant tower had an ID of 1.1 ft. and an OD of 3.2 ft. and consisted of 8 modular sections with multiple access ports as shown in Figure 2-2. Design specifications for the vertical tower are indicated in Table 2-1. The BSF can be used to simulate a wide range of time/temperature profiles by positioning water cooled panels or rods appropriately in the furnace.

The horizontal convective section contained air-cooled tube bundles that simulated the superheaters, economizers and air heaters in a boiler. Cooling air was supplied by an FD fan with a damper to control flow. The convective section was the same one used in previous BSF programs, thus complete documentation can be found in an earlier report (14).

2.2 Distributed Mixing Burner (DMB)

The furnace was equipped with a versatile DMB modeled after the EPA prototype burner. The burner is shown schematically in Figure 2-3. Two secondary air streams supplied the burner. The secondary air swirl could be controlled by modifying the swirl and axial air flow rates. The burner had four external staging air ports supplied with separately metered tertiary air. The tertiary air injection velocity could be modified by changing the air injector size. The burner was designed to fire coal or natural gas. NO_x levels were minimized with the DMB due to the fuel-rich core that was produced in the flame zone.

For the natural gas studies, H_2S was doped into the gas line and injected at the burner to simulate the sulfur content of coal. For those tests involving burner injection, sorbent fed from a twin-screw volumetric feeder

TABLE 2-1. RADIANT TOWER DESIGN SPECIFICATIONS

Internal Dimensions	22" ID x 18 ft long
External Dimensions	38" OD x 21.5 ft long (includes slag trap)
Maximum Design Gas Temperature	3200°F
Furnace Volume, V	47.52 ft^3
Internal Surface Area, A	103.7 ft^2
Surface to Volume, A/V	2.18/ft
Modules	3 High Temperature Modules 4 Medium Temperature Modules 1 Burner Module 2 Transition Modules
Wall Construction	• High Temperature Modules 3 Layers (inside to outside) (AP Green) 3" Greencast 97 3" Kast-O-Life 30 2" Castible 22 • Medium Temperature and Transition Modules 2 Layers (AP Green refractories) 3" Mizzou 5" Kast-O-Life 25 • 3/16" Carbon Steel Casing
Residence Time (to transition) @ 1 x 10^6 Btu/hr SR = 1.2	2.2 sec
Firing Density Btu/ft^3	2.1 x 10^4
Estimated Overall Heat Transfer Coefficient U_T(Btu/hr F ft^2)	High Temperature Modules 0.63 Medium Temperature Modules 0.60
Estimated Heat Loss Per Module Btu/hr, % of Load	High Temperature Modules 15,040 / 1.5% Medium Temperature Modules 12,240 / 1.2%
Sample/Viewport/Slag Panel Area, Total ft^2/% of Surface	7.56 ft^2/8.5%

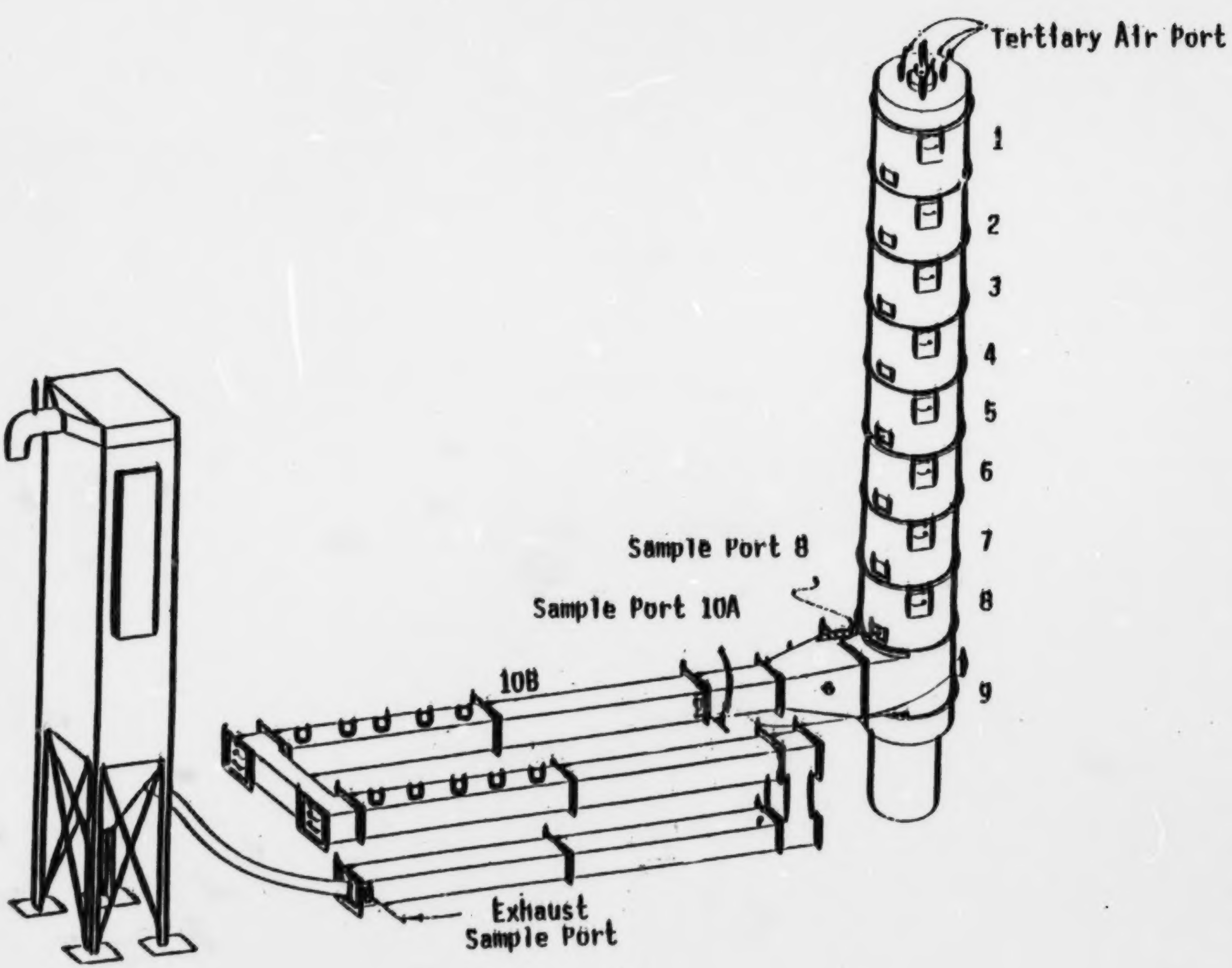
Tertiary Air Port
1
2
3
4
5
6
7
8
9
Sample Port 8
Sample Port 10A
10B
Exhaust
Sample Port

Figure 2-1. Boiler simulator furnace (BSF).

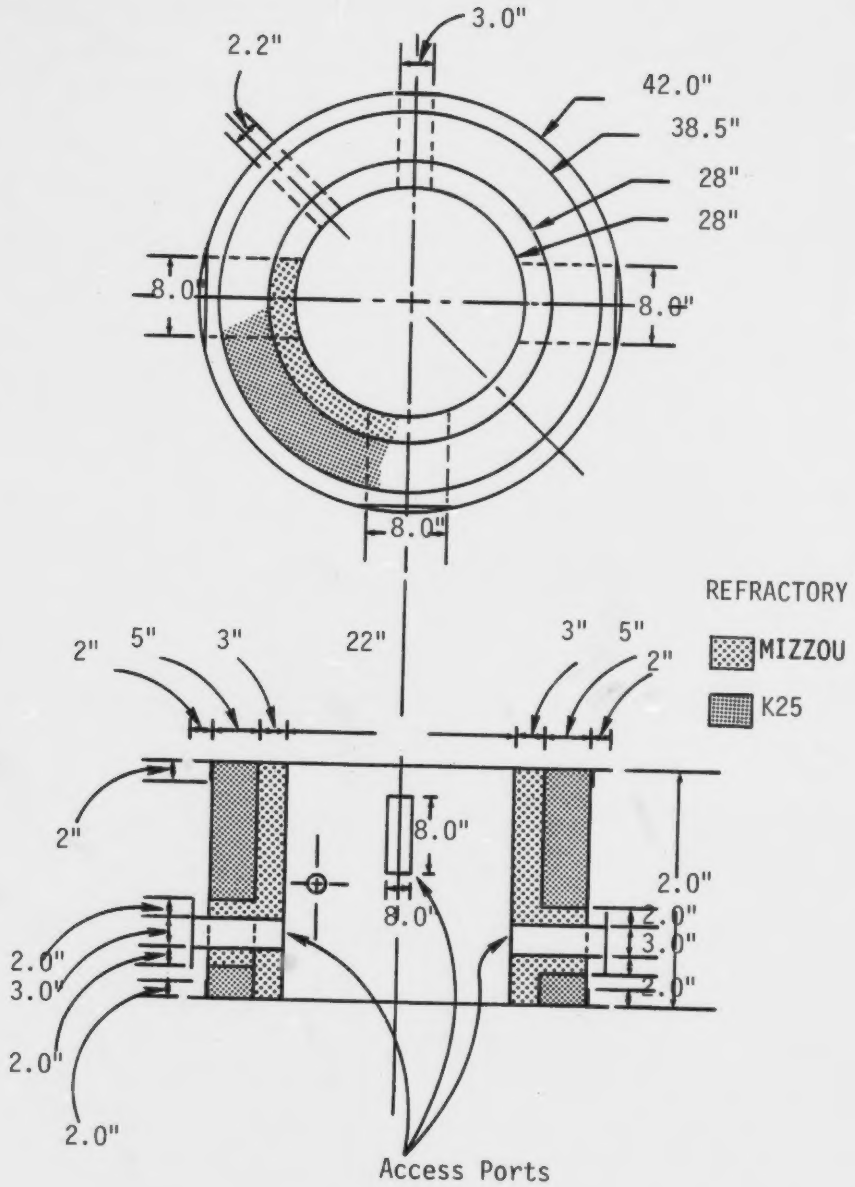
3.0"
2.2"
42.0"
38.5"
28"
28"
8.0"
8.0"
8.0"
REFRACTORY
▨ MIZZOU
▨ K25
2"
5"
3"
22"
3"
5"
2"
2"
8.0"
8.0"
2.0"
2.0"
3.0"
2.0"
2.0"
3.0"
2.0"
2.0"
2.0"
Access Ports

Figure 2-2. BSF tower module.

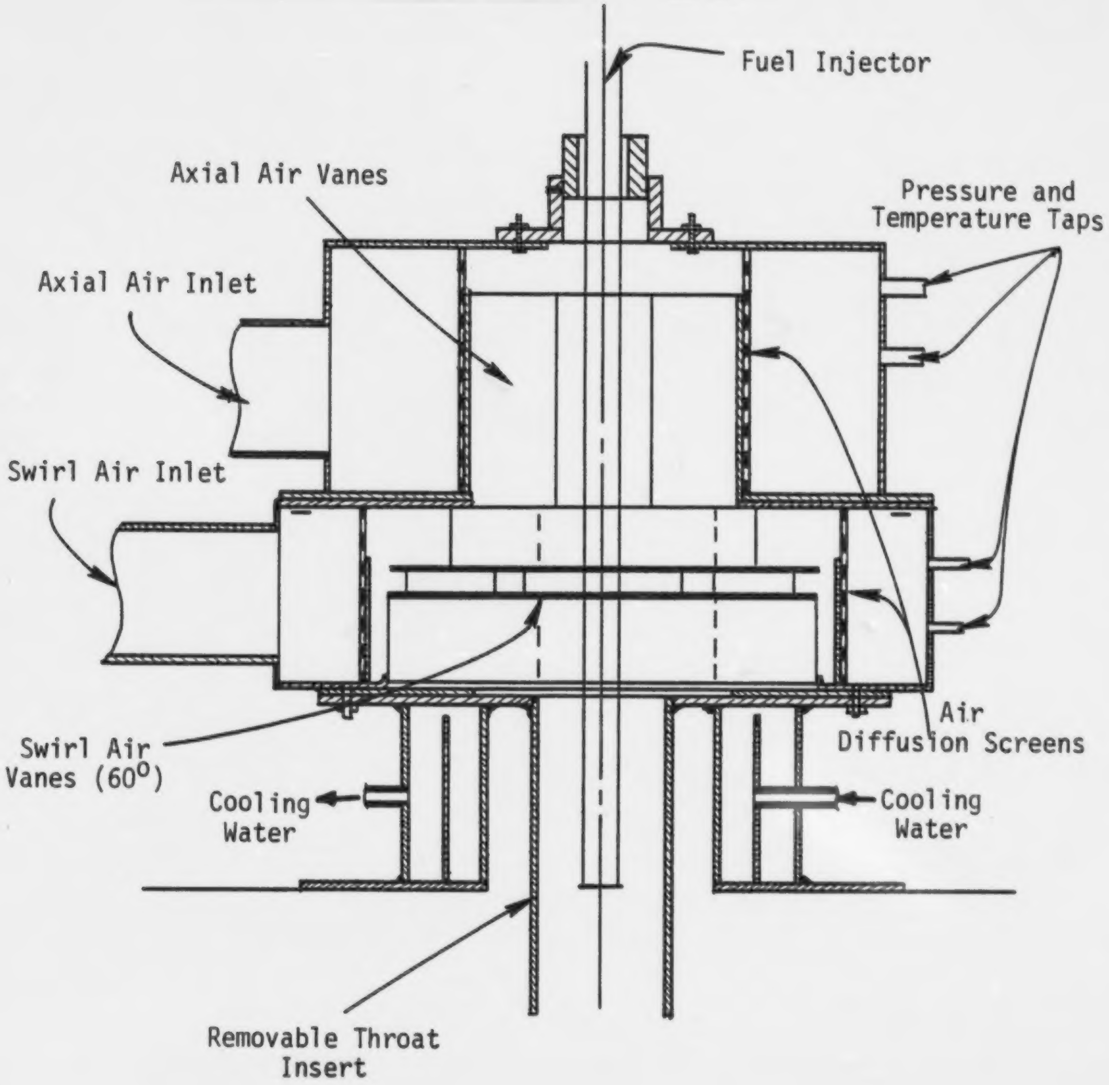
Fuel Injector
Axial Air Vanes
Pressure and Temperature Taps
Axial Air Inlet
Swirl Air Inlet
Air Diffusion Screens
Swirl Air Vanes (60°)
Cooling Water
Cooling Water
Removable Throat Insert

Figure 2-3. Distributed mixing burner (DMB) schematic (tertiary air ports not shown).

involving burner injection, sorbent fed from a twin-screw volumetric feeder was added to the main coal pipe or to a concentric pipe around the natural gas line. For both fuels, sorbent was injected downward through the center of the burner.

2.3 Support Facilities

2.3.1 Ash Handling and ID Fan

Fly ash which passes through the furnace was collected from the exhaust in a baghouse. The baghouse was equipped with special fabric bags which allowed high temperature (to 550°F) operation when needed. The baghouse was exhausted with an induced draft fan and the clean exhaust gas was discharged. The ID fan was equipped with a damper and the furnace/convective sections were generally run at ambient or slightly (up to 6" H_2O at the burner) positive pressure to prevent dilution by in-leakage of air.

2.3.2 Water Recirculation System

All of the cooling water requirements for the BSF were supplied by a closed-loop water recirculation system. Water at a pressure of about 40 psi was pumped up one leg of the platform as a supply manifold. Cooling water for the various panels and rods was taken off the supply manifold and dumped into another leg for the return manifold. The hot water was then returned to an automatic cooling tower and then recycled through the system.

2.3.3 Coal/Sorbent Delivery Systems

Pulverized coal was delivered to the DMB through a 1 inch pipe with air as the transport medium. Coal was fed from a K-tron loss-in-weight feeder into a cyclone/aspirator assembly. The primary transport air passed through the aspirator creating a negative pressure that pulled coal from the cyclone into the transport line. Coal was fed from ground level up to the burner approximately 25 feet off the ground. The coal feeder provided an accurate and constant fuel rate that could be used with the input air and flue gas oxygen measurements to obtain a mass balance.

Sorbent was fed in a similar fashion from a twin-screw volumetric feeder located at the top of the platform. The sorbent transport air passed through a cyclone/aspirator assembly similar to the coal system. An air bypass value allowed adjustment of the cyclone pressure which was maintained at a constant negative pressure of 2 inches of water. The sorbent feeder was calibrated before every set of runs to ensure that the correct feedrate was delivered to the transport line. Sorbent feedrates were dependent upon the weight percent of calcium in the sorbent and the desired calcium to sulfur molar ratio.

2.3.4 Air Delivery System

All of the air requirements for the BSF were supplied by a 300 cfm @ 100 psi air compressor. During normal operation, compressed air passed through an oil filter and dryer and entered a large receiving tank. Air was then drawn from the tank to a supply manifold for each of the separately metered air lines. Each line contained a factory calibrated laminar flow element. The pressure drop across the element is converted to a numerical value of SCFM by a pressure transducer and input to a continuous data reduction system. Up to five different air streams could be individually monitored and injected in the furnace at various locations.

2.4 Measurement Systems

Measurements that were performed during the course of this program included:

- Gaseous species concentrations
- Solid composition and physical characteristics
- Furnace wall and gas temperatures

Table 2-2 summarizes the gas and solid species measured and the solid characteristics determined. The methods and instruments used for these

TABLE 2-2 MEASUREMENTS

MEASUREMENT	PROBE AND CONDITIONING	ANALYTICAL METHOD/INSTRUMENT
Gases		
O_2	Standard or Phase Discrimination - Continuous	Beckman 755
CO_2		Non-dispersive Infrared (Anarad) AR-600R
CO		Non-dispersive Infrared (Anarad) AR-500R
NO_x		Chemiluminescent (TECO)
SO_2	Phase Discrimination, Continuous	Non-dispersive Ultraviolet (DuPont) 400 Photometric Analyzer
Temperatures		
Furnace	Wall Thermocouples	Type S or K Thermocouple
Gas	Suction Pyrometer	Type S or B Thermocouple
Solids		
Mass Loading	Isokinetic Solids Probe or Grab Sample with Glass Cyclone	Mass Basis, Ash as Tracer
Carbon		CO_2 Evolution, Combustion (Perkin-Elmer 240B)
Hydrogen		H_2O Evolution Combustion
Nitrogen		N_2 Evolution Combustion
Oxygen		
Sulfur		SO_2 Evolution (Leco)
Ash		Combustion
Heating Value		ASTM
CaO		
Size Distrib.		Sedimentation
Surface Area		N_2 Adsorption BET (Quantachrome)
Hydration Wt.Gain		H_2O Uptake
Dissolution Rate		Acid Titration

measurements are listed, as are the probes and sample conditioning systems used to obtain samples. This section describes the standard sampling and analytical systems used for the bench-scale studies.

2.4.1 Gas Samples

The measurement of sulfur species in combustion products containing active sorbents poses several special problems. Sulfur species are water soluble and highly reactive with calcium-based sorbents. It is imperative that gas-solid contacting be minimized and contact between the gas and any condensed water be avoided. Therefore, a phase "discriminating probe" which was previously (14) developed and tested was used for all continuous gas species measurements. The probe was designed so that the sulfur species sample was extracted from the main particle-laden sample steam at right angles to the main flow and at a relatively low velocity (see Figure 2-4). The probe supplied two gas streams simultaneously: the main, particle-laden stream which was used for continuous monitoring of O_2, CO, CO_2, NO_x and the side, nearly particle-free, stream which was used for SO_2 measurement. Sample conditioning for the two streams was somewhat different (see Figure 2-5). The main sample (O_2, CO, CO_2, NO_x) was dried using an iced-condenser, filtered, pressurized, filtered again and delivered to the continuous instrumentation listed in Table 2-2. The SO_2 gas sample was transported in a heated Teflon line maintained above 115°C under vacuum to a heated filter followed by a permeation tube drier. The permeation tube drier selectively removed water-vapor from the gas sample. Dry air was used as the dry gas medium in the permeation drier. The sample was then pressurized and delivered to the analytical system (see Figure 2-6). SO_2 concentration was measured using a non-dispersive ultraviolet instrument manufactured by DuPont. The NDUV system was selected for simplicity, lack of interferences or quenching (a problem with pulsed-fluorescent SO_2 instruments) and linearity. The majority of SO_2 sampling was performed at Port 10B. In some cases samples at different locations along the furnace and at the exhaust port were also obtained for analysis.

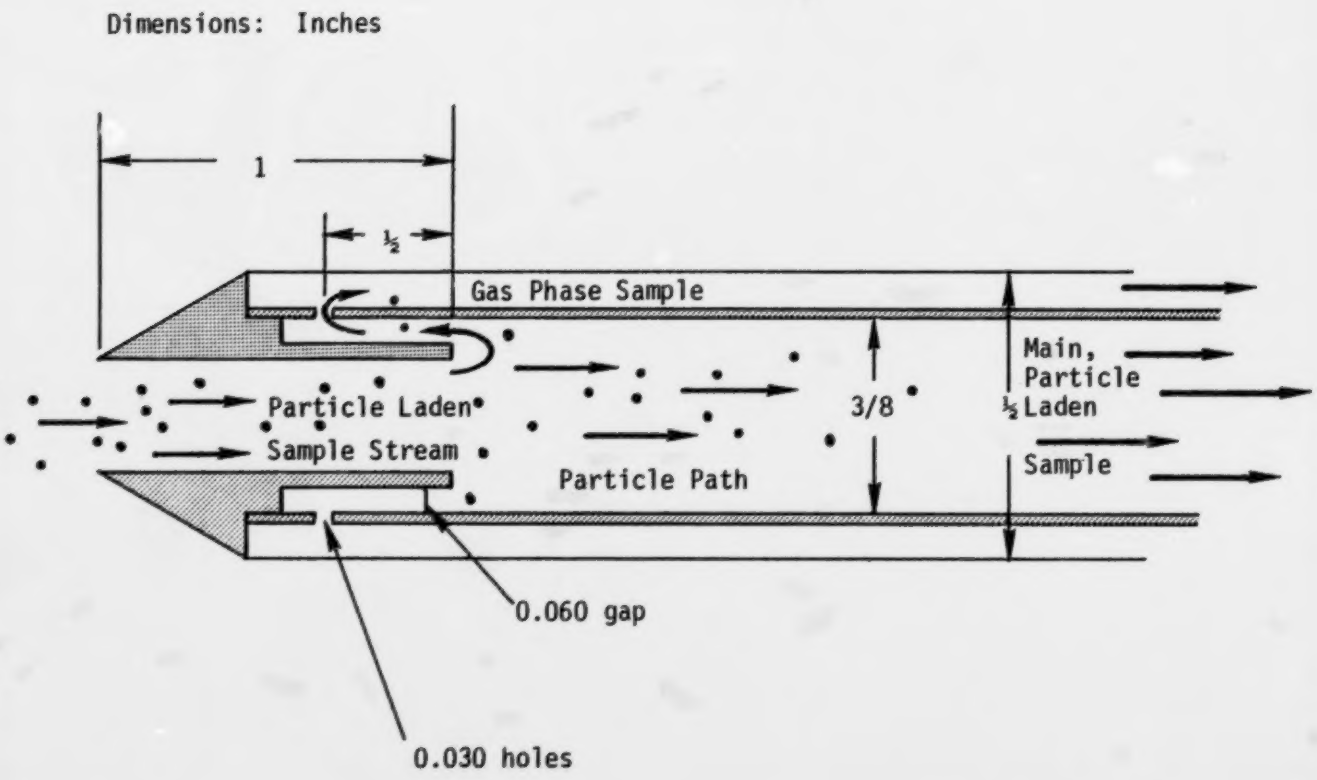
Dimensions: Inches
1
½
Gas Phase Sample
Main,
Particle
½ Laden
Sample
3/8
Particle Laden
Sample Stream
Particle Path
0.060 gap
0.030 holes

Figure 2-4. Phase discrimination probe.

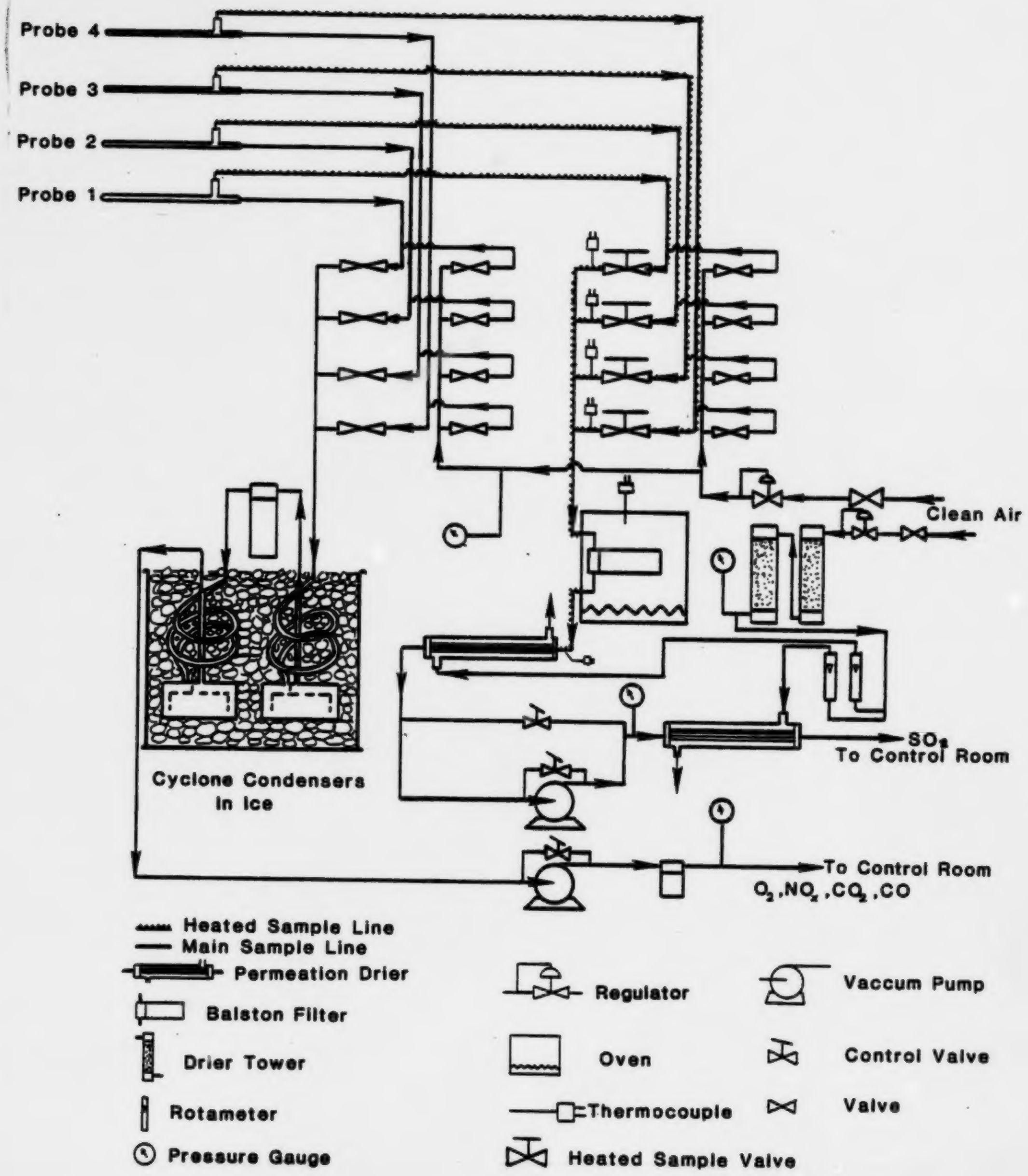
Probe 4
Probe 3
Probe 2
Probe 1
Clean Air
SO_2
To Control Room
Cyclone Condensers
in Ice
To Control Room
O_2,NO_x,CO_2,CO
Heated Sample Line
Main Sample Line
Permeation Drier
Balston Filter
Drier Tower
Rotameter
Pressure Gauge
Regulator
Oven
Thermocouple
Heated Sample Valve
Vaccum Pump
Control Valve
Valve

Figure 2-5. Sample conditioning for gas streams.

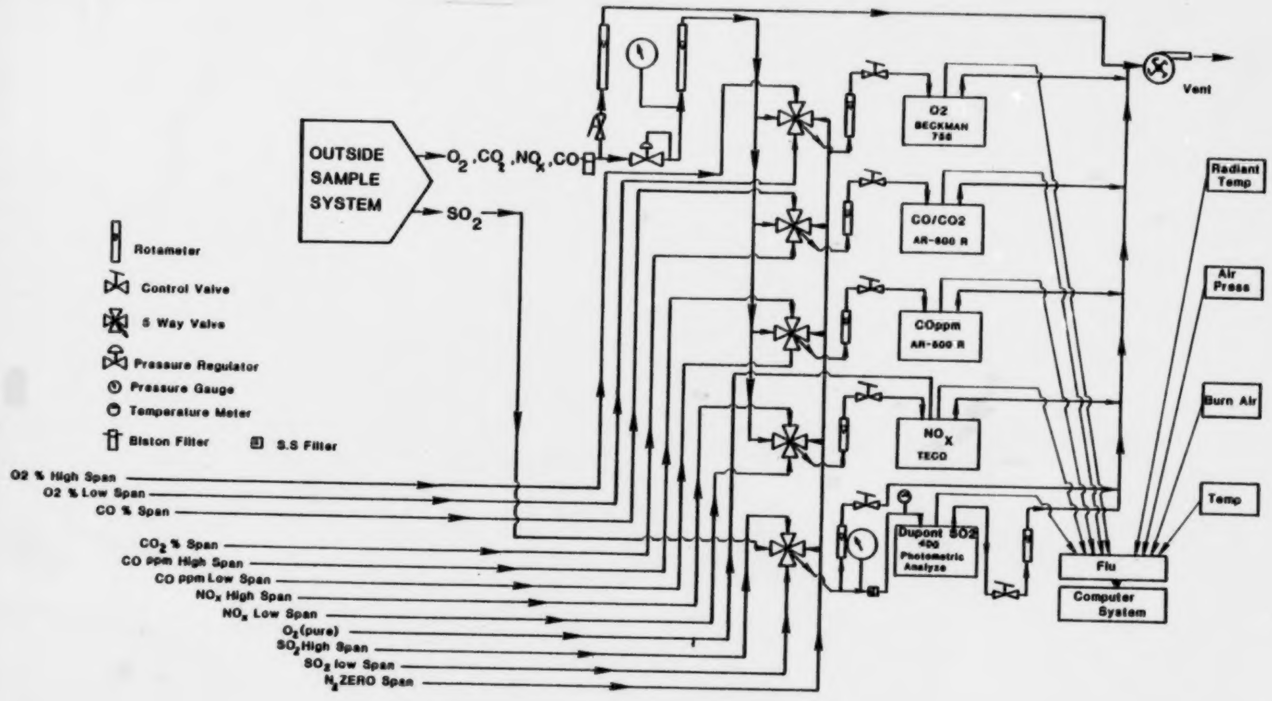
OUTSIDE SAMPLE SYSTEM
O_2, CO_2, NO_x, CO
SO_2
Rotameter
Control Valve
5 Way Valve
Pressure Regulator
Pressure Gauge
Temperature Meter
Biston Filter
S.S Filter
O2 % High Span
O2 % Low Span
CO % Span
CO_2 % Span
CO ppm High Span
CO ppm Low Span
NO_x High Span
NO_x Low Span
O_2(pure)
SO_2 High Span
SO_2 low Span
N_2 ZERO Span
O2 BECKMAN 755
CO/CO2 AR-600 R
COppm AR-600 R
NO_x TECO
Dupont SO2 400 Photometric Analyze
Vent
Radiant Temp
Air Press
Burn Air
Temp
Flu
Computer System

Figure 2-6. Analytical Systems.

2.4.2 Solid Samples

Three different types of solid samples were taken from the furnace: isokinetic solids-loading samples, isokinetic samples for surface area measurement, and non-isokinetic "grab samples". Solids loading samples were taken with an IFRF (International Flame Research Foundation) type probe which is shown in Figure 2-7. Solids were collected in the stainless steel filter and the remaining flue gas then passed through a pump, dry gas meter, and rotameter for measurement of the sample flow rate. Grab Samples were taken from the furnace with a standard, stainless-steel, water-cooled probe. Particles were separated from the gas stream with the use of a glass cyclone which is shown schematically in Figure 2-8.

Surface area measurements were taken isokinetically to ensure that a representative sample was obtained. The flow stream entered a water-cooled probe and was subsequently quenched with nitrogen and accelerated through a smaller tube to keep particle carrying velocity high. The sample then entered a heated teflon line and then into an oven containing a stainless-steel filter holder. Particles were deposited on a paper filter and the remaining flue gas passed through a water condenser, pump, and rotometer. The gas sample was maintained above 150°C until the flue gas left the oven to ensure that no water condensed and affected particle surface area. This system is shown schematically in Figure 2-9.

2.4.3 Temperature Measurements

Furnace wall temperatures were measured using thermocouples embedded in the refractory walls. Temperatures in the radiant section were measured using platinum/platinum-rhodium (Type S or Type B) thermocouples. Temperatures in the convective sections were measured using chromel/alumel (Type K) thermocouples.

Gas temperature measurements were measured using a water-cooled stainless-steel suction pyrometer as shown in Figure 2-10. A closed-end

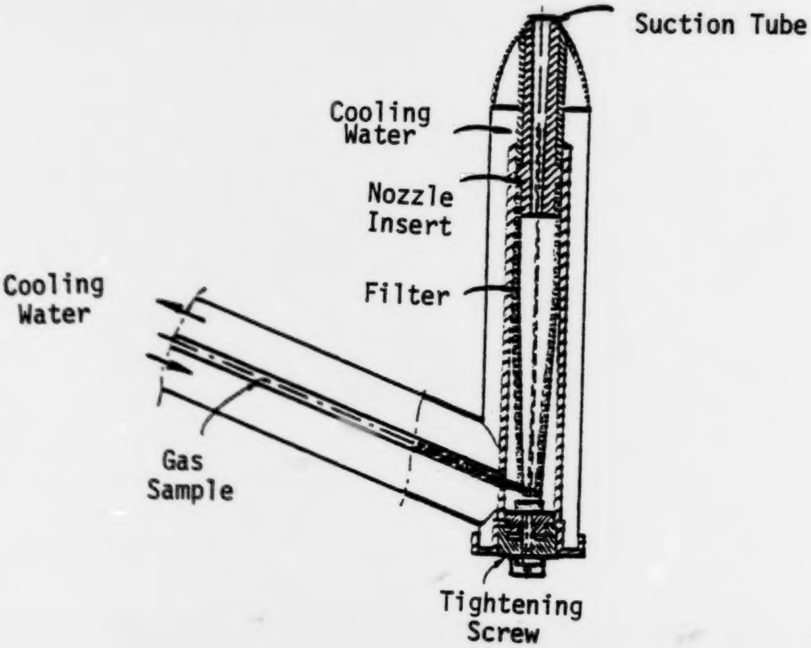
Suction Tube
Cooling Water
Nozzle Insert
Filter
Cooling Water
Gas Sample
Tightening Screw

Figure 2-7. International Flame Research Foundation solid sampling probe.

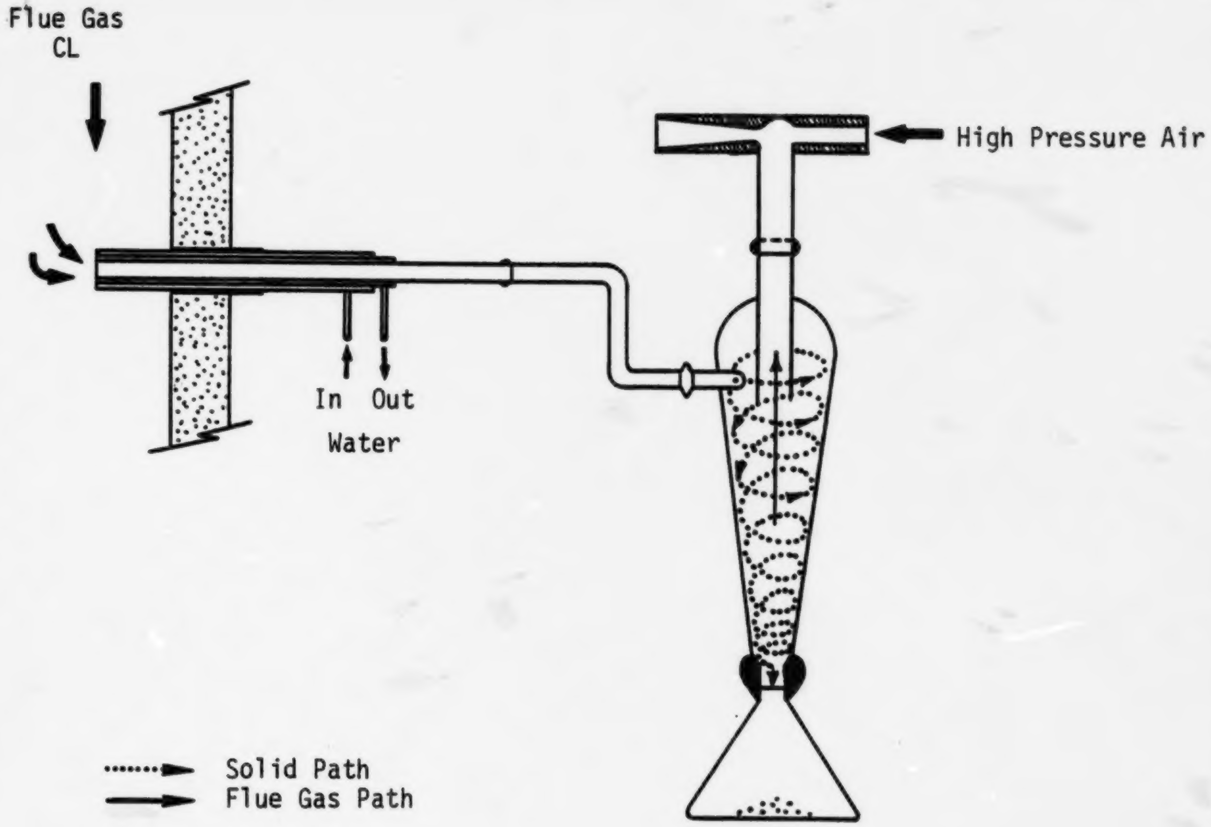
Flue Gas
CL
High Pressure Air
In
Out
Water
Solid Path
Flue Gas Path

Figure 2-8. Grab Sample.

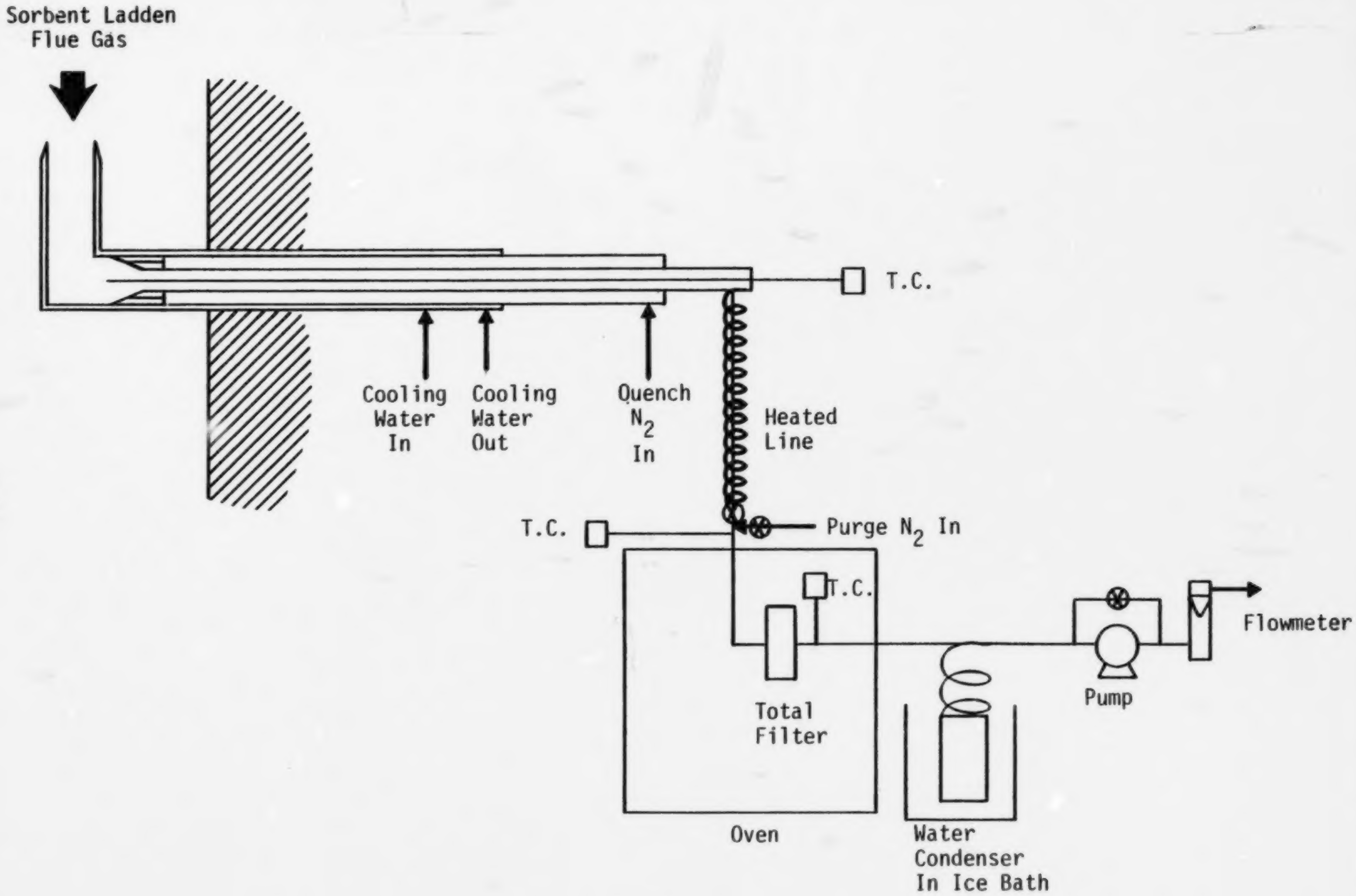
Sorbent Ladden Flue Gas
Cooling Water In
Cooling Water Out
Quench N_2 In
Heated Line
T.C.
T.C.
Purge N_2 In
T.C.
Total Filter
Oven
Water Condenser In Ice Bath
Pump
Flowmeter

Figure 2-9. Surface area sample train.

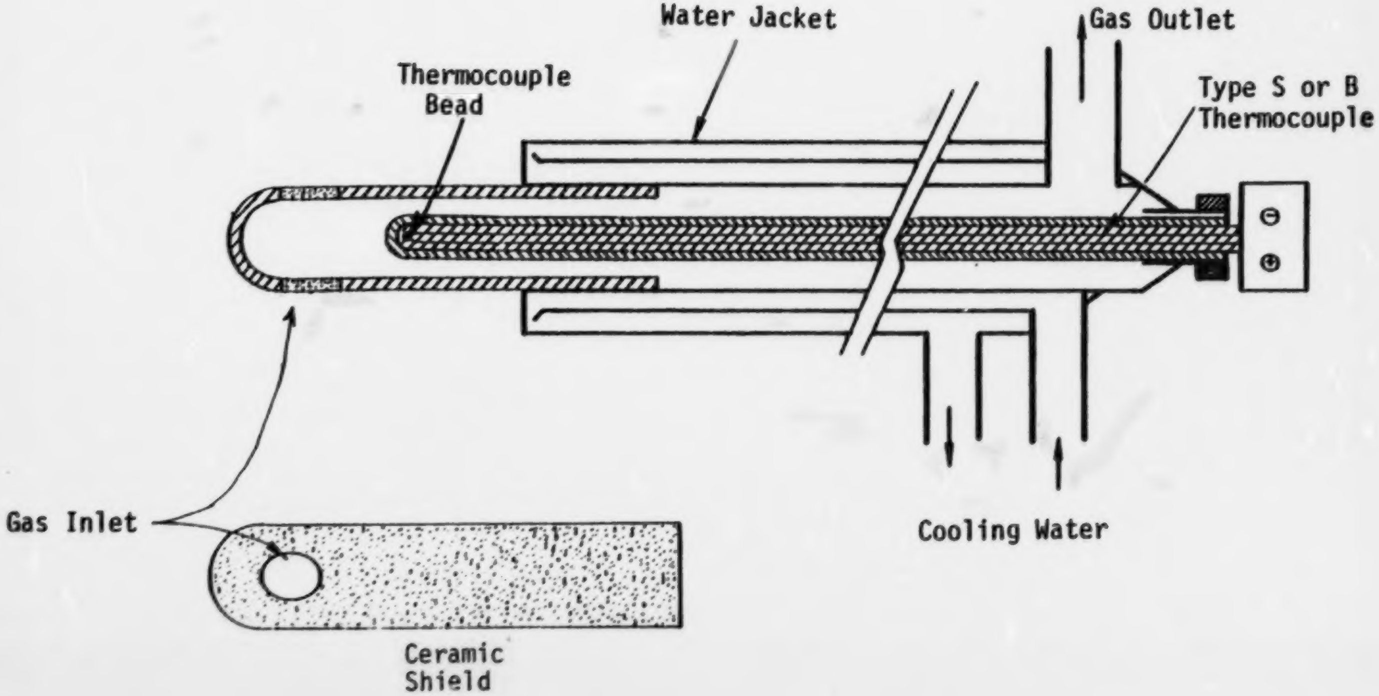
Water Jacket
Gas Outlet
Thermocouple Bead
Type S or B Thermocouple
Gas Inlet
Cooling Water
Ceramic Shield

Figure 2-10. Suction Pyrometer Schematic.

ceramic shield with a hold parallel to the gas flow was used for temperature measurements in both gas and coal flames.

2.5 Data Acquisition

Data for the BSF facility was obtained with the use of a continuous on-line computer and real-time data acquisition program. The program obtained input data every 30 seconds from each of the continuous gas monitors and from the pressure transducers on each of the five laminar flow elements. With this information, the computer could calculate firing rates, various stoichiometries, air and flue gas flow rates, and gas species concentrations on a 0 percent O_2 basis. This information was displayed on a display screen and a printer if desired every 30 seconds. Temperature information was also displayed. The operator could interact with the computer as desired to set up a particular experiment or change variables.

3.0 SORBENTS AND FUELS

3.1 Sorbent Properties

Table 3-1 lists the chemical and physical properties for the major sorbents used in this program. Sorbent types included calcites, hydroxides, dolomites, and pressure slaked dolomitic limes. Calcium percentages went from 30 percent to nearly 54 percent and magnesium content went from close to 0 to 16 percent. Overall, a broad range of sorbents was considered in terms of sulfur capture performance.

The type S pressure hydrated sorbents were the primary group that had not been tested in earlier BSF programs. The type "S" designation indicated that the sorbent was hydrated under pressures exceeding atmospheric; normally in the range of 60 to 120 psi. A type "N" hydroxide implied that the hydration process was done at atmospheric pressure.

Both type N and type S processes have specific advantages depending on the application. The type N process is less expensive since pressure vessels are not required and is generally used with high Calcium limes. The type S process is generally used with dolomitic limes because magnesium oxide will not hydrate at atmospheric pressure. Hydration at high pressure produces a dihydrated ($Mg(OH)_2 \cdot Ca(OH)_2$) dolomitic lime of very small particle size. Both of these factors are advantageous in terms of sulfur capture. High calcium limes can also be hydrated with a type S process if very high conversion is desired or if the raw lime is particularly unreactive.

3.2 Fuel Properties

The fuels used during this program were primarily natural gas and Indiana #3 coal. At the beginning of the program, two other coals were also examined briefly: an Alberta and a Danish Import coal. Table 3-2 gives proximate and ultimate analyses for all of these fuels.

TABLE 3-1. PHYSICAL AND CHEMICAL PROPERTIES OF SORBENTS

Sorbent	○ Vicron	◇ Colton Hydrate	⬡ Warner Hydrate	△ Dolomite	✤ Genstar Blend	✙ Genstar Dolomitic Hydrate (s)	⬯ Warner Dolomitic Hydrate (s)	◊ Warner Hydrate (60 psi)
Petrographic Character	Calcite	Hydrated Lime	Hydrated Lime	Dolomite	Pressure Hydrated Lime + Pressure Hydrated Dolomitic Lime	Pressure Hydrated Dolomitic Lime	Pressure Hydrated Dolomitic Lime	Pressure Hydrated Lime
Composition	$CaCO_3$	$Ca(OH)_2$	$Ca(OH)_2$	$CaCO_3$ $MgCO_3$	$Ca(OH)_2$ + $Ca(OH)_2 \cdot$ $Mg(OH)_2$	$Ca(OH)_2 \cdot$ $Mg(OH)_2$	$Ca(OH)_2 \cdot$ $Mg(OH)_2$	$Ca(OH)_2$
Mean Size (μm)	9.8	4.0	3.5	11.8	1.8	1.4	3.5	3.5
Density (g/cm^3)	2.7	2.3	2.3	2.9	2.3	2.3	2.3	2.2
Chemical Composition (%)								
Ca	39.2	51.4	53.9	24.8	45.0	30.3	29.5	53.2
Al	0.02	0.21	0.37	0.04		0.26	0.21	
Si	0.09	3.30	0.51	0.16		0.13	0.94	
Fe	0.06	0.10	0.21	0.09		0.07	0.42	
Na	0.007	0.007		0.007				
Mg	0.33	0.25	0.20	11.3	6.2	16.0	15.9	
K	--	0.05		0.008				

TABLE 3-2. FUEL ANALYSES

	IND #3	Alberta	Danish Import	Natural Gas
Proximate (as Received)				
H_2O	5.07	13.84	4.28	--
Ash	9.34	15.12	14.44	--
Volatile Matter	30.24	32.58	29.74	--
Fixed Carbon	55.35	38.46	51.54	--
Ultimate (dry)				
C	72.16	57.83	69.39	72.15
H	4.71	3.76	4.33	23.04
N	1.32	1.28	1.33	1.94
S	1.06	0.59	0.86	--
Ash	9.88	17.55	15.09	--
O	10.87	18.99	9.00	0.59
Heating Valve				
Btu/lb	12545	8256	11394	22714
ASTM Classification	High Vol C Bit	Sub-Bit B	High Vol. C Bit.	--

4.0 FURNACE CHARACTERIZATION

Since this version of the Boiler Simulator Furnace was specifically designed and built for this program, it was necessary to obtain characterization data for the new facility before testing could proceed. Initially, this was accomplished through a series of mass balance, solids loading, and thermal history tests.

4.1 Thermal History Data

The thermal profile produced at a load of 1.0 MBtu/hr in the new furnace was quite different from that of the old BSF at the same load. Since it was desired to compare capture data between the two facilities, it became necessary to first match the thermal profile of the old BSF in the new furnace as part of the shakedown tests. Several load and cooling variations were tried before one at 1.0 MBtu/hr with five cooling panels was found that closely matched the old BSF profile.

4.2 Initial Capture Data

Figure 4-1 shows a comparison of the two thermal profiles and the baseline Vicron capture data that was obtained for each profile. Capture data for the old BSF was significantly higher at all of the ports measured. At a Ca/S molar ratio of 2.0 the new BSF showed about 20 percent overall capture while the old BSF attained nearly 60 percent overall capture. Figure 4-2 shows similar data for the two furnaces fired with coal. In this case, the results were very similar at about 20-25 percent capture. Figure 4-3 shows a comparison of old and new data for Vicron injected downstream. Percent SO_2 capture is presented as a function of Ca/S ratio (Ca/S refers to the molar ratio of calcium to sulfur in the furnace throughout the report). For the new BSF, capture increased slightly when the sorbent was injected downstream for both gas and coal. For the old BSF, capture increased with downstream injection for coal but decreased for gas. Overall, the baseline results between the old BSF and the new BSF appeared anomalous.

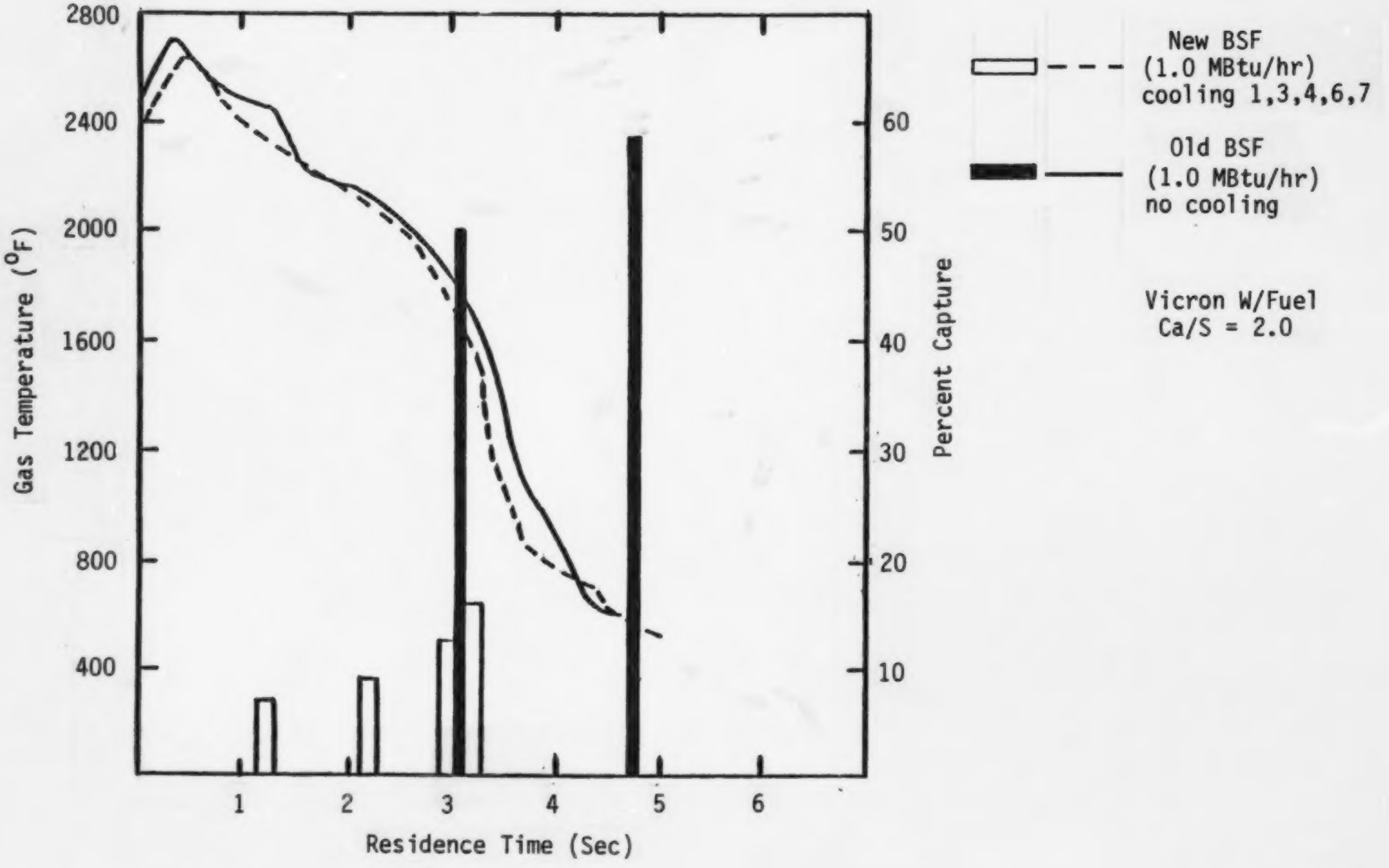

Figure 4-1. Comparison of furnaces with natural gas.

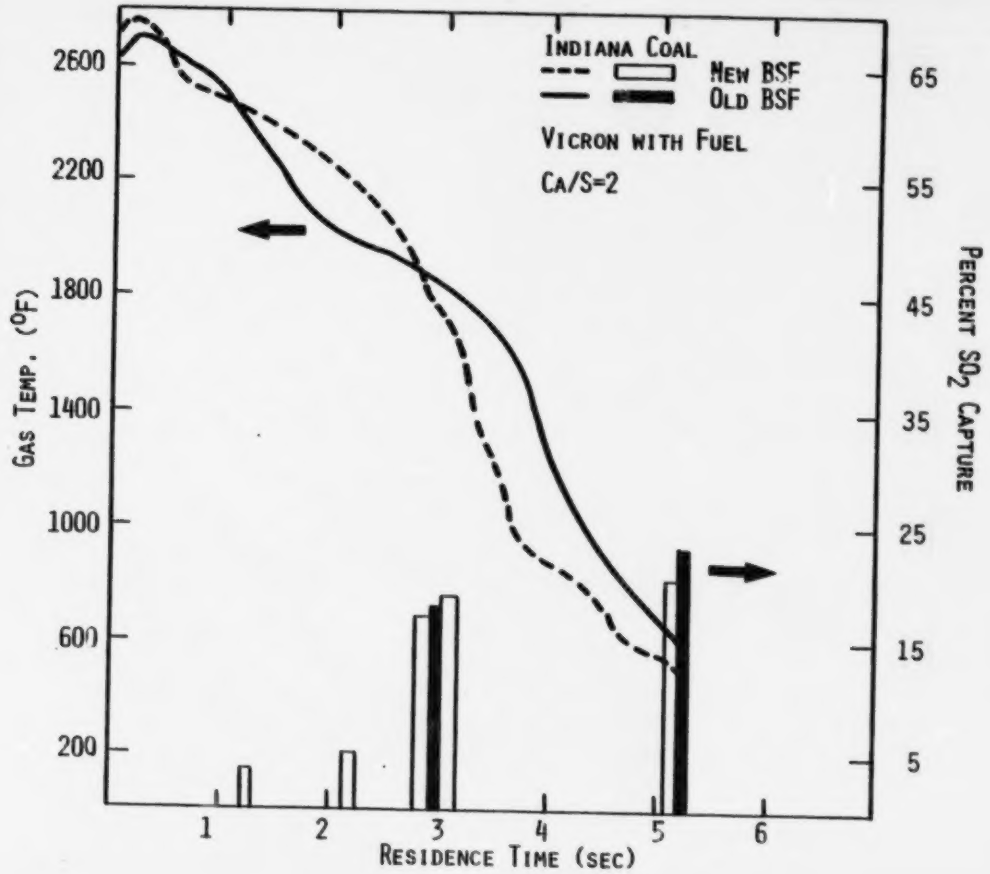

Figure 4-2. Comparison of furnaces with coal.

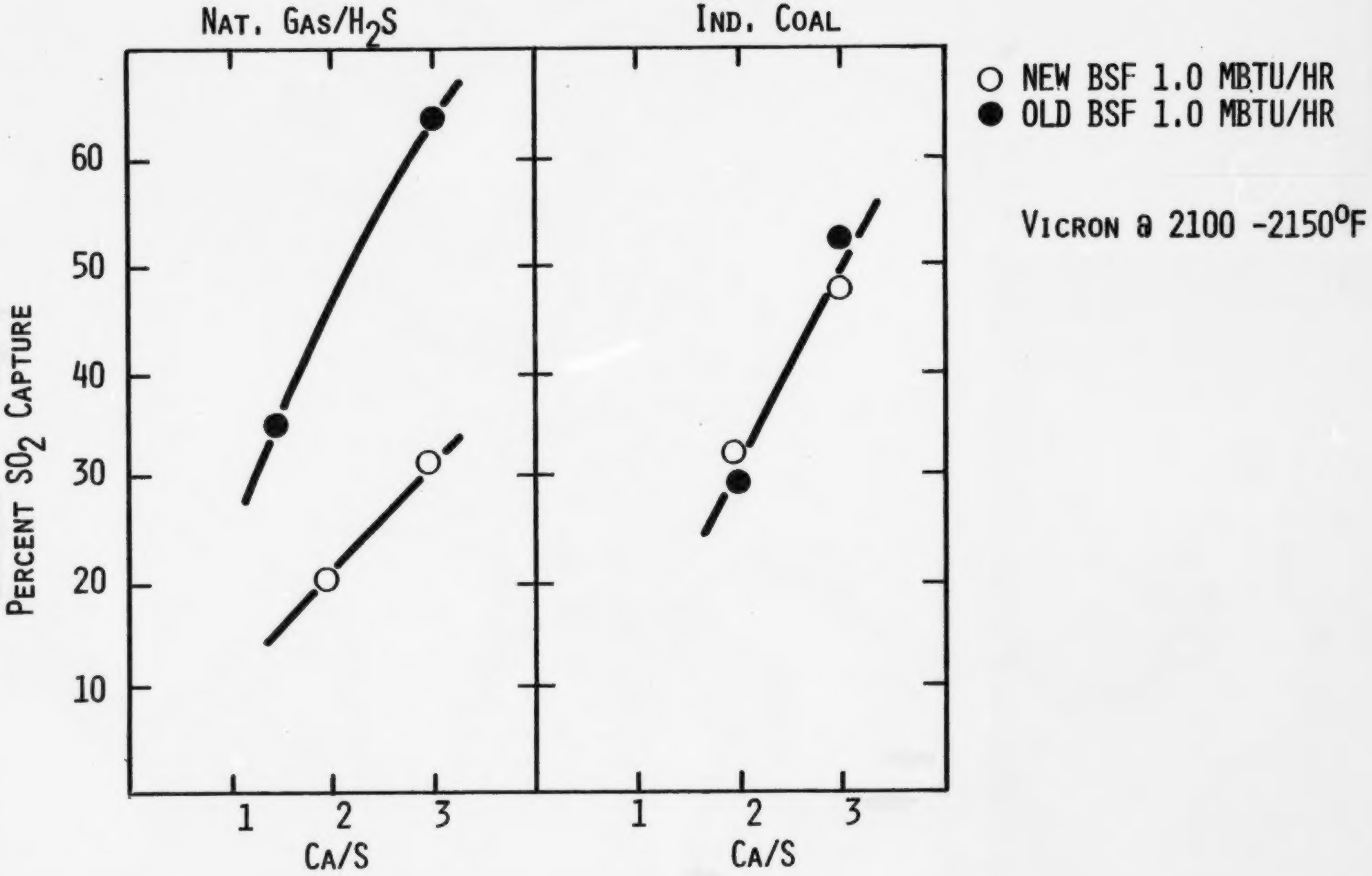

Figure 4-3. Capture comparison for downstream injection.

4.3 Model Predictions

The results produced by EER's sulfation pore model seemed to lend support to the new BSF data because only moderate captures could be predicted. The model predictions and the actual data with Vicron as the sorbent and natural gas as the fuel are illustrated in Figure 4-4. Overall, the model predicts the data quite well for two different profiles - one at low load (0.75 MBtu/hr) and another at normal load (1.0 MBtu/hr). The predictions were certainly much closer to the new BSF data than the high captures generated in the old BSF. The low load and normal load temperature profiles for the new BSF are shown in Figure 4-5 for the upper temperature region. Cooling configurations are indicated for each profile on the figure. Both curves experienced a sharper temperature drop at the convective region because of greater heat losses. For the normal load, this point occurred in the middle of the sulfation window and the resulting quench rate (average rate of temperature drop between 2250 and 2000°F) was approximately 340°F/sec. For the low load case the temperature drop was near the end of the sulfation window, resulting in a lower quench rate of 225°F/sec.

Measured peak temperatures were very close for both profiles and, consequently, the model predicted that the low load profile should produce better capture for both fuel and downstream injection due to longer residence time in the sulfation zone. Figure 4-6 indicates that this was the case for downstream injection, however fuel injection showed the opposite trend. This may have been due to the fact that the peak temperature might not occur precisely at the measurement port and, thus, a sorbent particle may experience higher peak temperature than measured which would decrease surface area.

4.4 Preliminary Mineral Matter Interactions

An interesting conclusion that emerged from the characterization period on the new furnace was that SO_2 capture with coal was similar to capture with natural gas doped with H_2S. Several coal types and a variety of high calcium sorbents were run at two loads and two injection locations. Fuel injection

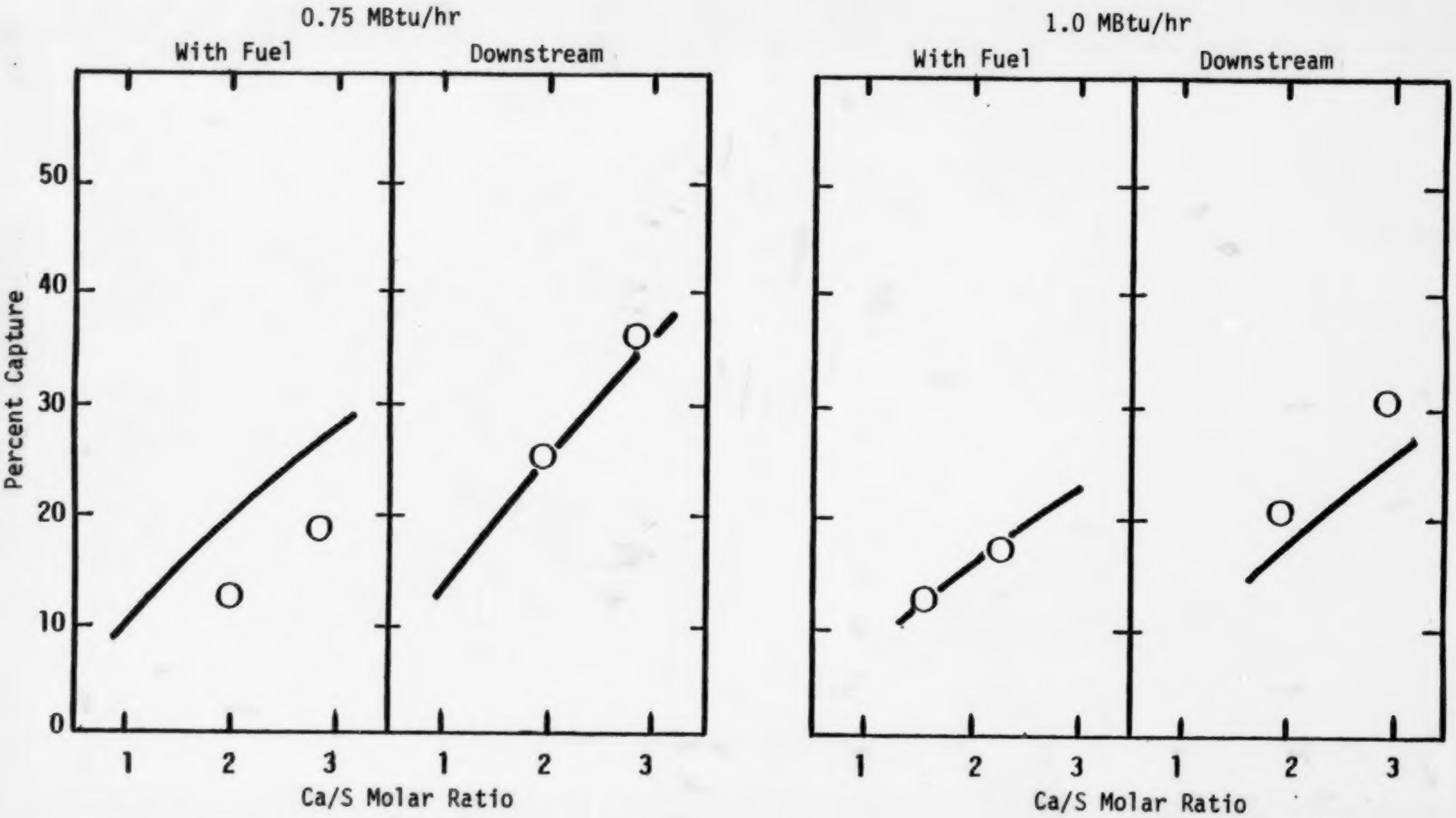

Figure 4-4. Comparison of model predictions and measurements for new BSF.

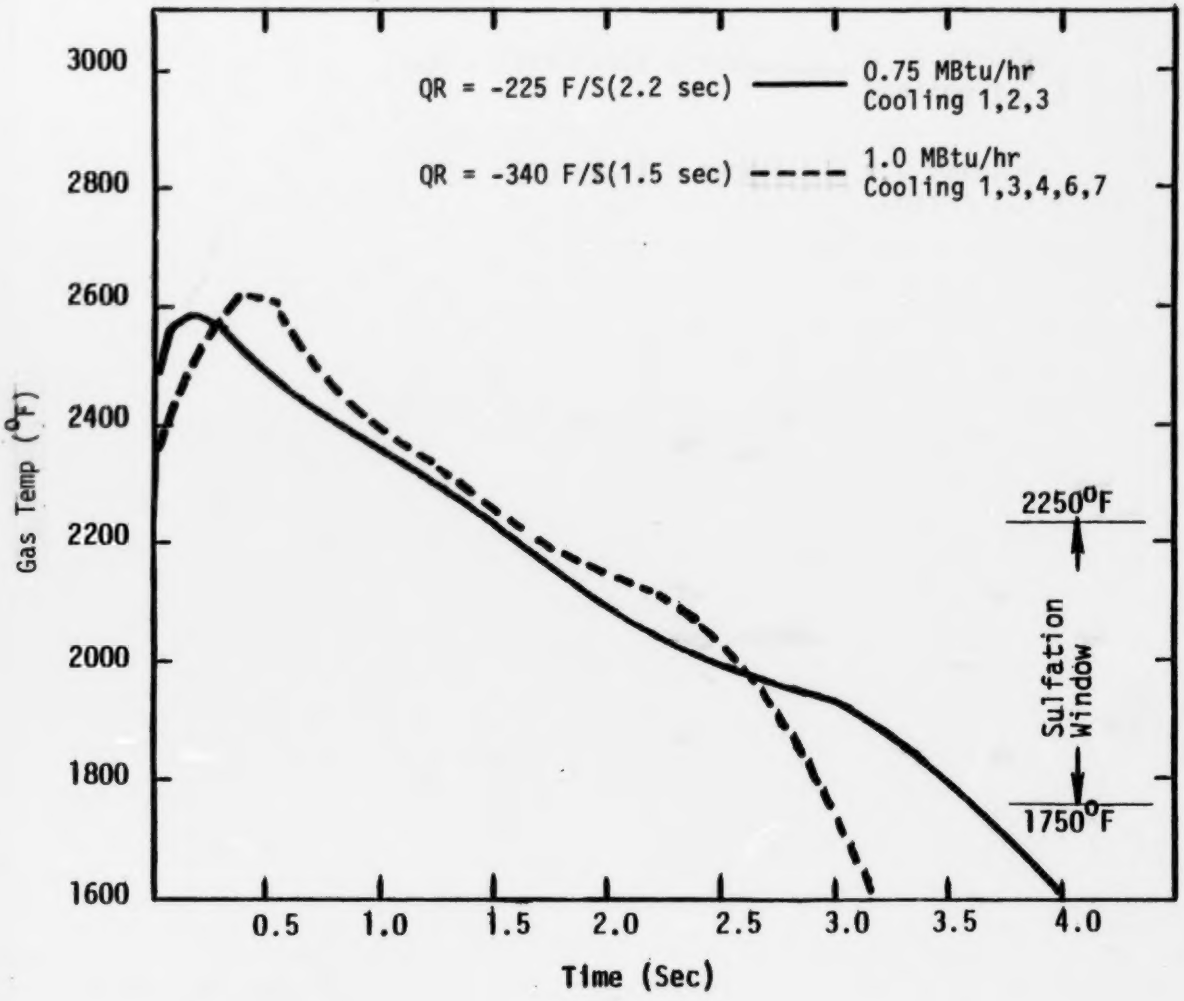

Figure 4-5. Comparison of low and normal temperature profiles.

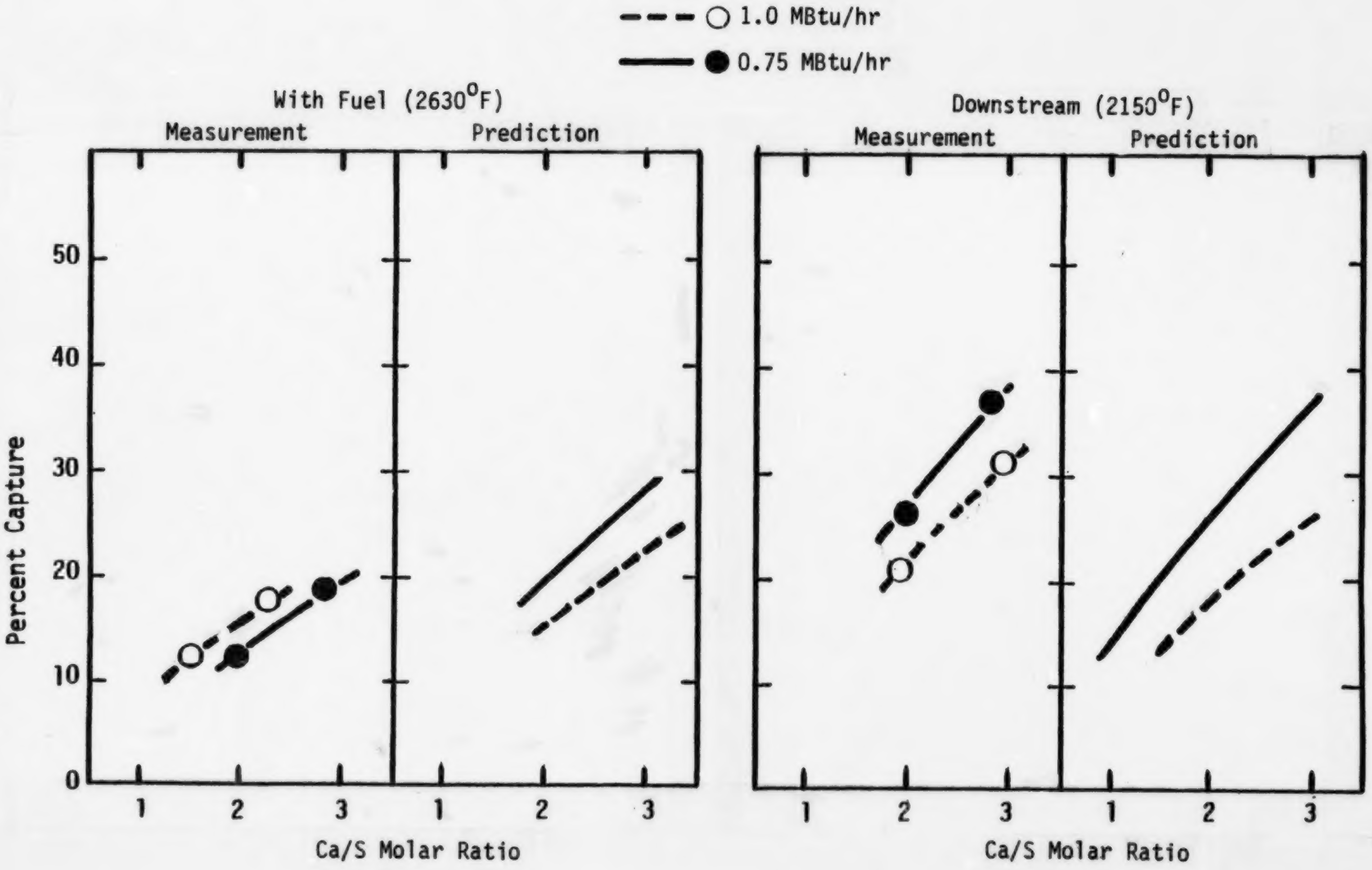

Figure 4-6. Influence of thermal history on capture and model predictions.

produced similar results and for downstream injection coal capture was slightly higher. SO_2 capture with coal was relatively insensitive to coal type and, as expected, downstream injection produced consistently higher captures than fuel injection for both gas and coal. This effect was due to the more favorable calcination environment with downstream injection. These results are presented in Figures 4-7 and 4-8 for 0.75 and 1.0 MBtu/hr loads.

The coal vs gas results were somewhat surprising since the old BSF data indicated that gas capture was dramatically better than coal. In an attempt to explain the difference in coal and gas data in the old furnace, a series of experiments were run whereby sorbent and coal ash were mixed and injected into the furnace. The results of these tests are shown in Figure 4-9. With Vicron alone, capture was very high in the old BSF but when coal ash was mixed in, capture dropped off dramatically. Evidently, mineral matter interacted unfavorably with the sulfation reaction to reduce capture. In order to determine if mineral matter had the same effect on capture in the new furnace, the old BSF experiments were duplicated by mixing Vicron and Kaolin in a 1:1 ratio and injecting the mixture at the fuel and downstream. These results are illustrated in Figure 4-10. For injection with the fuel, mineral matter addition decreased capture significantly which was consistent with the old data except for the range at which it occurred. For downstream injection at approximately 2150°F, the Kaolin had little effect on capture.

Early in the project it became apparent that the new BSF could not achieve capture levels as high as those observed in the old furnace. Consequently, all of the possible differences in the two facilities were looked at in greater detail. As part of this process a comparison of all of the refractories used in both furnaces was made. The new BSF refractories were primarily composed of Al_2O_3 and SiO_2 with only traces of iron, calcium and magnesium oxides. The old furnace refractories contained essentially the same compounds except for the high-temperature zone which was made of a refractory containing 10% Cr_2O_3. In order to check the possible effects of Cr_2O_3 on capture, a 5% (by weight) Cr_2O_3/Vicron mixture was injected at the burner and downstream. These results are shown with the baseline and ash data in Figure 4-10. For injection at the fuel the results were dramatic,

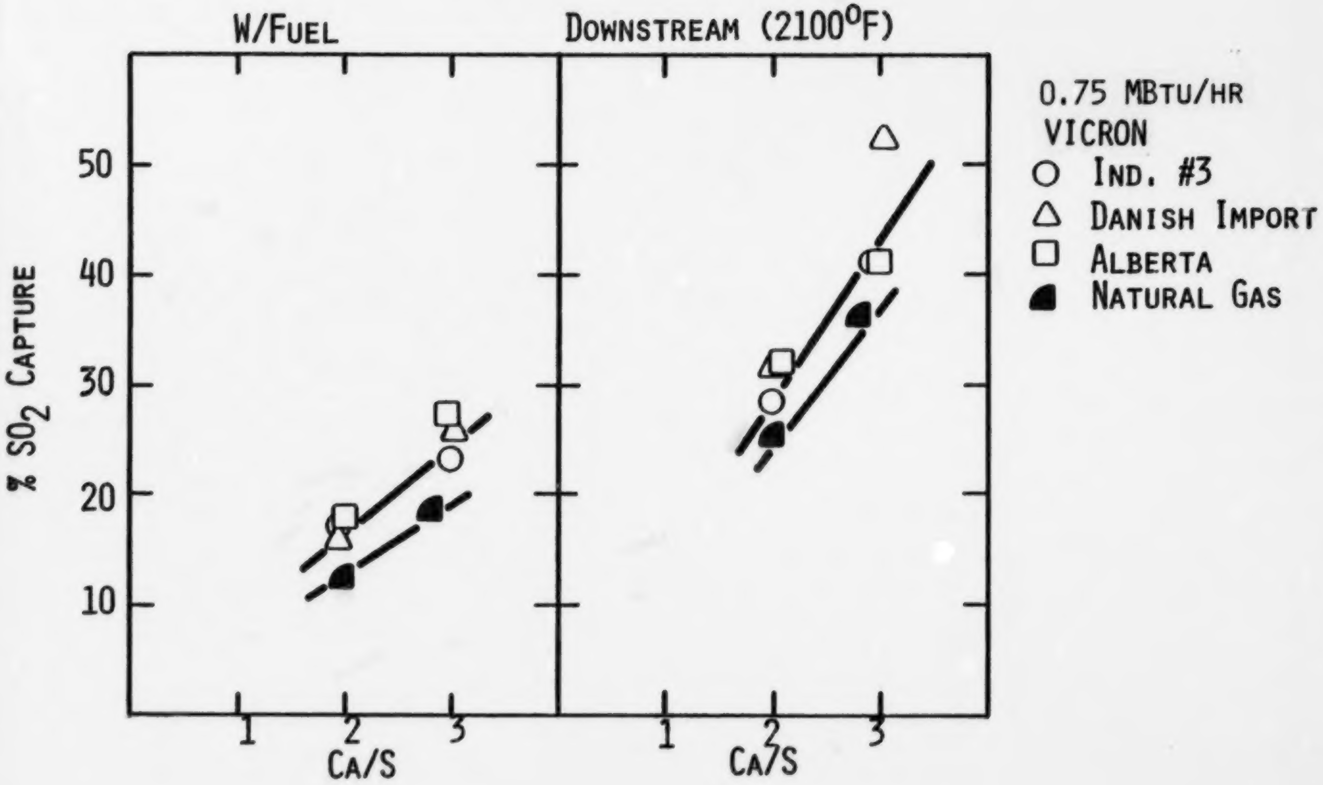

Figure 4-7. Coal vs. gas capture at low load.

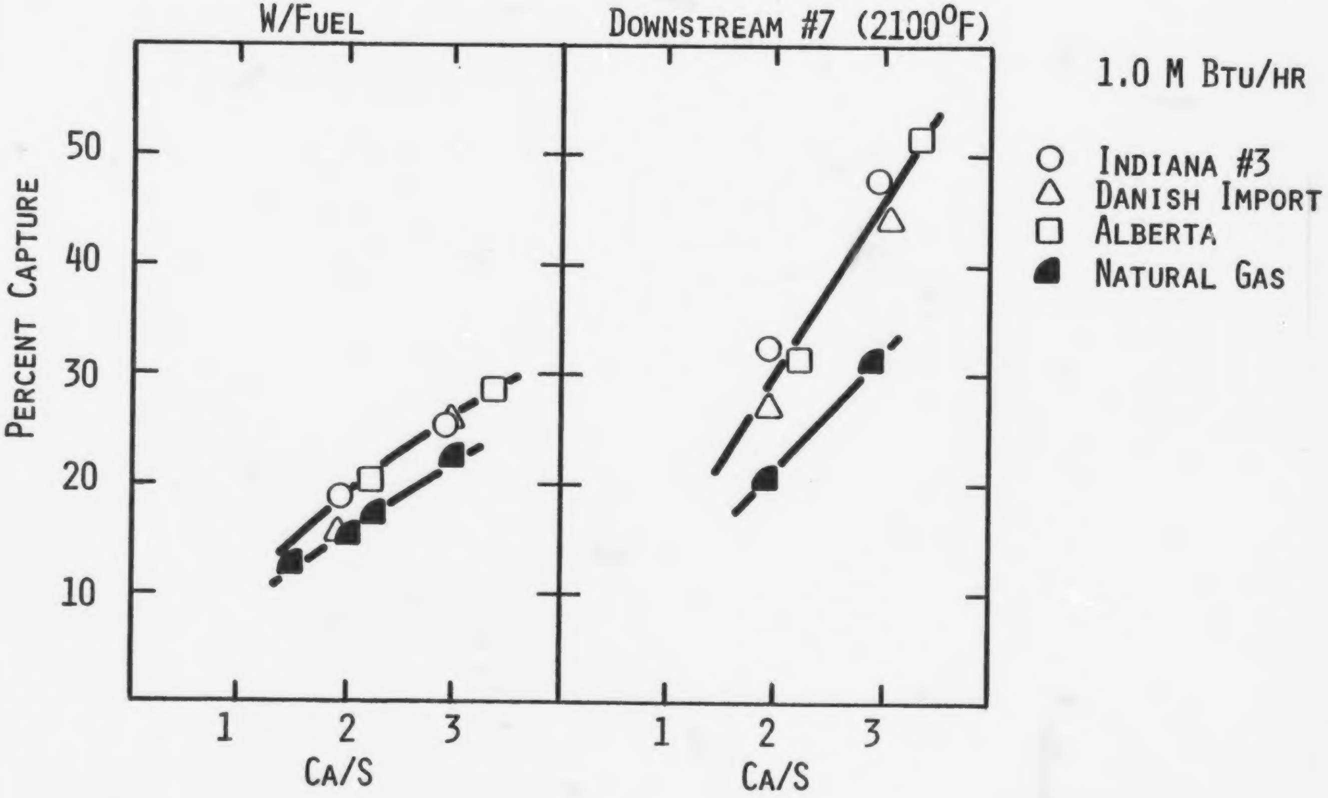

Figure 4-8. Coal vs. gas capture at normal load.

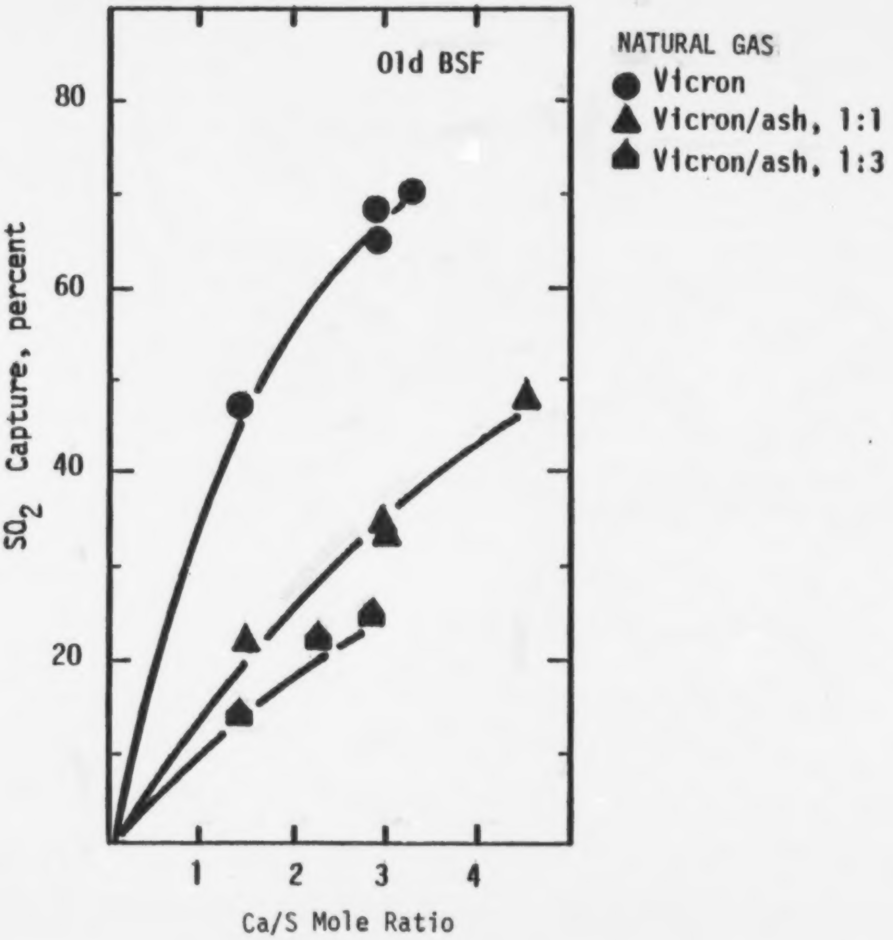

Figure 4-9. Ash deactivation in old BSF.

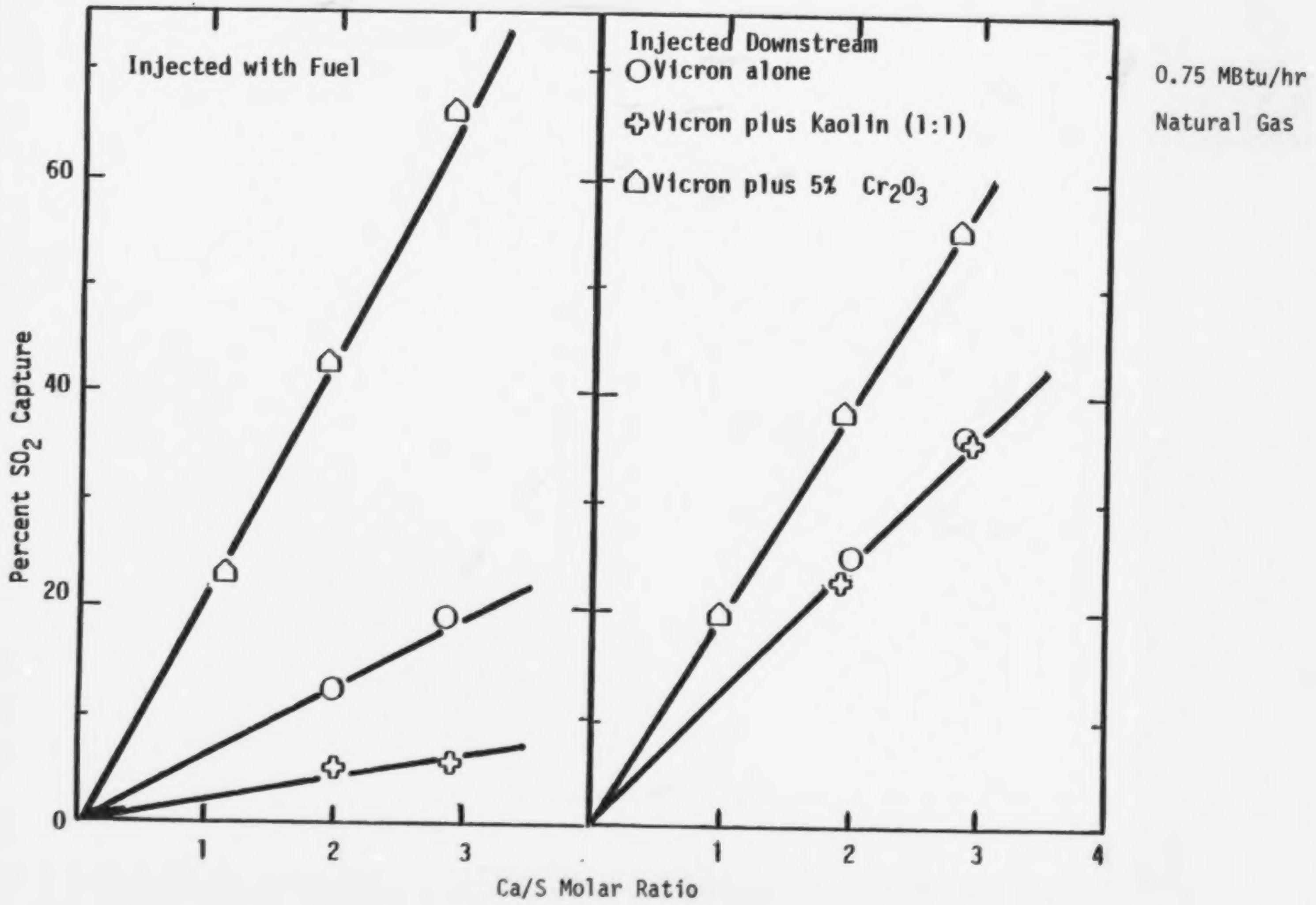

Figure 4-10. Overview of mineral matter effects.

increasing capture by better than a factor of three. Injection downstream produced a significant increase in capture however, the results were lower than the fuel data even though sorbent surface area should have been higher at the downstream location. Apparently the Cr_2O_3 in the old BSF refractory catalyzed the capture reactions to yield high-SO_2 removal efficiencies.

In an attempt to determine the combined effect of mixing mineral matter components, the 5% mixture of Cr_2O_3/Vicron was again mixed in a 1:1 ratio with kaolin and injected at the burner and downstream. These results are shown with the baseline Vicron and the Vicron plus 5% Cr_2O_3 results in Figure 4-11. For injection at the fuel, the presence of kaolin decreased capture significantly compared to the Vicron plus Cr_2O_3 data. Downstream, the kaolin had little effect just as was seen in Figure 4-10 where no Cr_2O_3 was present. Figure 4-11 explains much of the apparent anomaly between the old and new furnaces. The presence of Cr_2O_3 in the old furnace obscured much of the data and explained why the old BSF data was so much higher than the new data.

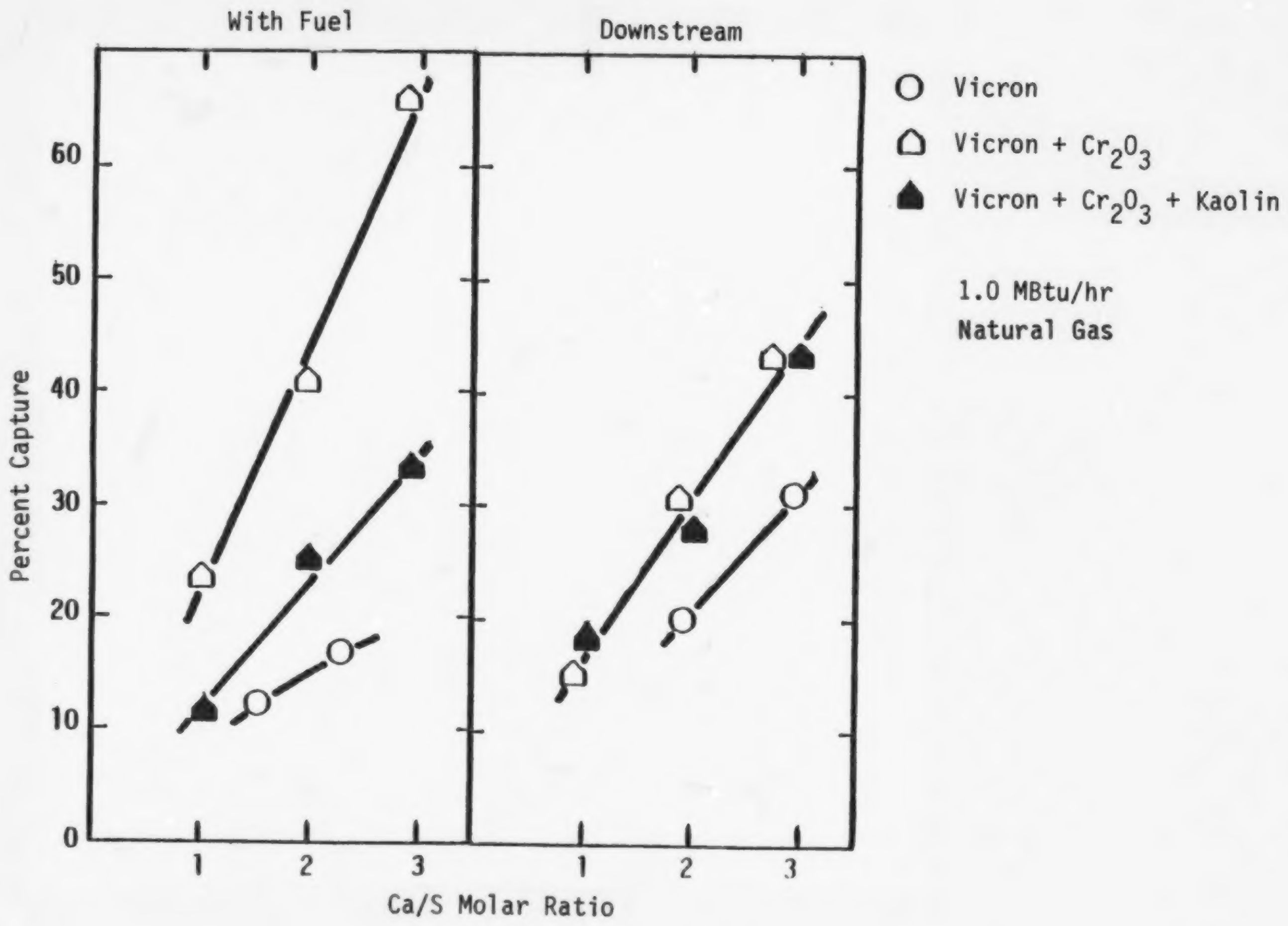

Figure 4-11. Combined mineral matter effects.

5.0 OPTIMIZATION OF SULFUR CAPTURE

At the conclusion of the characterization period, testing focused on techniques for optimizing sulfur capture. Most of the experimental work in this phase of the program fell into two categories: sorbent screening and thermal parameters. In the sorbent screening phase many different sorbent types were studied at several baseline conditions. In the thermal parameters phase, most of the sorbents were run under a variety of thermal conditions with the goal of optimizing sulfur capture. All of the data presented in this chapter were run with natural gas as the fuel in order that capture optimization could be studied in the absence of mineral matter effects. In Chapter 6.0 the influence of mineral matter is discussed in conjunction with the data in this chapter.

5.1 Sorbent Screening

Two temperature profiles on the BSF were chosen as baseline profiles and these represent the time/temperature histories under which most of the data were taken. One of the profiles was termed "American Boiler" which represented current field practice and the other termed "reduced load" which had a more favorable quench rate. These two profiles were chosen because they had a wide range of quench rates and because the "American Boiler" profile should give results that might be expected from real utility boilers. These two profiles are shown in Figure 5-1 along with the results of detailed heat transfer calculations for the temperature profiles of three full-scale utility boilers. The same five temperature profiles are plotted again in Figure 5-2 with only the temperature region below 2250°F shown. The solid lines are the real boilers and the slashed lines represent the two BSF profiles. In this plot, time zero was arbitrarily defined to be the point in the boiler where the gas temperature reached 2250°F. The profiles were characterized in terms of an average quench rate within the region 2250°F to 2000°F since this is the most critical zone in the sulfation window. These results indicated that the quench rate of commercial boilers may vary by as much as a factor of 5 and that in typical utility boilers the time available in the sulfation window (2250°F to 1700°F) may be as little as one second.

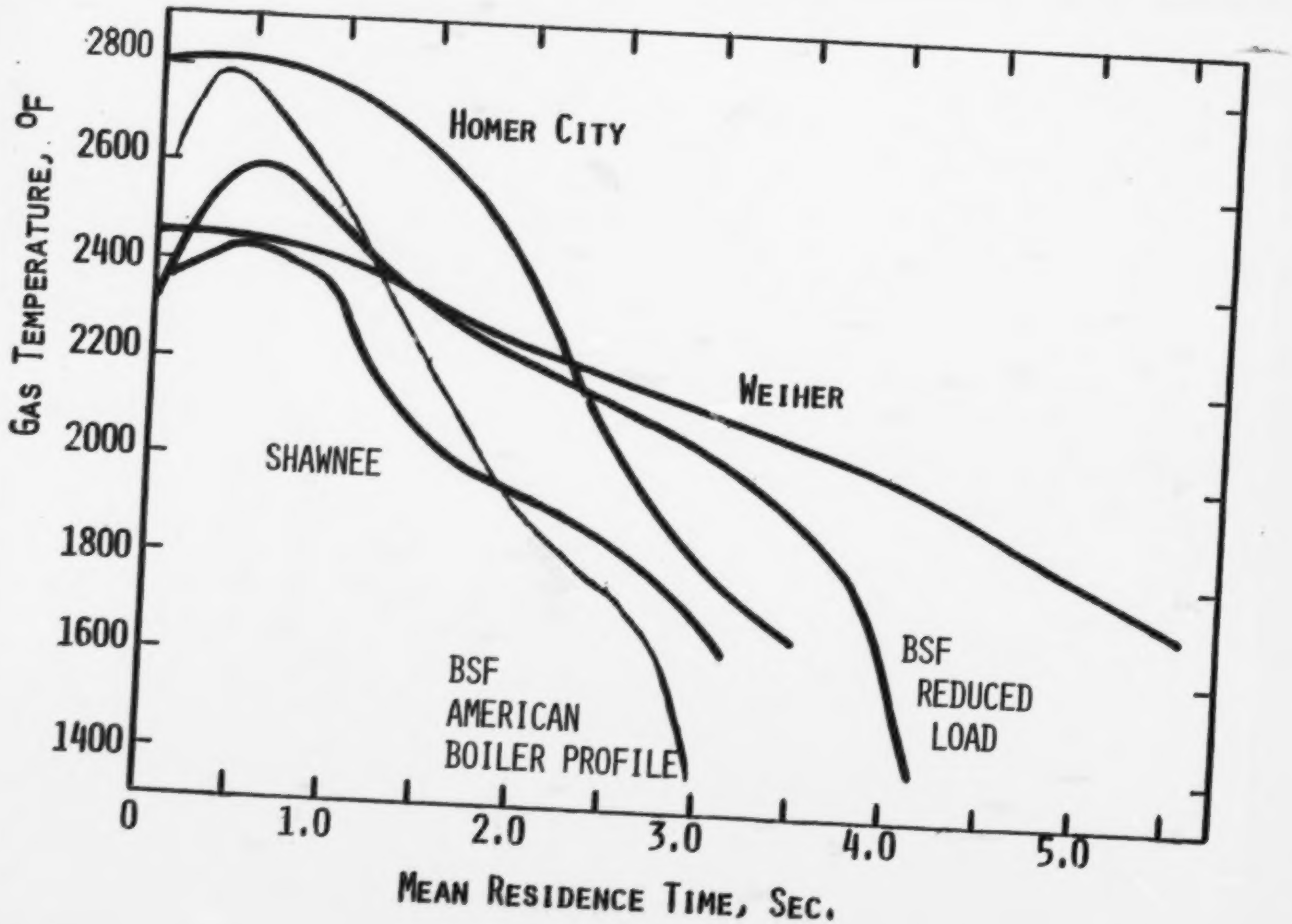

Figure 5-1. Thermal history comparison.

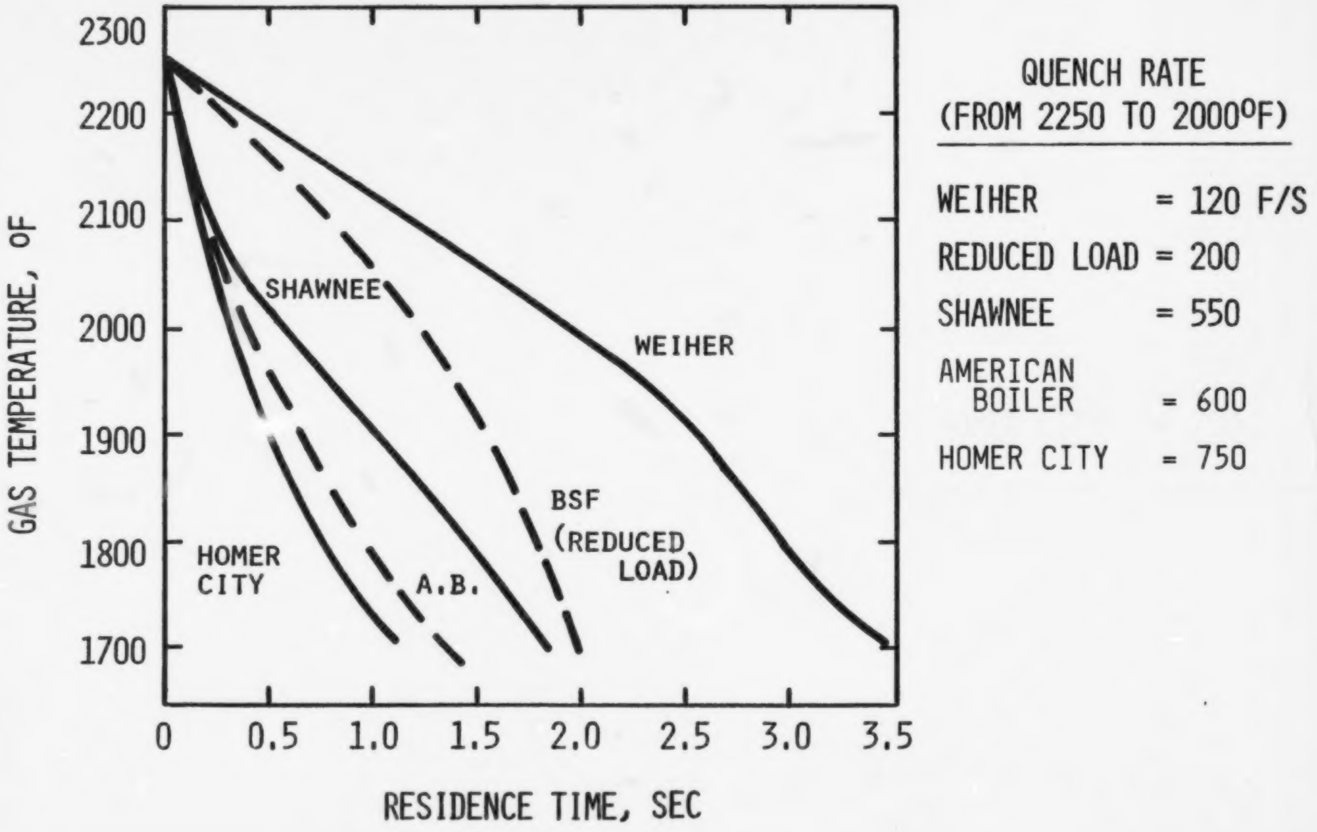

Figure 5-2. Thermal history in the sulfation zone.

5.1.1 Sorbent Comparison

Sorbent composition and other physical properties are probably the most important factors in determining overall capture performance. With all other variables held constant, a wide range of sulfur capture can be produced with different sorbent types. This fact is clearly illustrated in Figure 5-3 which shows that for the reduced load, capture with downstream sorbent injection ranged from 30% for Vicron to over 75% for pressure slaked dolomitic sorbents at a calcium to sulfur ratio 2.0. The range in capture with high temperature injection (with the fuel) was not as broad (20 to 40% at Ca/S = 2.0), because the final surface area was less dependent on the initial sorbent characteristics when the calcination occurred at flame zone temperatures (16). In general the capture results tend to be grouped primarily by general sorbent type. On a calcium molar basis, the three pressure slaked dolomitic sorbents gave the best capture with downstream injection. They were followed by the natural dolomite, the two limes slaked at atmospheric pressure, and finally the Vicron limestone. For injection with the fuel, both the natural dolomite and the pressure slaked dolomite gave the highest capture while the calcitic carbonate (Vicron) and the calcitic hydroxide gave the lowest capture.

Since the sorbents shown in the composite comparison included both calcitic and dolomitic materials, the total mass feed rate can vary substantially for a given Ca/S molar ratio; hence, both the initial sorbent cost and the amount of ash which must ultimately be disposed of are variable. In order to compare the different sorbents on a total mass output basis, the abscissa in Figure 6 was converted to the mass parameter, MgO + CaO divided by the inherent coal ash (assuming a 10% ash coal) as shown in Figure 5-4. Compiling the data on this basis gives an indication of the capture that can be achieved relative to the amount of additional material that must be removed from the particulate collection devices. Even on this basis the dolomitic pressure slaked limes appear extremely attractive as does the Warner hydrate. Again the poorest performance was achieved with the Vicron limestone. These results suggest that capture in excess of 60% can be achieved with approximately a 50% increase in the dry ash handling

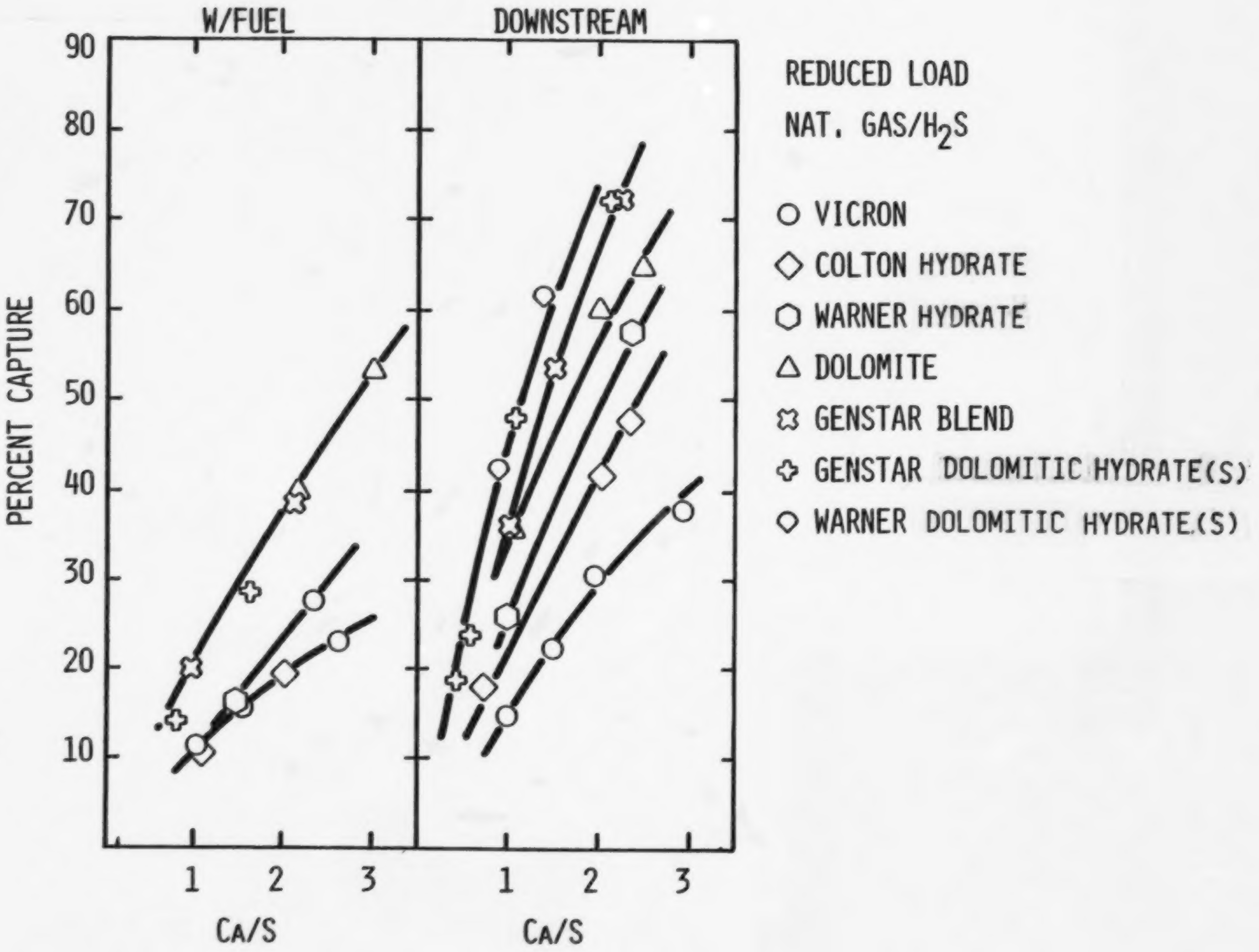

Figure 5-3. Sorbent comparison at reduced load.

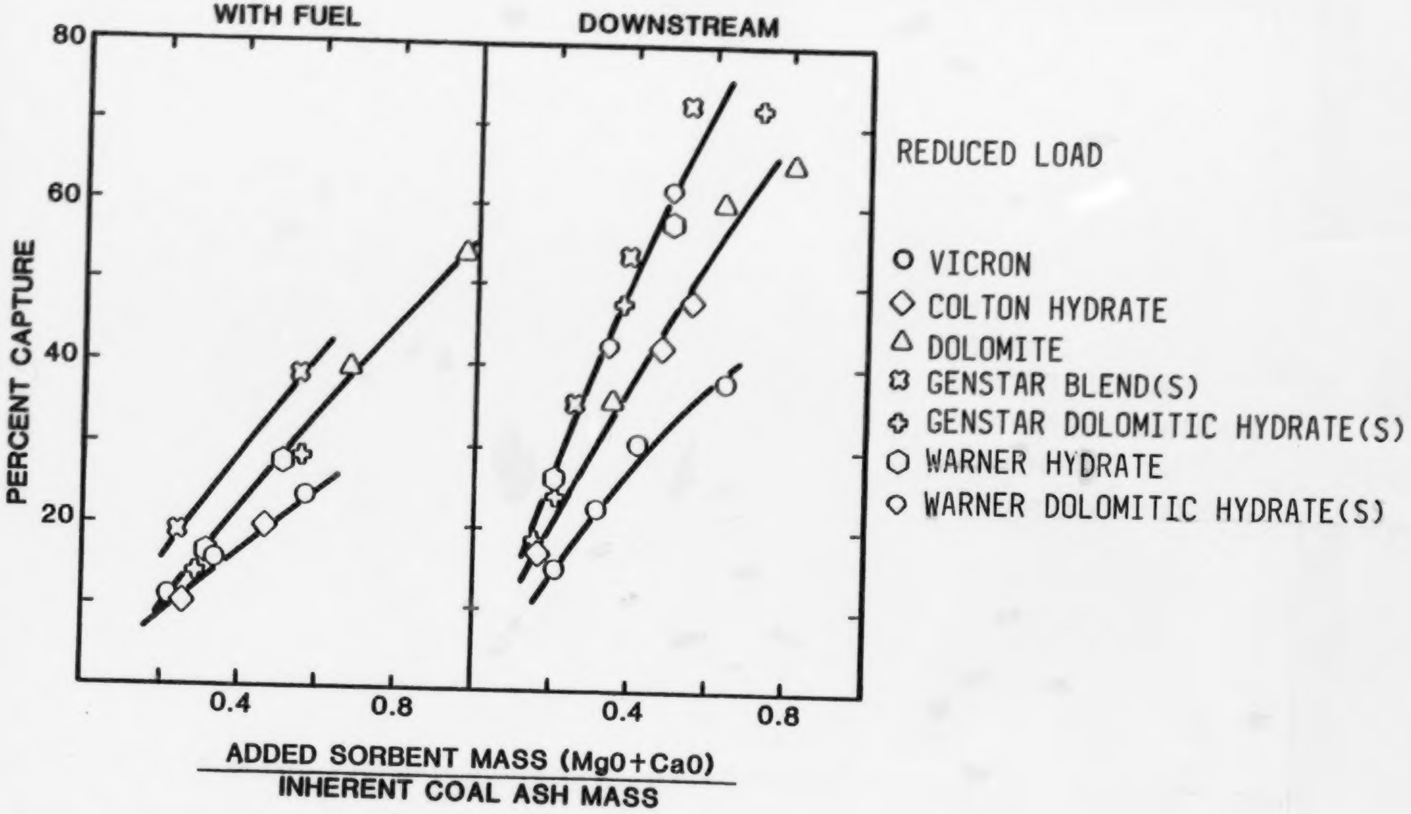

Figure 5-4. Sorbent comparison at reduced load on a mass basis.

requirements (i.e. sorbent addition is like switching from a 10 to a 15% ash coal).

Some of the same sorbents are shown on a calcium basis for the American Boiler profile in Figure 5-5. Although not all of the sorbents were tested, the trends were identical to those obtained with the reduced load. Downstream injection gave better results than fuel injection and the best capture was achieved with the pressure slaked dolomitic sorbent followed by dolomite, the hydroxide, and finally the Vicron. In general, the results with the reduced load were more favorable than those obtained with the American Boiler profile.

5.1.2 Influence of Hydration

The effect of slaking is shown in Figure 5-6 for several calcitic sorbents that were run at the reduced load. The two high calcium sorbents (Colton hydrate and Warner hydrate) are compared against Vicron for both fuel and downstream injection. On the downstream side, both hydroxides produced better capture than the carbonate with the Warner hydrate highest overall. For fuel injection, the effect was smaller with only the Warner hydrate showing a small increase over the Colton and Vicron.

A similar set of data is shown in figure 5-7 for calcitic sorbents run at the American Boiler profile. In this figure, two sorbents slaked at atmospheric pressure (Colton hydrate and Western hydrate) are compared against Vicron for downstream injection. In addition, some of the raw Western lime was pressure slaked at 60 psi and run to determine what effect pressure slaking might have with calcitic materials. The results indicate that the difference between the pressure slaked Western lime and the standard Western hydrate was small. Apparently, pressure slaking did not produce a significant change in either particle size or percent conversion for this particular sorbent. All of the hydroxides showed an increase in capture over the Vicron baseline as was the case with the reduced load.

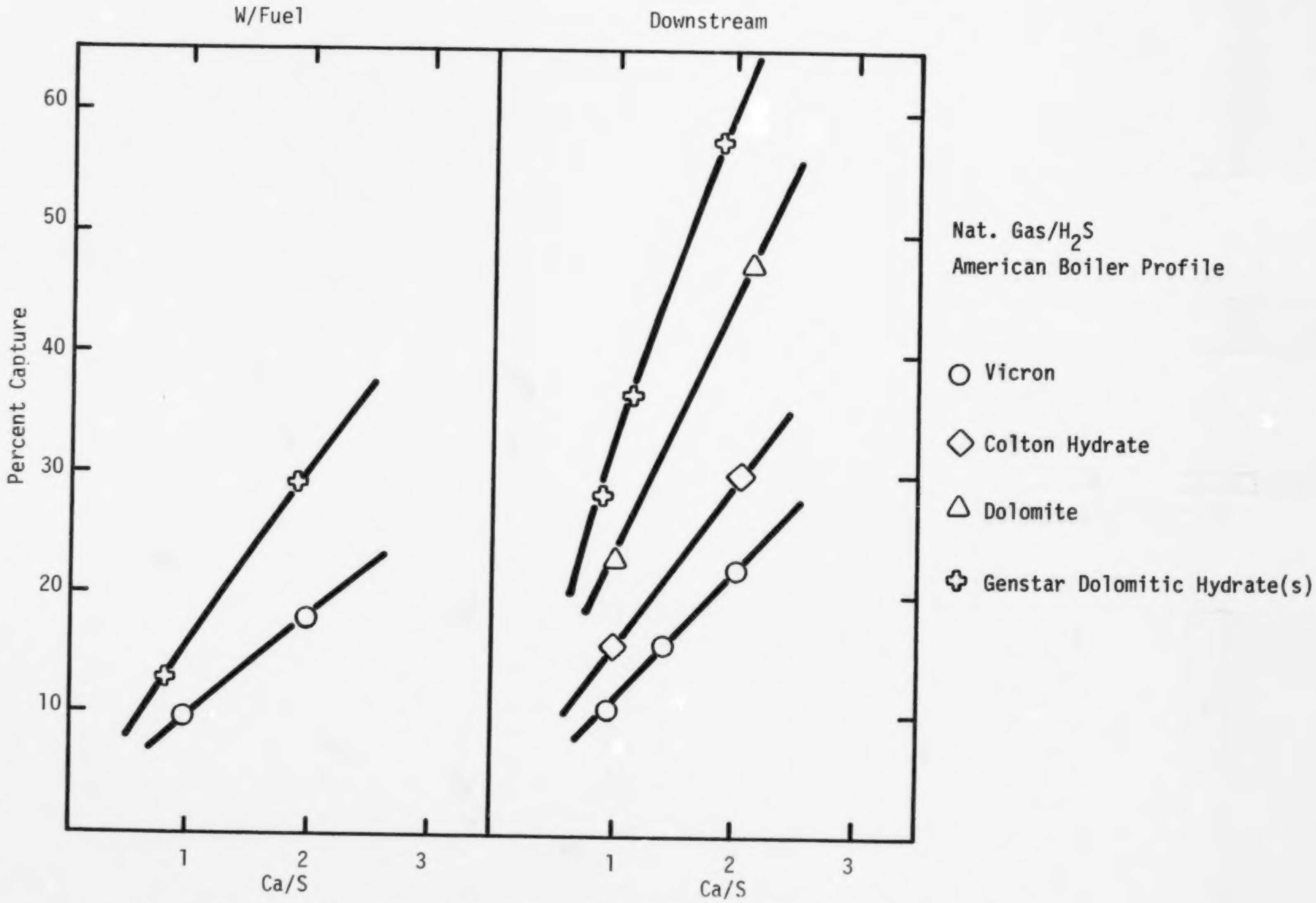

Figure 5-5. Sorbent comparison for American Boiler profile.

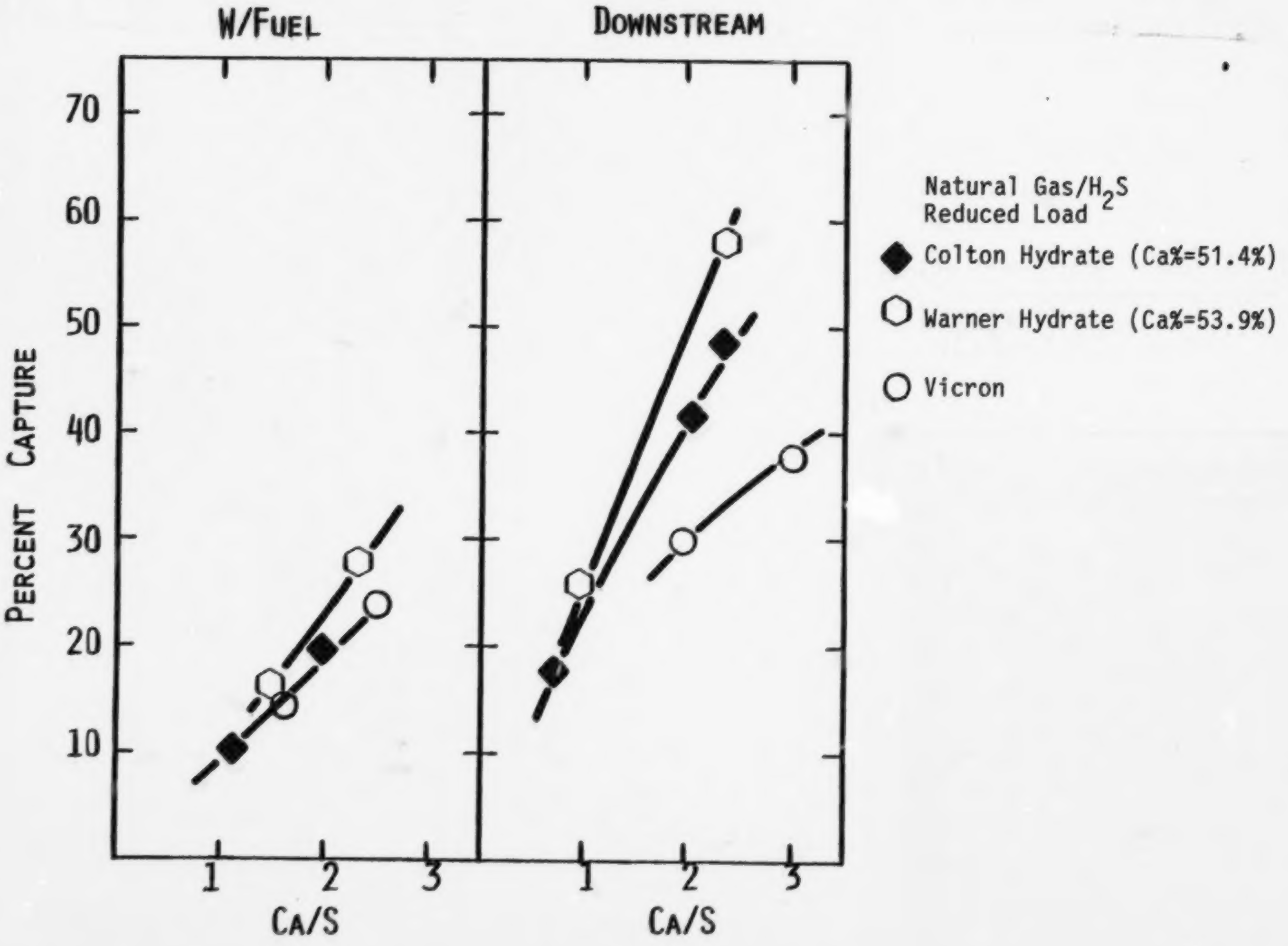

Figure 5-6. Influence of slaking for calcitic sorbents at reduced load.

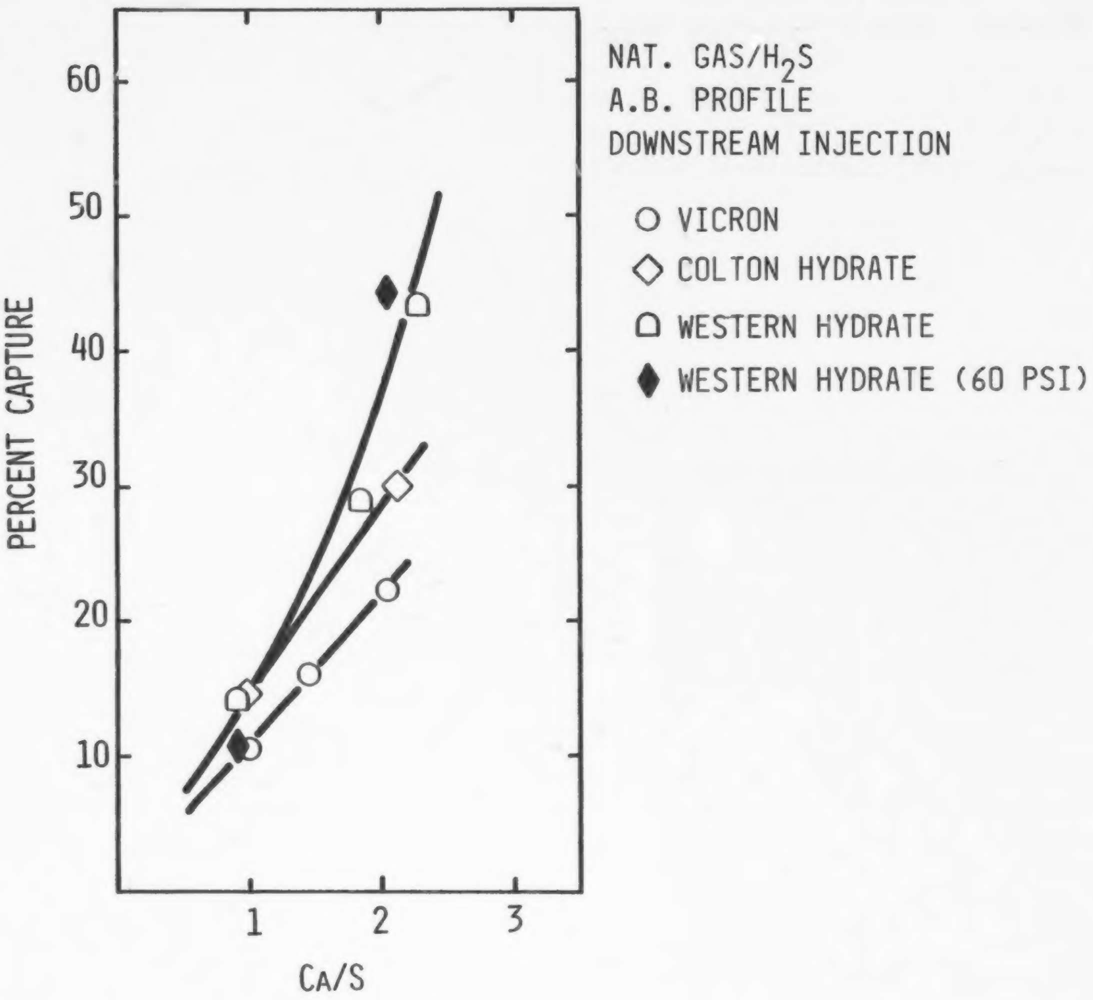

Figure 5-7. Influence of slaking for calcitic materials at American Boiler profile.

The influence of pressure slaking for dolomitic materials is illustrated by Figure 5-8 for downstream injection at two thermal profiles. For each case, type S pressure slaked dolomitic hydroxide were compared against a standard dolomite in the carbonate form. The figure indicates that pressure slaking clearly increased capture for downstream injection. This effect may have been due to a decrease in particle size and the relative reactivity of dolomite in the hydroxide form as compared to the carbonate form.

5.1.3 The Role of Magnesium

Since the results shown in the previous section indicated that dolomitic sorbents were extremely effective in achieving sulfur capture, the role of magnesium was of particular interest. Figure 5-9 shows the influence of magnesium content for several slaked sorbents at two different thermal profiles. As magnesium content increased from near zero to 16 percent, capture increased significantly.

The role of magnesium was examined directly by injecting $MgCO_3$ alone and in a mixture with the Vicron limestone to achieve a "simulated dolomite". The Ca/Mg molar ratio of the mixture was kept the same as the real dolomite and the results from these tests are shown in Figure 5-10. The data from the downstream injection of $MgCO_3$ alone suggest that it does not significantly react with SO_2 to form magnesium sulfate prior to the sampling point (1700^{o}F) which is consistent with both theoretical considerations and previous practical expereince. The simulated dolomite gave esentially identical capture to that measured previously for the Vicron limestone alone; again confirming that $MgSO_4$ formation was not significant. Apparently, the role of magnesium in the dolomitic materials is that of a promoter rather than sorbent since mere physical mixing of the two materials does not yield the high capture produced with dolomite where the magnesium is present as an integral part of the sorbent matrix. It has been previously suggested that the magnesium prevents pore blockage, but the characteristic particle size in the Genstar pressure slaked dolomite is less than one micron and with such small sorbent particles, the pore diffusion resistence is insignificant. A

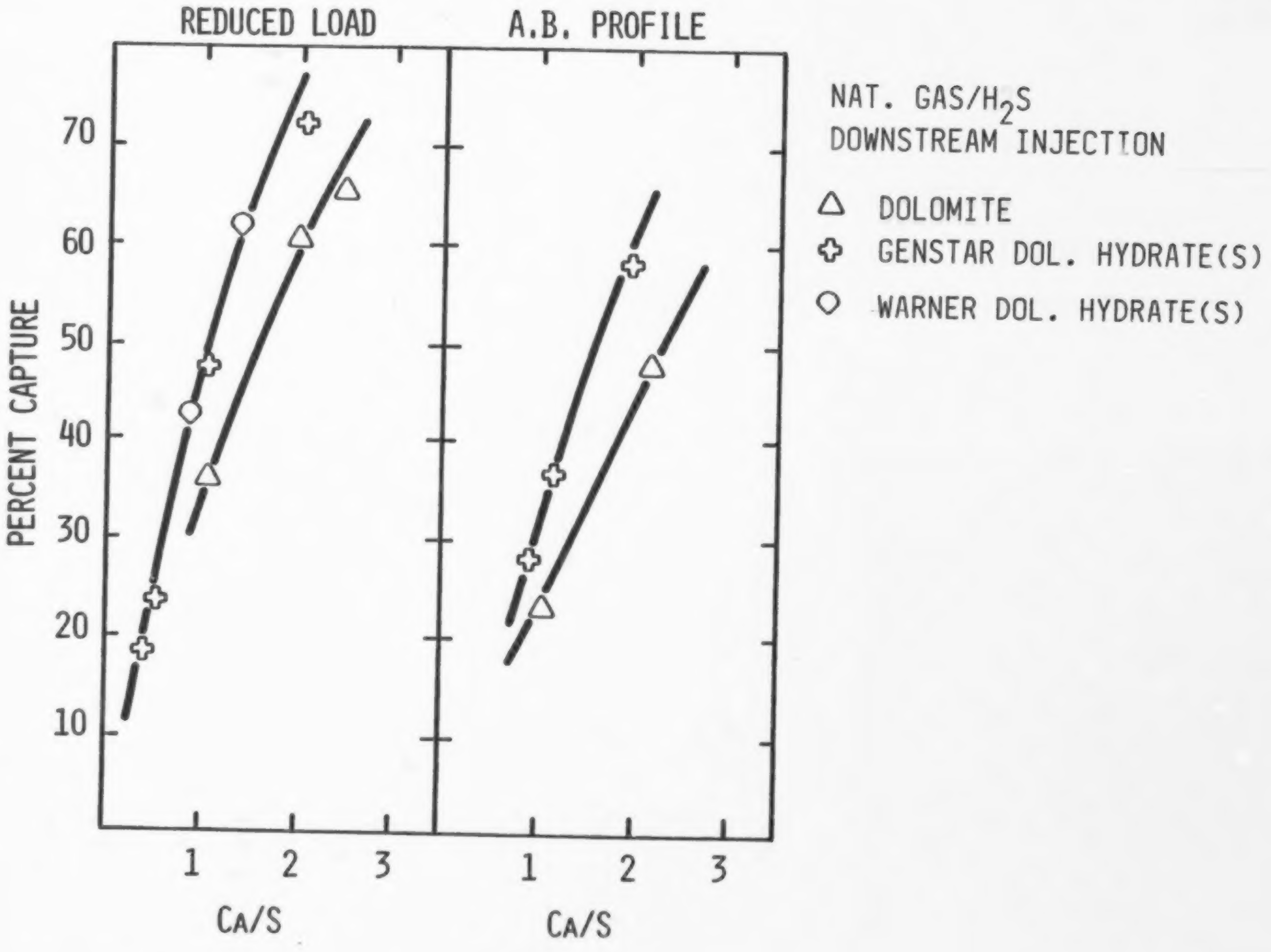

Figure 5-8. Influence of pressure slaking with dolomitic materials.

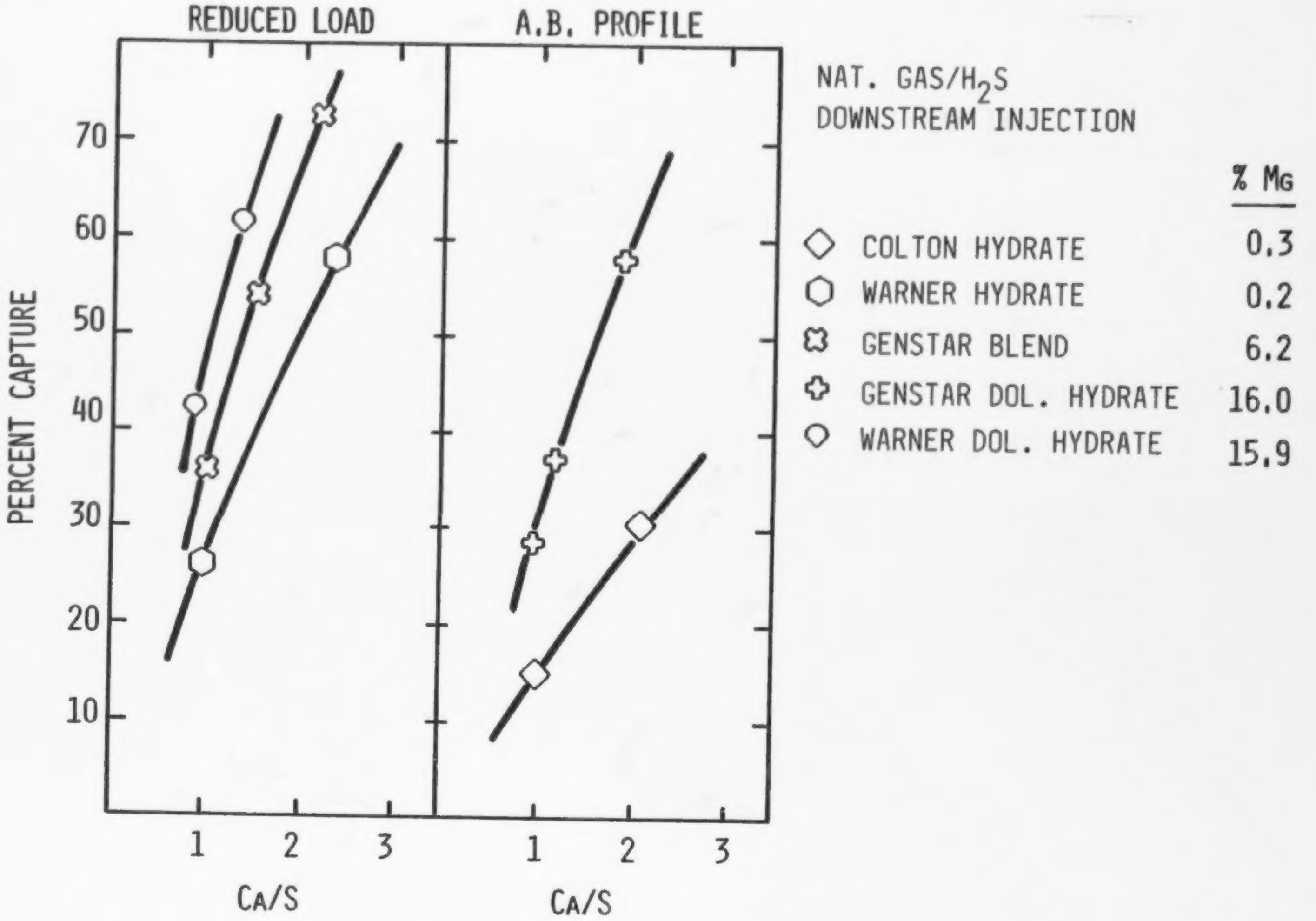

Figure 5-9. Influence of Magnesium content.

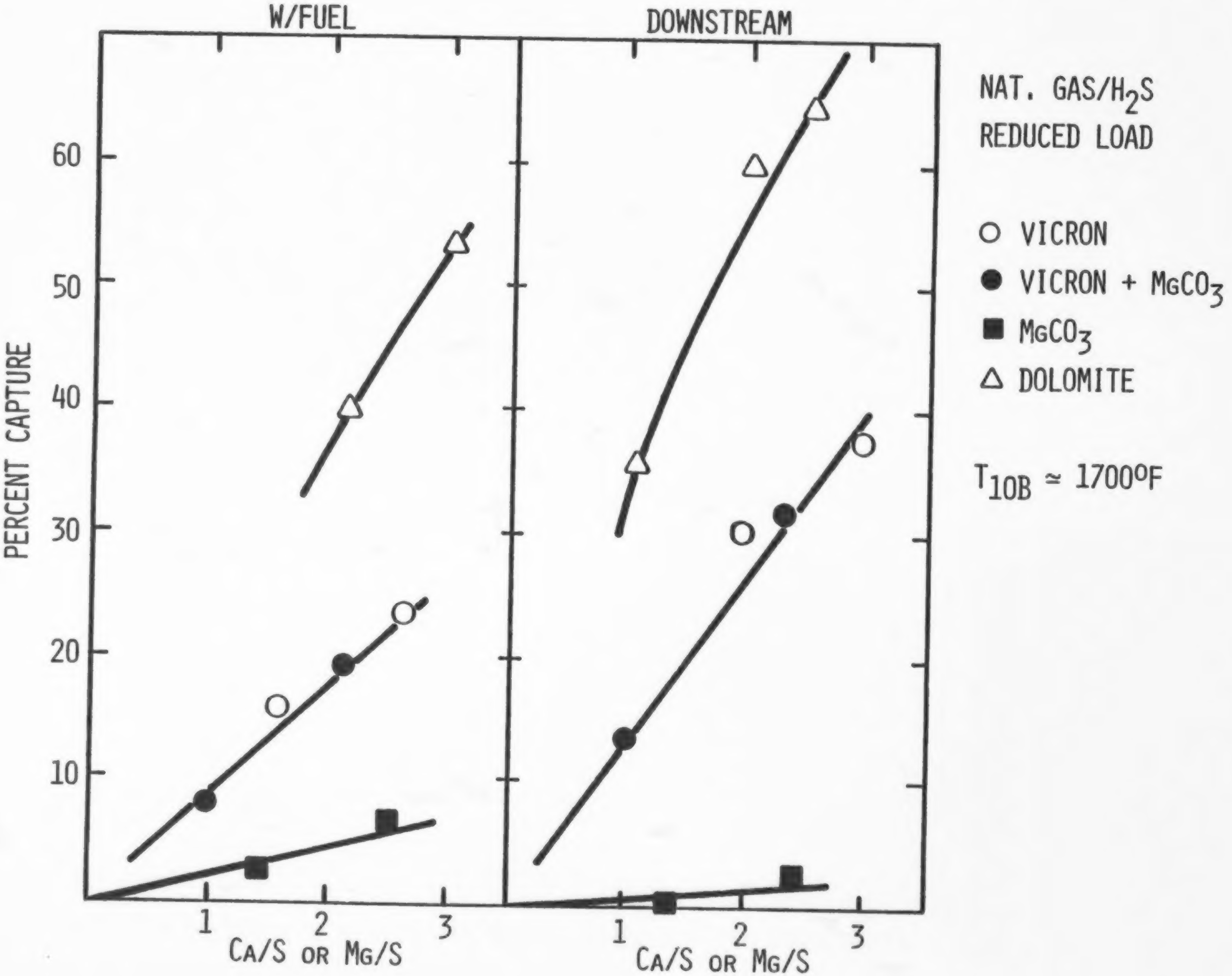

Figure 5-10. Sulfur capture with magnesium.

more likely explanation appears to be that the Mg enhances product layer diffusion and/or initial chemisorption of the sulfur species.

5.1.4 Low Temperature Capture

All of the data presented thus far in this chapter were taken at sampling port 10B where gas temperatures were measured at approximately 1700°F. Beyond port 10B, the flue gas encountered the convective tubes that removed heat from the hot exhaust gases. The presence of many tubes in the flow path allowed sorbent to deposit on the surfaces and increase the effective Ca/S ratio. Thus, exhaust sulfur measurements were not normally taken. In this section however, some low temperature data is presented for purposes of studying the reactions below 1700°F.

Figure 5-11 shows the increase in capture obtained between 1700°F and 400°F for several carbonate type sorbents. Input Ca/S ratio was 2.0 for each test and the open bars represent the capture at port 10B and the shaded bars indicate additional capture to the exhaust. Vicron alone showed little low temperature capture, but the sorbents containing magnesium produced an increase in capture. For downstream injection, $MgCO_3$ showed significant low temperature capture compared with the port 10B results and the dolomite gave the most low temperature capture for injection at the fuel.

Low temperature capture results for the various hydroxide type sorbents are shown in Figure 5-12. For these sorbents, only the Genstar Blend (6.2% Mg) showed significant sulfur capture below 1700°F. Both the hydrates and the dolomitic sorbents showed small increases in capture thus, port 10B was used as the comparison point for all subsequent data because of the uncertainty in Ca/S ratio in the convective section.

In order to compare sorbent reactivity under low temperature conditions, two sorbents (Vicron and Genstar dolomitic) were injected at port 10A at a temperature of approximately 1750°F. Sulfur concentrations were then measured at port 10B and at the exhaust. Port 10B was only 0.2 seconds in residence time from the point of injection. Figure 5-13 shows these results.

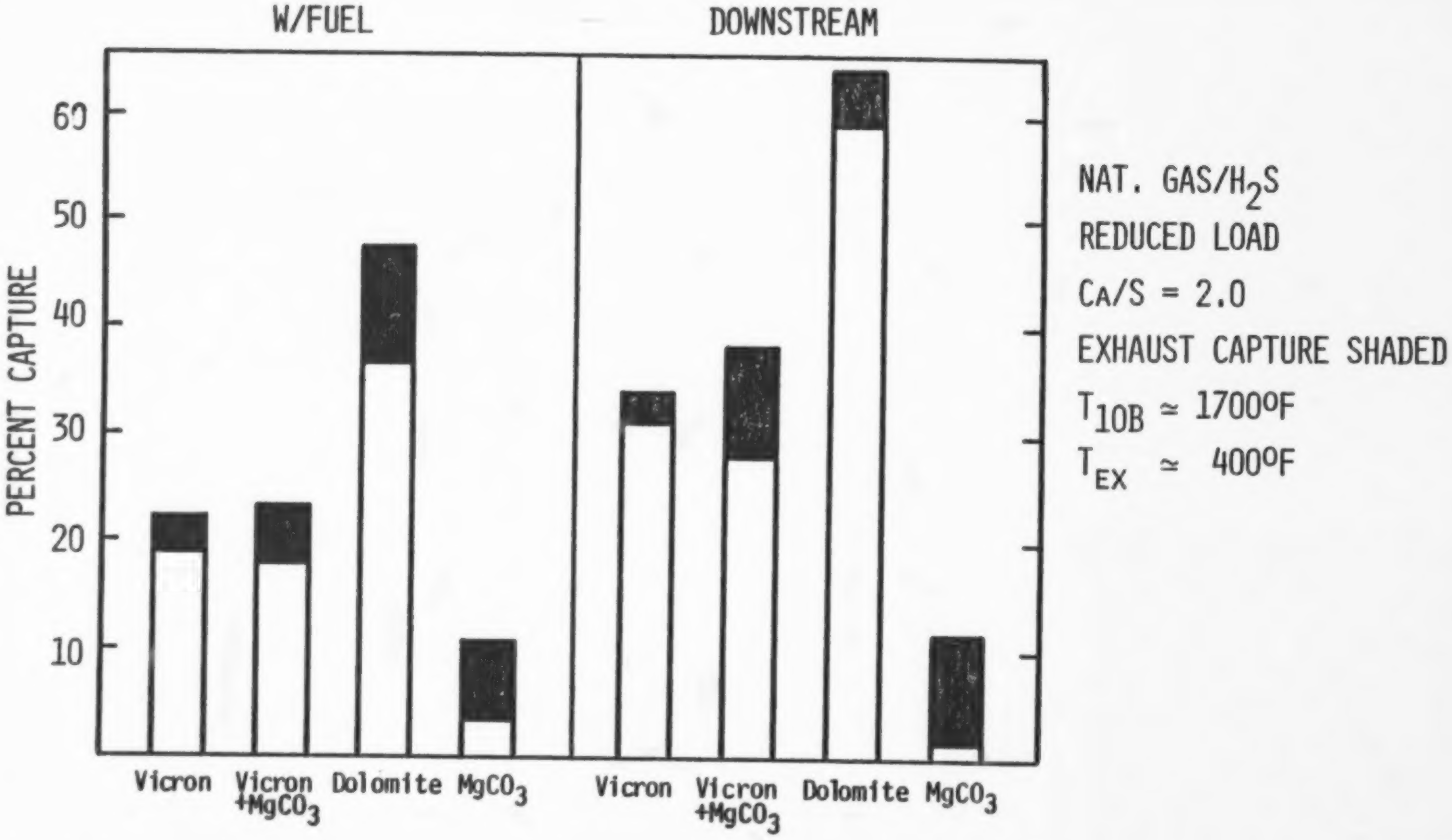

Figure 5-11. Low temperature capture for carbonates.

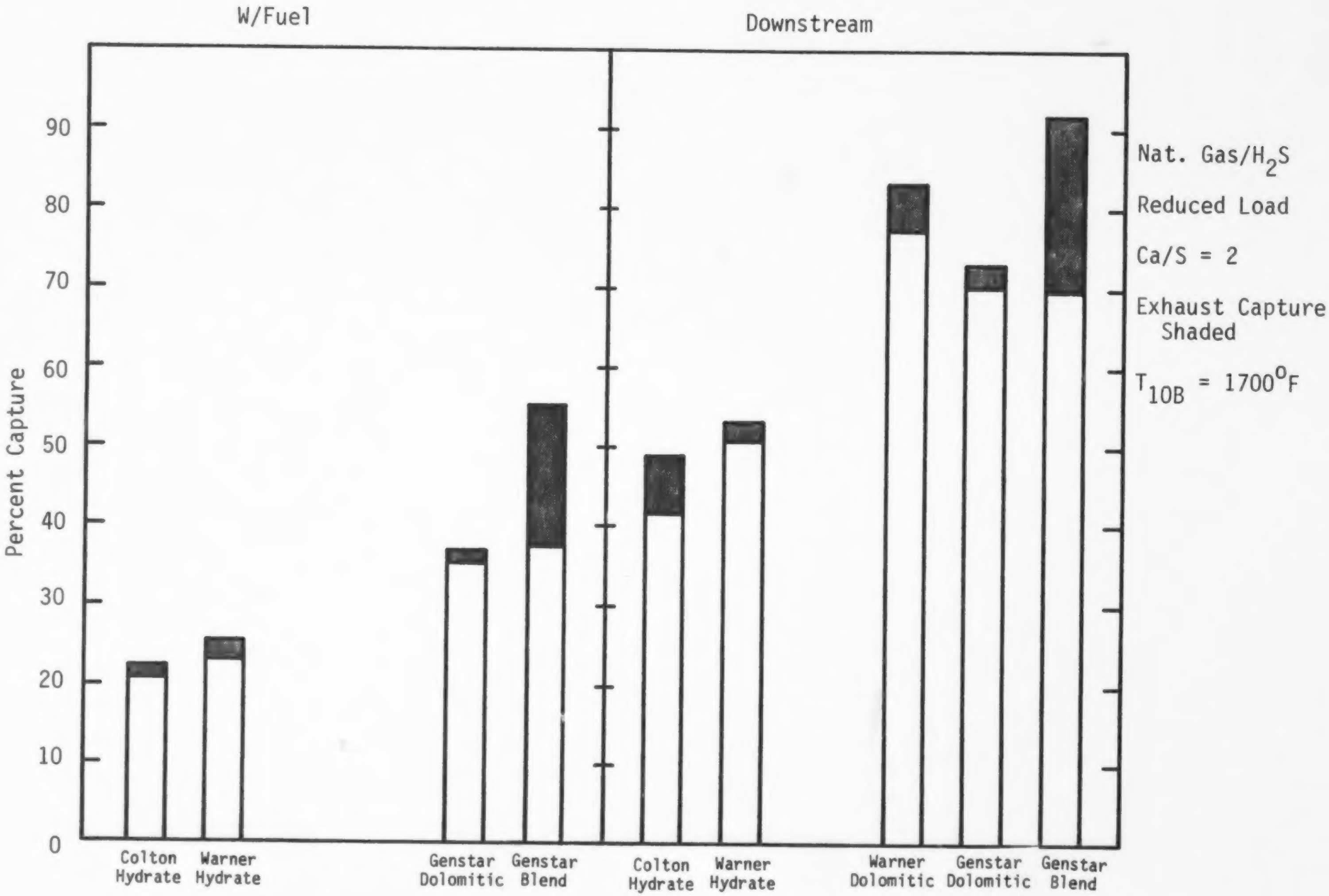

Figure 5-12. Low temperature capture for hydroxides.

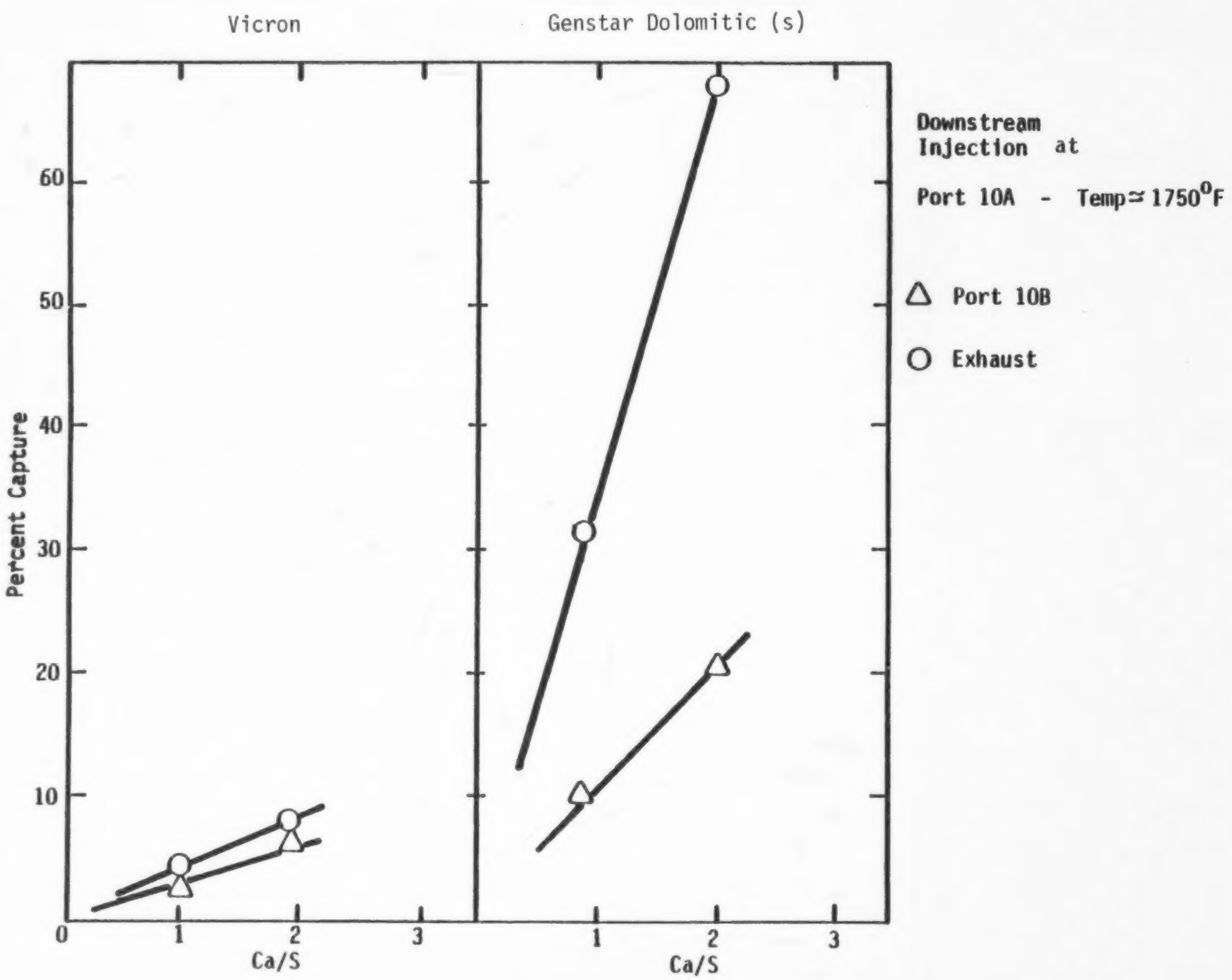

Figure 5-13. Low temperature sorbent injection.

As expected, the Vicron showed very low capture at both sample ports. Captures with the Genstar dolomitic however, were suprisingly high. At a Ca/S of 2.0, the Genstar captured about 20 percent of sulfur in the first 0.2 seconds and almost 70 percent by the exhaust. These results indicate that the Genstar dolomitic is very reactive initially and probably produces a high specific surface area even with low temperature injection.

5.2 Thermal Parameters

The two temperature profiles that were used for most of the data in this report are shown together in Figure 5-14. The American Boiler profile had a peak temperature of about 2800°F and a quench rate through the sulfation zone of 600 °F/sec. The reduced load profile which was obtained at a load of 0.75 MBtu/hr had a lower peak temperature (2600°F) and quench rate (200°F/sec) than the higher load profile. Both curves had approximately the same shape with the main difference due to the amount of mass flow or velocity through the furnace.

5.2.1 Influence of Peak Temperature/Quench Rate

The influence of quench rate is illustrated for four different sorbent types injected downstream at 2250°F in Figure 5-15. For all four sorbent types, capture increased for decreasing quench rate. At a Ca/S ratio of 2.0, the average increase in capture with the lower quench rate was about 35 percent. These results indicate that sulfur capture can be increased significantly by keeping the sorbent particles in the sulfation zone longer.

Figure 5-16 shows a comparison of the combination of peak temperature and quench rate effects for two sorbents injected at the burner. For the Vicron, there was virtually no difference in capture despite the difference in quench rates. The Genstar dolomitic showed only a slight increase in capture with the lower quench rate. These results can be explained in part by the surface area data shown in Figure 5-17. This data, obtained in an isothermal reactor, shows that each of the sorbents reached a maximum surface area when exposed to a temperature of about 1600°F for about 0.5 seconds. At higher

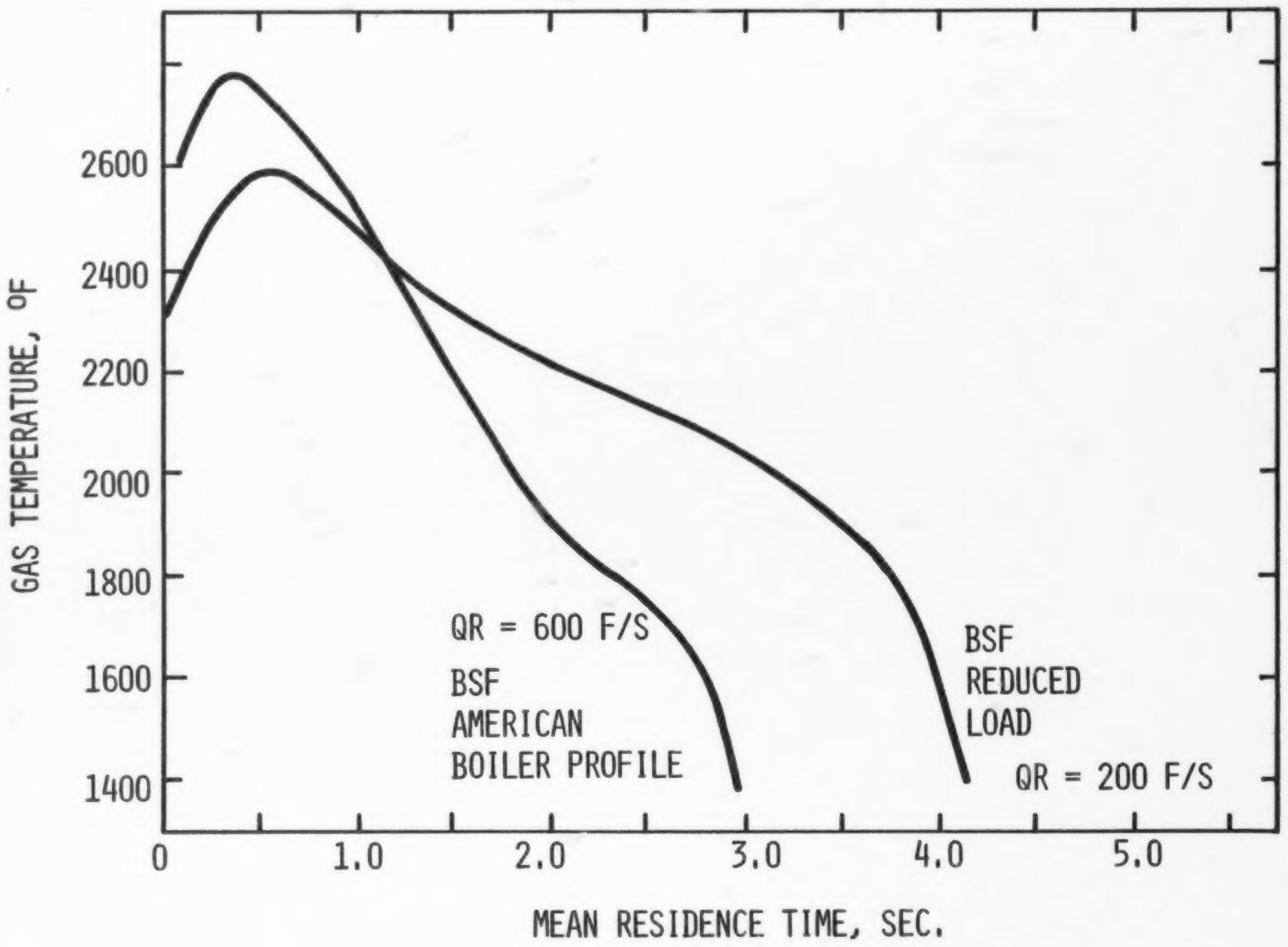

Figure 5-14. Thermal history comparison.

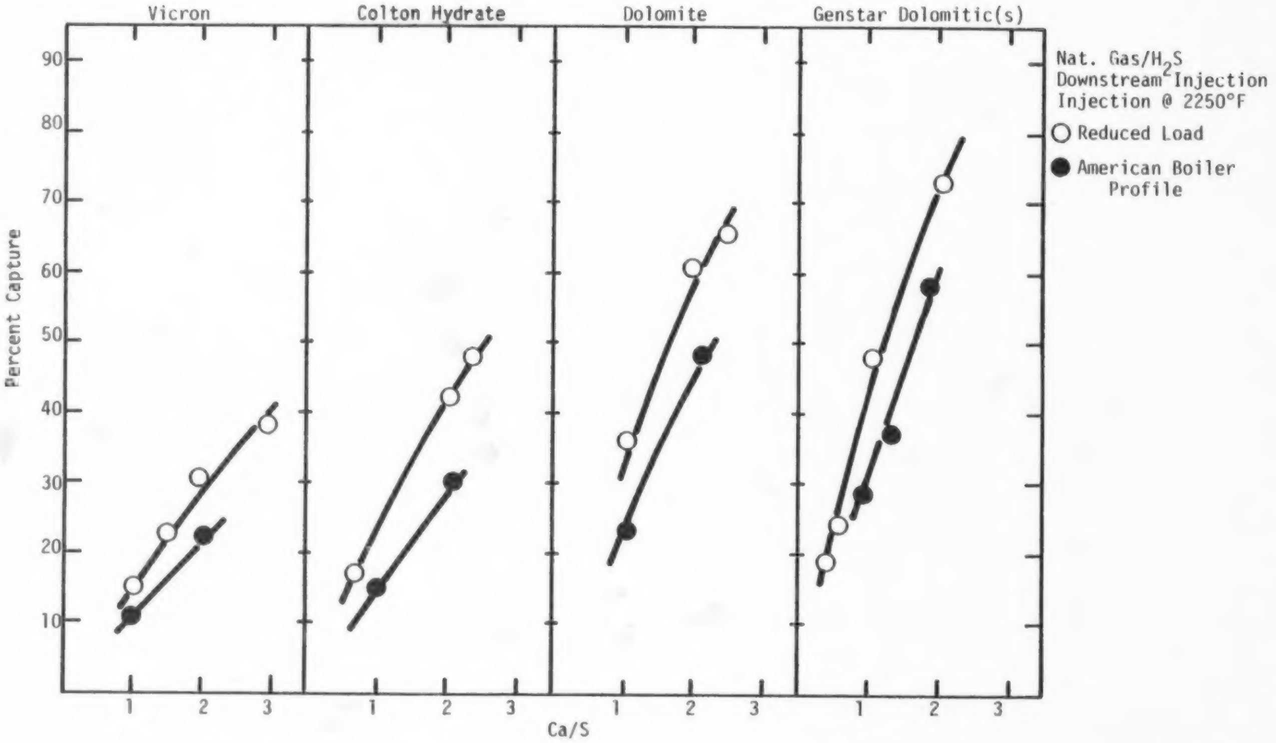

Figure 5-15. Influence of quench rate for downstream injection.

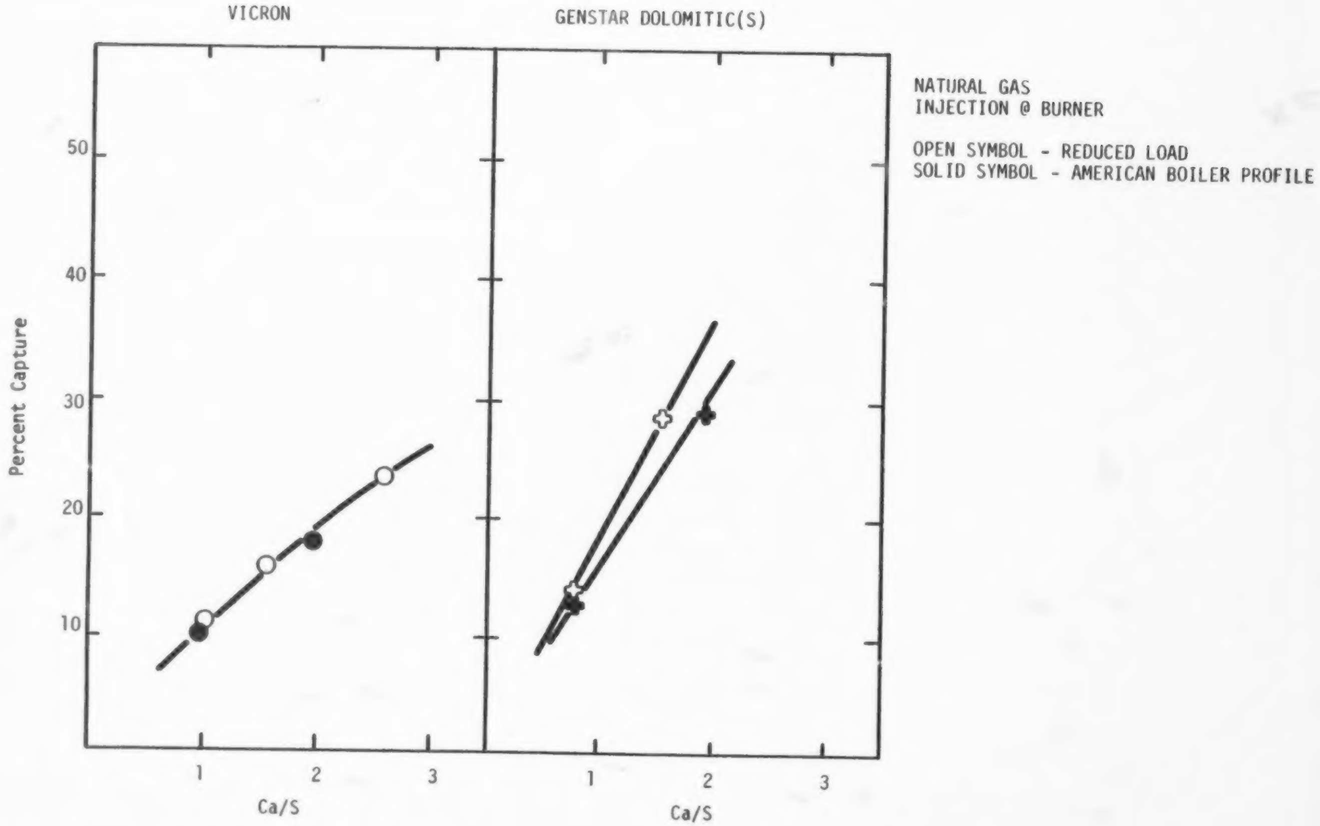

Figure 5-16. Influence of peak temperature/quench rate for burner injection.

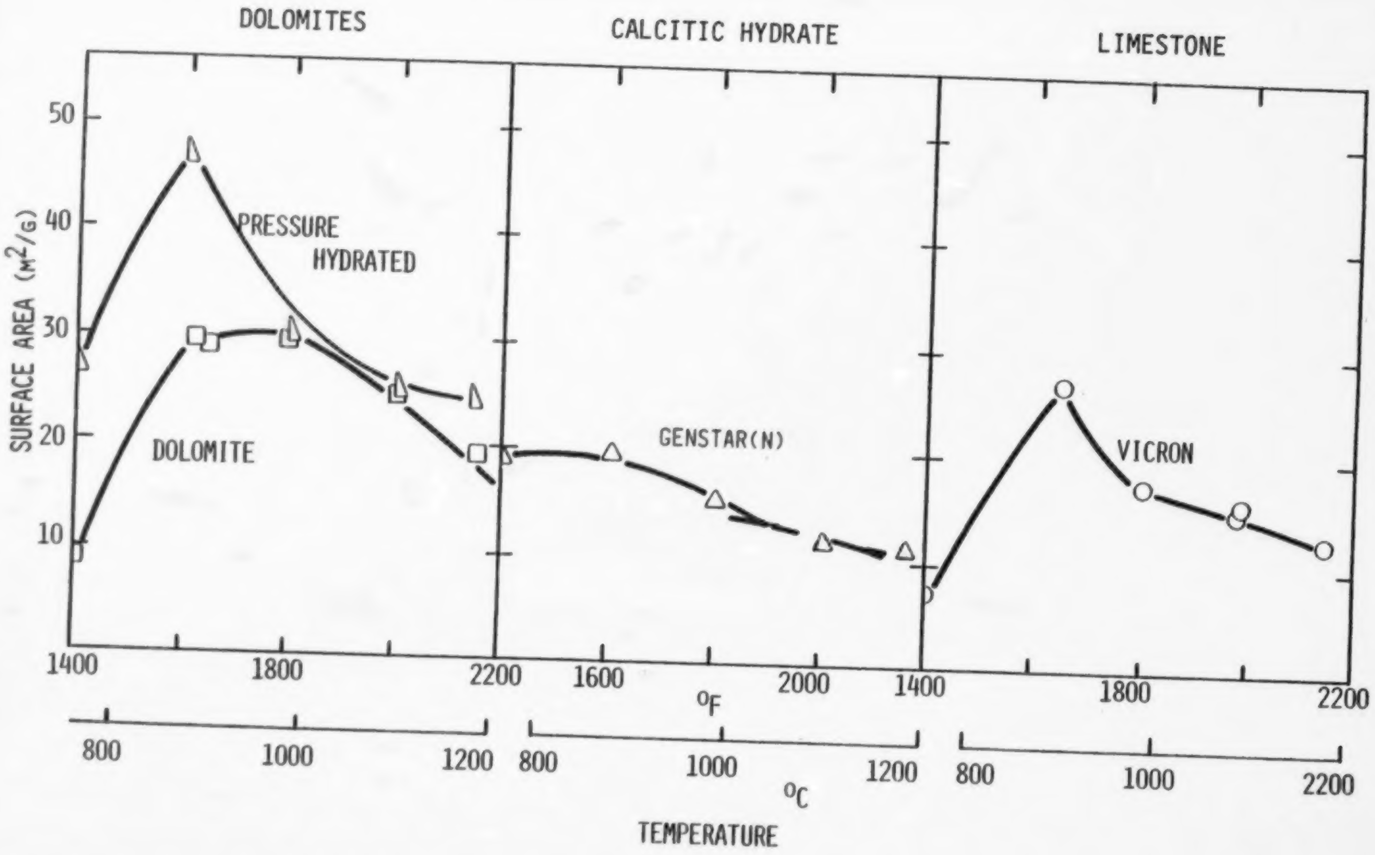

Figure 5-17. Available surface area data.

temperatures, the surface area decreased; primarily due to particle sintering. At injection temperatures of 2600°F and 2800°F, the surface area curves are quite flat and have reached a minimum. Thus, any difference in downstream quench rate has little effect on capture because the dominating parameter is the peak temperature. In this case, surface area is the limiting factor on overall capture and not residence time in the sulfation zone.

5.2.2 Model Predictions

EER's grain model was used to calculate the effect of quench rate for a variety of sorbents injected downstream. Figure 5-18 shows the model predictions for Vicron, Colton hydrate, dolomite, and Genstar dolomitic sorbents, along with the actual data. The surface areas used by the model are also shown in the figure. Overall, agreement between the data and the model was excellent for a broad range of sorbents and quench rates. Figure 5-19 illustrates the fuel injection data presented earlier along with the model predictions. In this case, agreement between the data and model is not as good as the downstream results. The model predicts a difference in capture resulting from the different quench rates while the data shows no effect. Apparently, the processes at work in the flame region are more complicated than those occurring downstream.

5.2.3 Influence of Injection Location

Another thermal parameter that has been known to be important in determining overall sulfur capture is injection location. Figures 5-20 and 5-21 illustrate the effect of injection location for the reduced load and the American Boiler profile, respectively. In every case, downstream injection produced significantly higher capture than burner injection. For the Colton hydrate and the Genstar dolomitic, downstream injection gave double the capture of burner injection. These two figures demonstrate clearly that in order to optimize sulfur capture, the sorbent must be injected downstream of the flame zone.

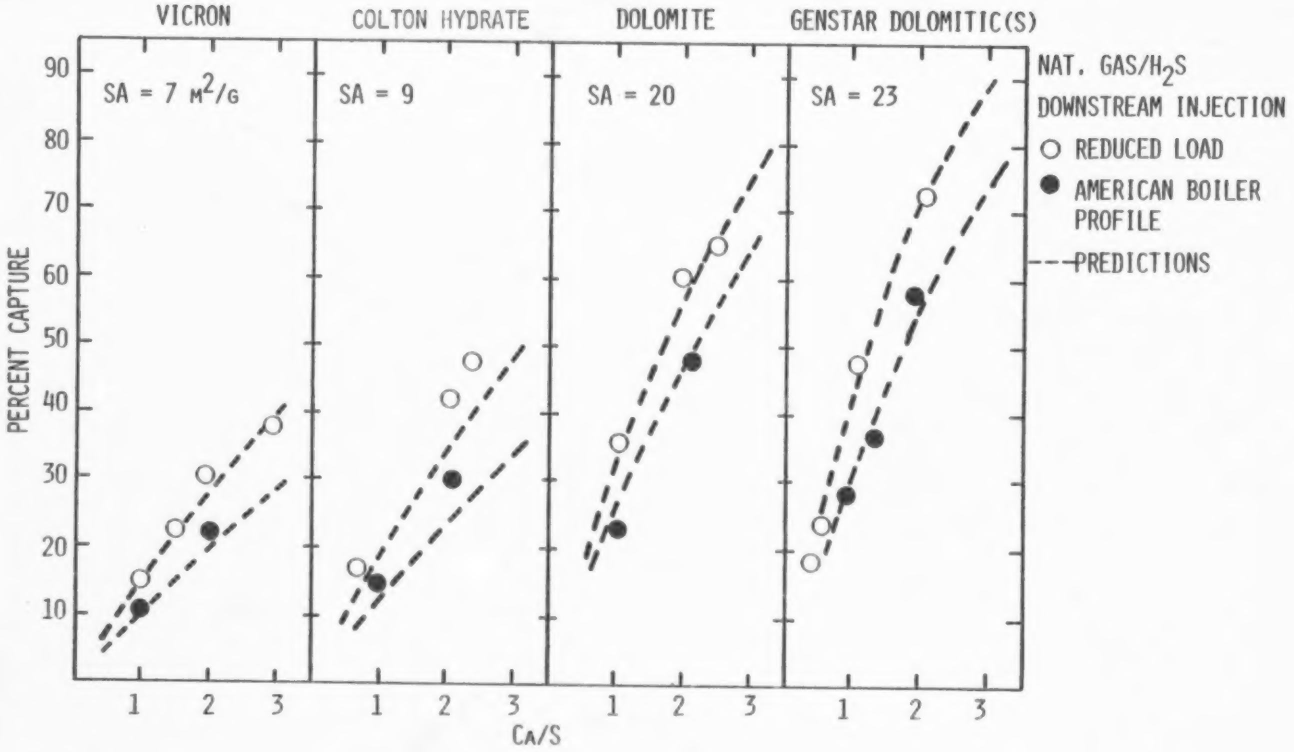

Figure 5-18. Model predictions for variable quench rate.

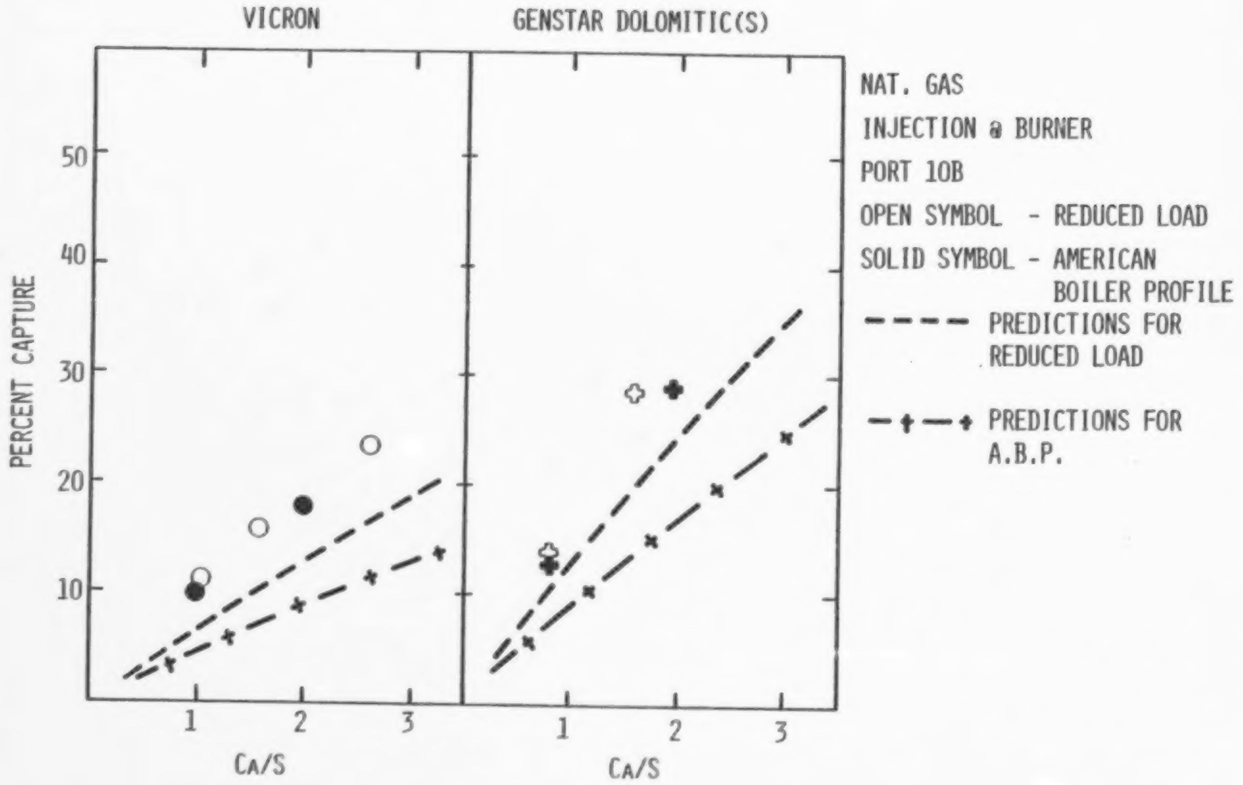

Figure 5-19. Model predictions for burner injection.

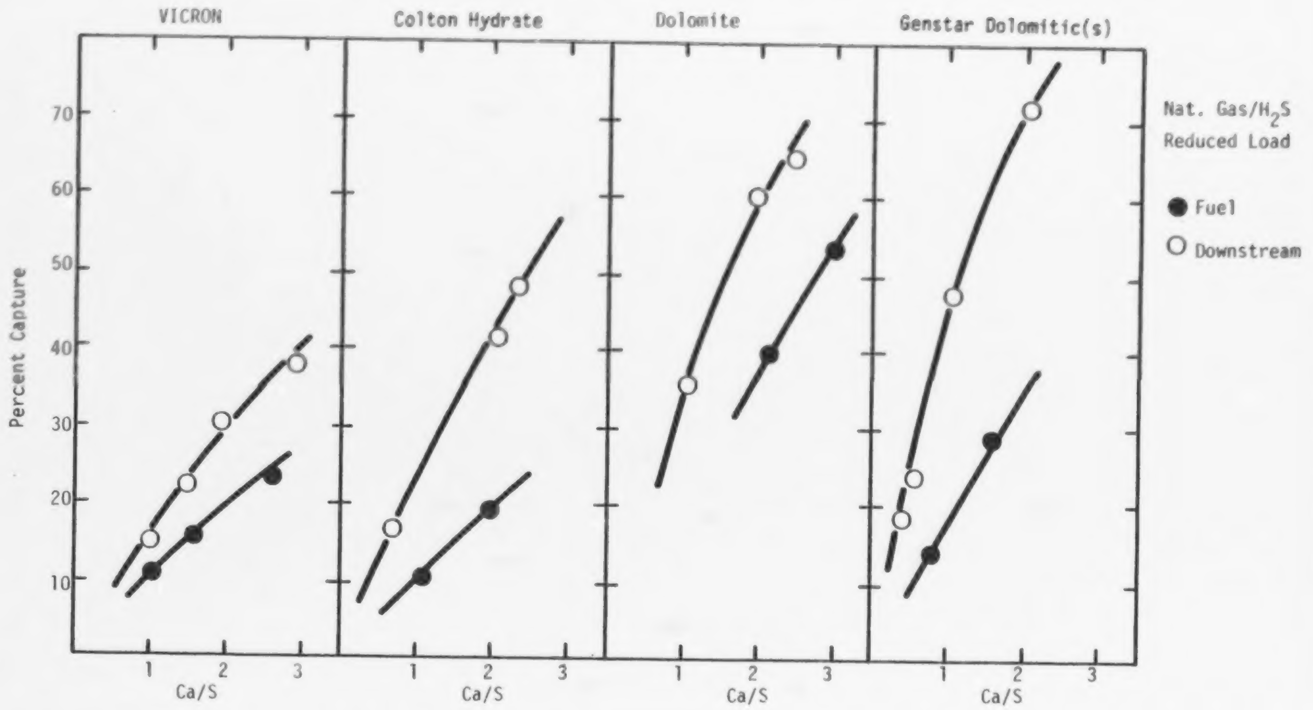

Figure 5-20. Influence of injection location at reduced load.

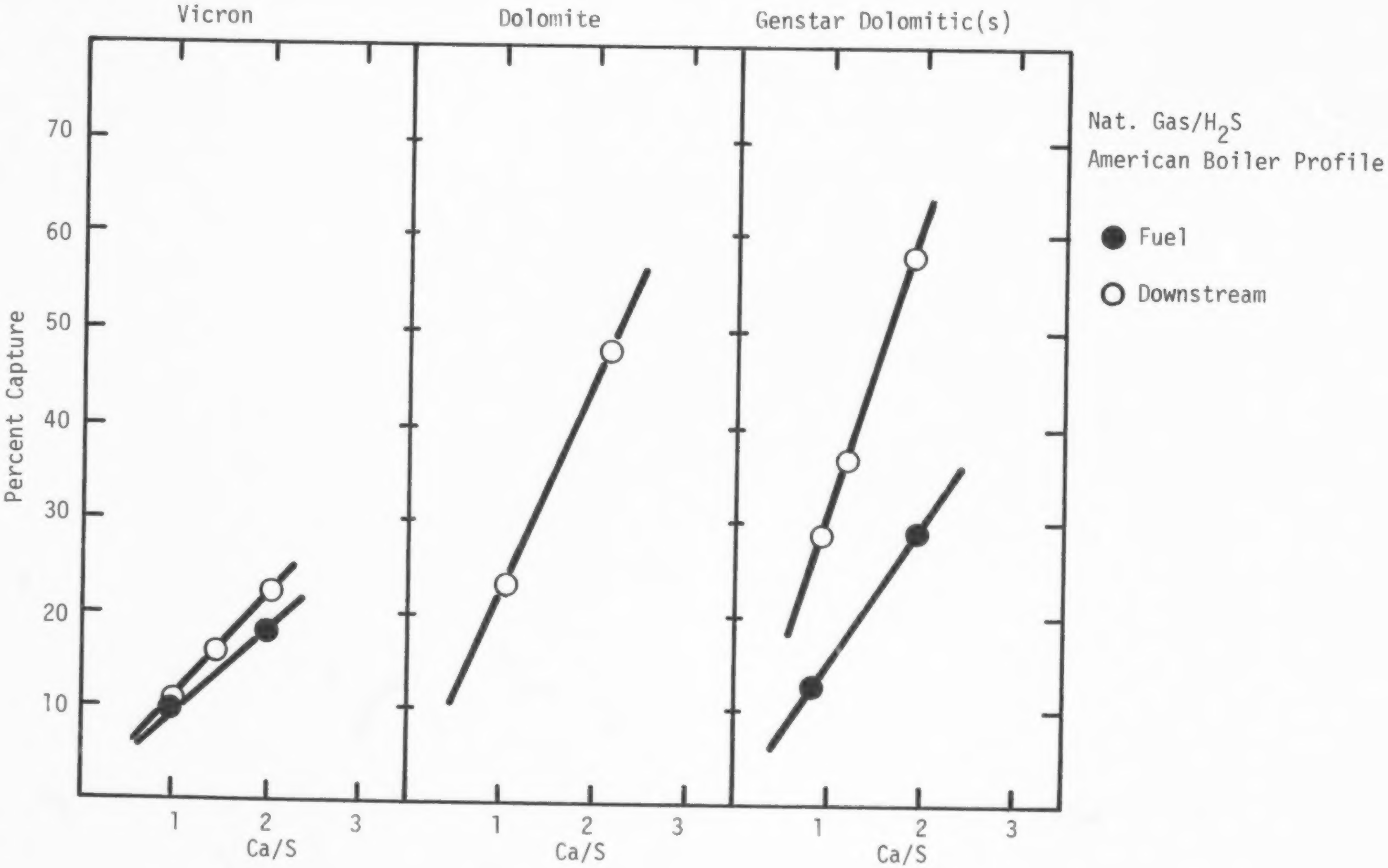

Figure 5-21. Influence of injection location at American Boiler Profile.

5.3 Summary

The results of the sorbent screening studies indicated that the best overall captures were obtained with the pressure slaked dolomitic sorbents which may have been due to a number of factors including particle size, magnesium content, and the initial reactivity of the sorbents. Even on a mass basis, the pressure slaked dolomitic sorbents were the most attractive. Dolomite gave the next best capture followed by the hydroxides and finally the Vicron.

Atmospheric slaking appeared to improve capture for calcitic materials and pressure slaking improved capture for the dolomitic materials. Pressure slaking had little effect for the one calcitic sorbent tested and magnesium content appeared to influence overall capture only when incorporated in the sorbent matrix. Magnesium carbonate alone as a sorbent gave poor capture results, however, magnesium did show some low temperature capture. The mechanism for the magnesium enhancement effect is uncertain but a probable explanation is that the magnesium enhances the product layer diffusion or the initial chemisorption of the sulfur species.

The thermal parameters studies indicated that for downstream injection, capture decreased with increasing quench rate which was predicted quite well by the model. For burner injection, captures were similar for both profiles and agreement with the model was not as good. As expected, downstream injection produced significantly higher captures for all types of sorbents than for burner injection. This effect was primarily due to the initial calcination environment the sorbent was exposed to and the resulting specific surface area.

6.0 EVALUATION OF MINERAL INTERACTIONS

The previous chapter dealt with capture optimization for a variety of sorbents and thermal conditions in natural gas flames. This chapter discusses capture data obtained with many of the same sorbents and thermal conditions for coal flames. Comparisons are made between coal and gas for a variety of injection schemes, and the results of the additive screening for both gas and coal are presented. Some of the mechanistic parameters of capture enhancement are also examined at the conclusion of this chapter.

6.1 Capture with Coal

6.1.1 Sorbent Comparison

Indiana #3 coal was used as the baseline fuel for all of the coal data presented in this chapter. This fuel was chosen primarily because of the existing data base from earlier BSF programs. The two thermal configurations that were used for most of the coal data were identical to the natural gas profiles; specifically, the reduced load (0.75 MBtu/hr) and the "American Boiler" profile (1.0 MBtu/hr).

Figure 6-1 shows the sorbent comparison for coal at reduced load. Included in the figure are two additives that appeared promising from the additive screening studies (see Section 6.3.3). For downstream injection at 2250^{O}F, the highest captures were obtained with the two dolomitic type S sorbents. The Warner lime gave the next best capture followed by the Vicron plus Cr_2O_3, and finally the Vicron plus Na_2CO_3 and Vicron alone. For injection at the burner, Vicron plus Cr_2O_3 produced the best results of those sorbents studied, followed by the Warner lime, Vicron plus Na_2CO_3, and Vicron which were all grouped together. In general, the sorbent ranking was about the same for coal as with gas. Figure 6-2 shows a similar sorbent comparison for the American Boiler profile for two injection locations. Again, for downstream injection, the type S dolomitic sorbents gave the best results and, in this case, were the only sorbents to achieve the EPA goal of at least 50 percent capture at a Ca/S ratio of 2.0. The standard dolomite nearly met

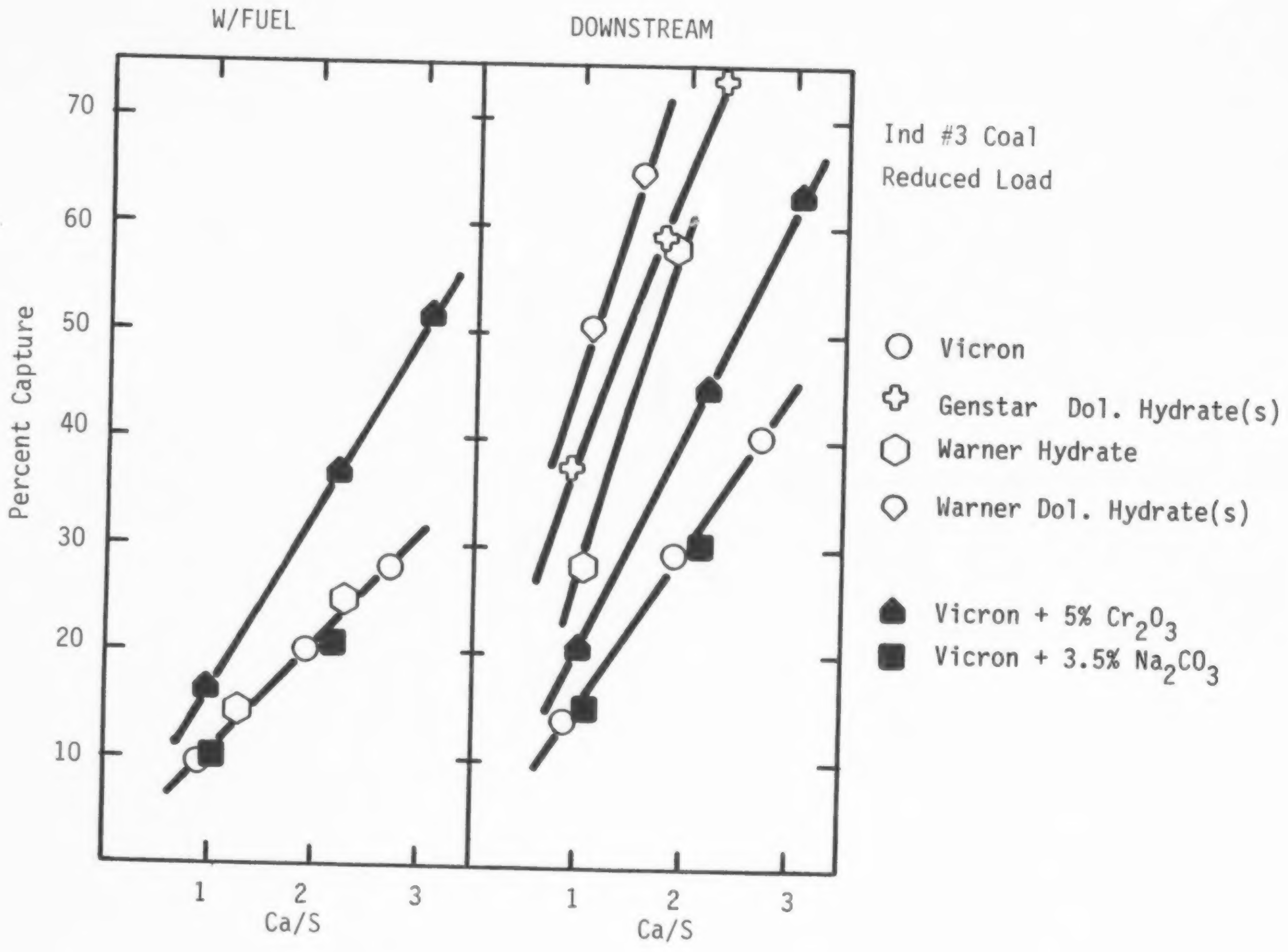

Figure 6-1. Sorbent comparison with coal at reduced load.

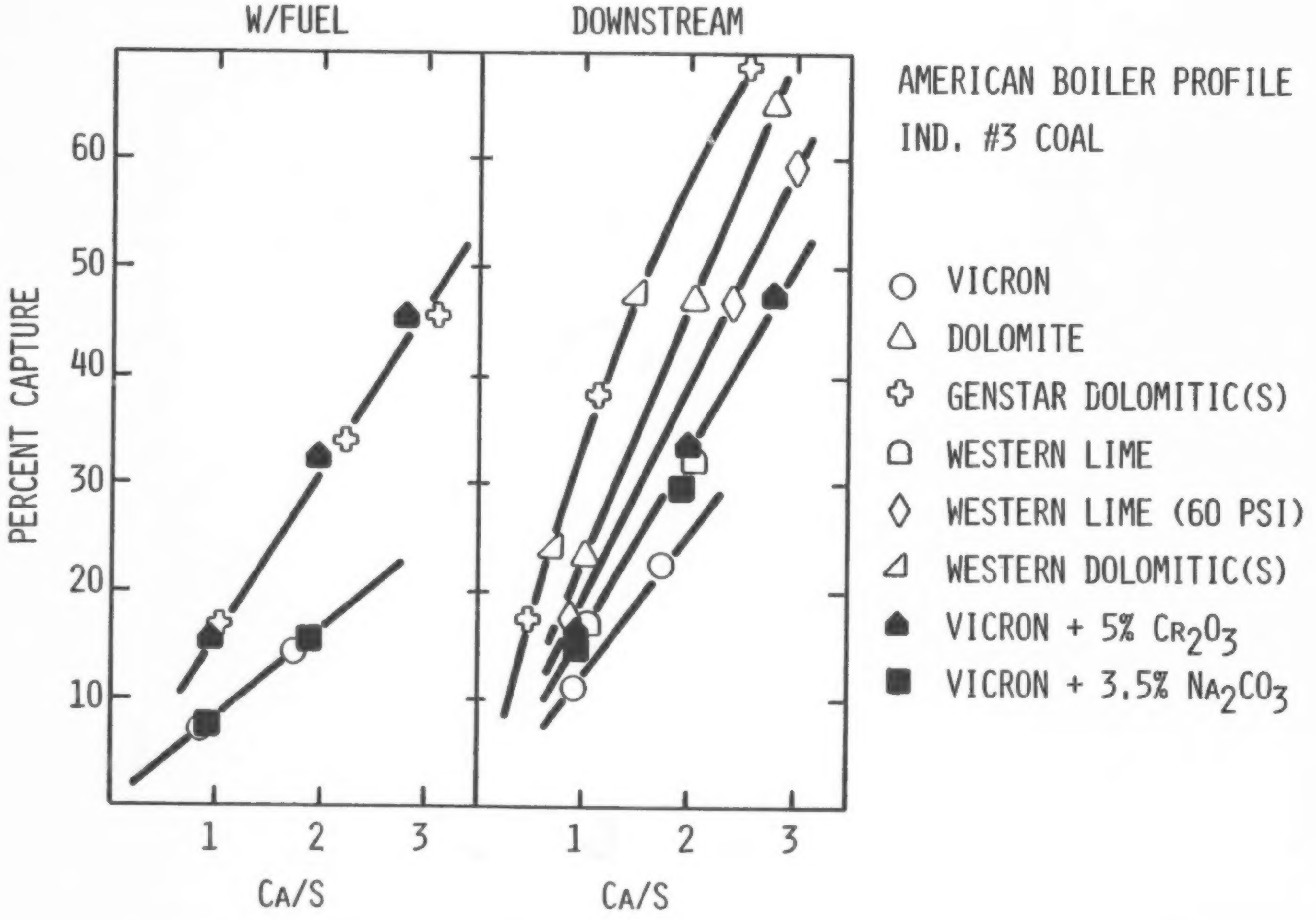

Figure 6-2. Sorbent comparison with coal for American Boiler profile.

the goal and was followed by the limes and the additives. For burner injection, the Genstar dolomitic and the Vicron plus Cr_2O_3, both achieved captures in excess of 30 percent at a Ca/S ratio of 2.0 as compared with a Vicron baseline of about 14 percent. Since the "American Boiler" profile is typical of many utility boilers, the results in Figure 6-2 should indicate achievable captures on real boilers.

6.1.2 Influence of Injection Location

Figures 6-3 and 6-4 illustrate the effect of injection location on capture for several sorbents. For both profiles, downstream injection was clearly better than burner injection regardless of sorbent type. These results were identical to the gas data shown in Chapter 5.0.

6.1.3 Influence of Thermal History

In order to determine the influence of time/temperature history, several sorbents were run with coal at both temperature profiles as shown in Figure 6-5. Vicron was injected downstream and at the burner and Genstar dolomitic was injected at the downstream location. For each set of data, the reduced load profile produced slightly better capture than the high quench rate American Boiler profile.

Thus far, all of the sorbent and thermal parameters studied with coal flames have generated the same results as with natural gas flames. Downstream injection was significantly better than fuel injection and captures decreased with increasing quench rate in the sulfation zone. The best overall captures for both gas and coal were obtained with the pressure hydrated dolomitic sorbents and the worst were obtained with Vicron. Evidently, sulfur capture for both fuels is similar with respect to the various thermal parameters.

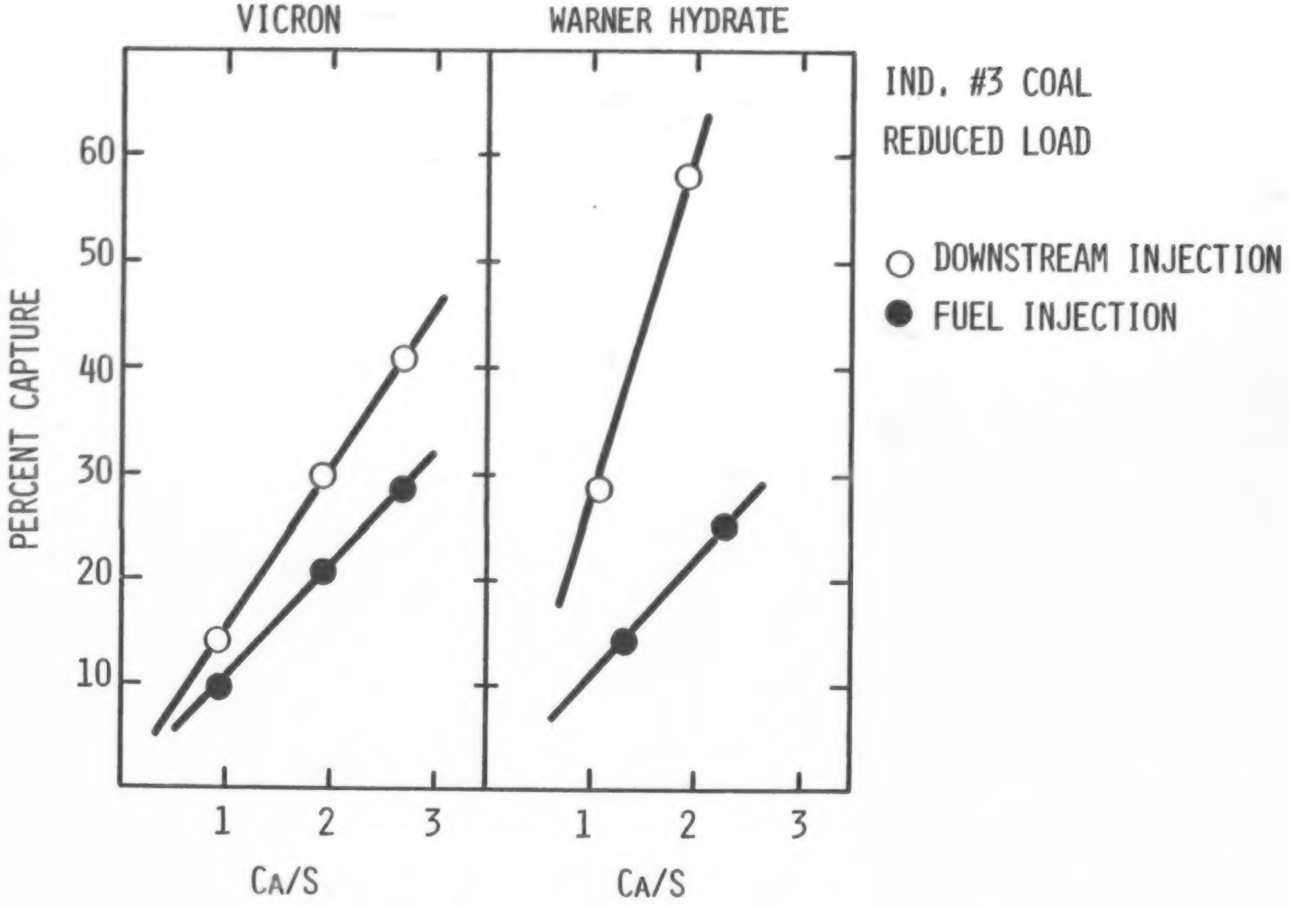

Figure 6-3. Influence of injection location at reduced load.

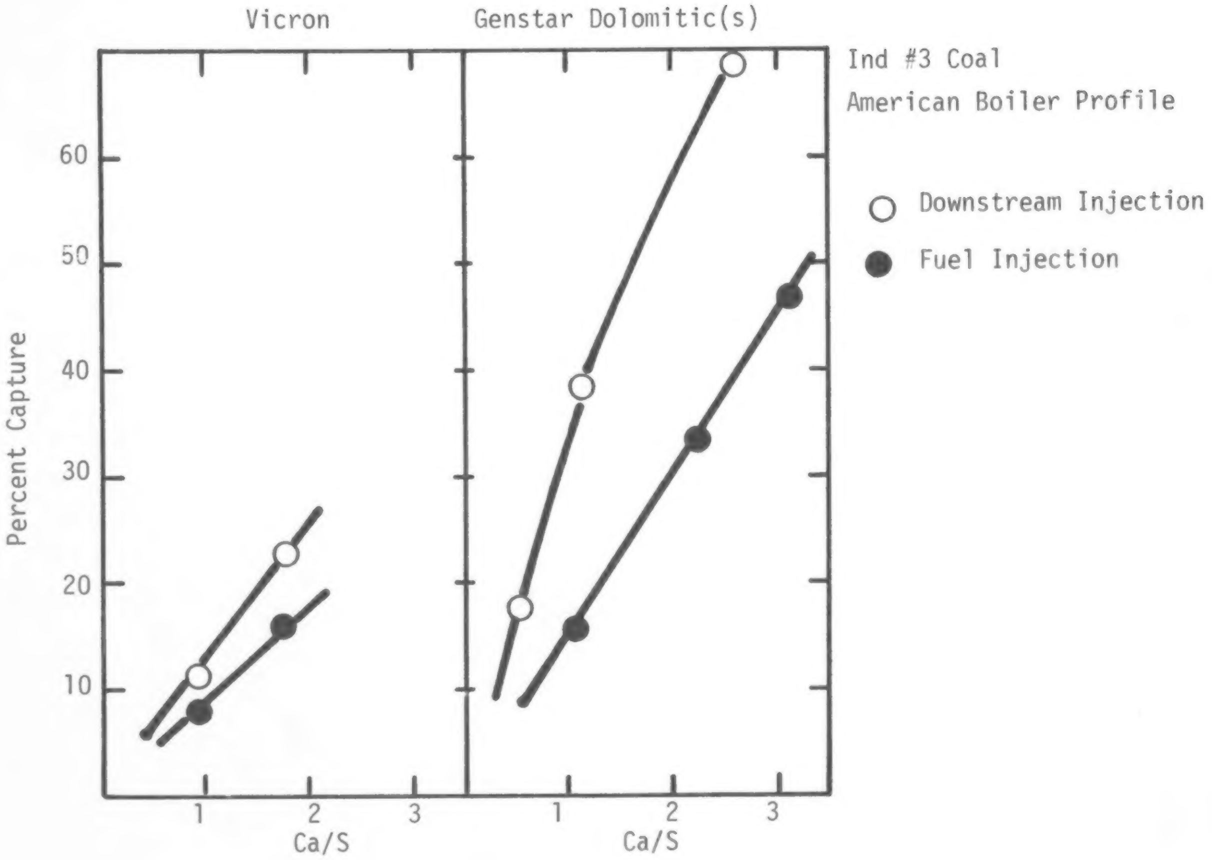

Figure 6-4. Influence of injection location for american boiler profile.

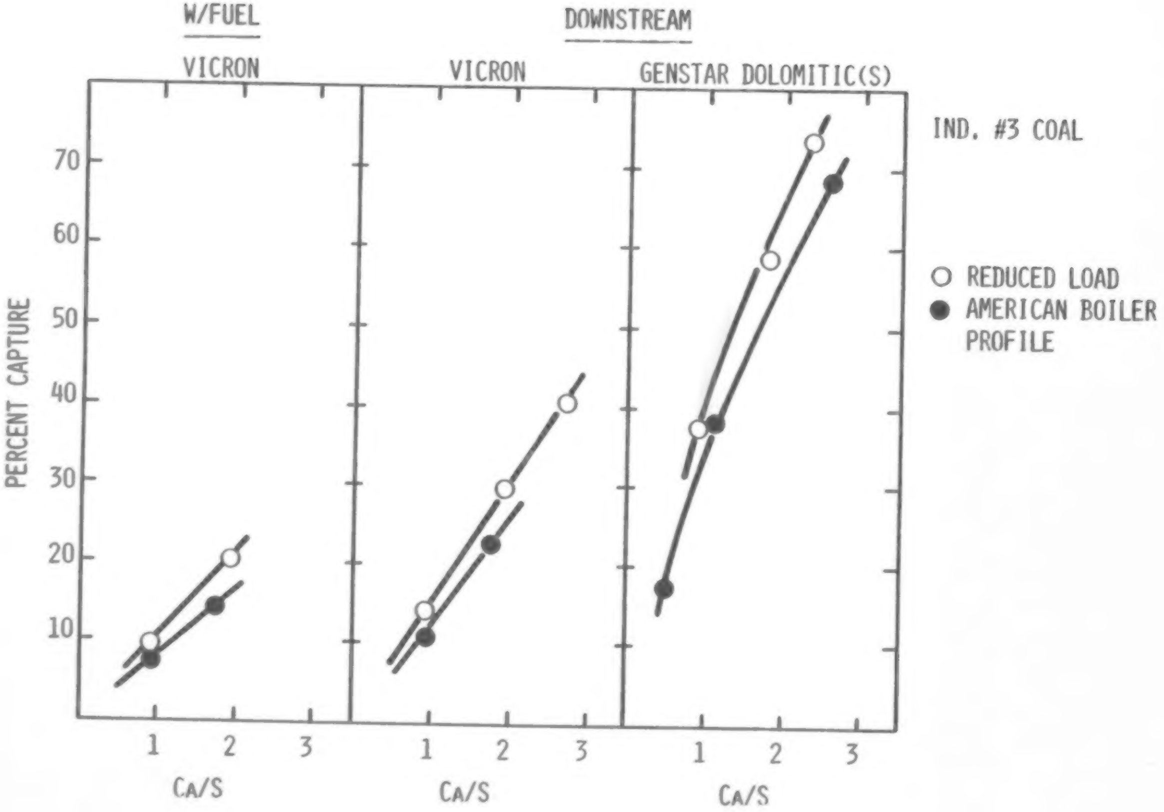

Figure 6-5. Influence of thermal history on capture in coal flames.

6.2 Capture Comparison Between Coal and Gas

In the last subsection, it was shown that similar trends were produced with coal and gas. In this subsection, coal and gas results are compared directly to determine which is better on an absolute level. A coal flame temperature profile was taken with the reduced load cooling configuration and compared to the gas profile in Figure 6-6. Although the peak temperature for the gas flame was somewhat lower than the coal flame, the quench rates were nearly identical and thus, it was decided that the data was comparable.

6.2.1 Burner Injection

The data presented in Figures 6-7 and 6-8 indicate the fuel effect for burner injection at reduced load and American Boiler profile, respectively. Vicron and Warner hydrate were run for the reduced load condition and Vicron and Genstar dolomitic were tested at the high load profile. For each of these comparisons, a single line can be drawn through the data which suggests that the mineral matter from the coal had no effect.

6.2.2 Downstream Injection

A gas vs. coal comparison is illustrated for downstream injection at two thermal profiles in Figures 6-9 and 6-10. As with burner injection, the downstream injection data indicates that there was very little difference between coal and gas capture, independent of the sorbent type used. Again, this data suggests that mineral matter does not influence sulfur capture with coal.

During the previous BSF program it was thought that the mineral matter in coal had an adverse effect on sulfur capture. Part of this reasoning was due to experimental data that was obtained from mixing fly ash and Vicron and injecting at the burner. Substantial decreases in capture occurred when this mixture was injected (see Figure 4-9). This experiment was repeated on the new BSF with essentially the same results as shown in Figure 6-11. Interestingly, the 1:1 mixture of ash and sorbent decreased capture when

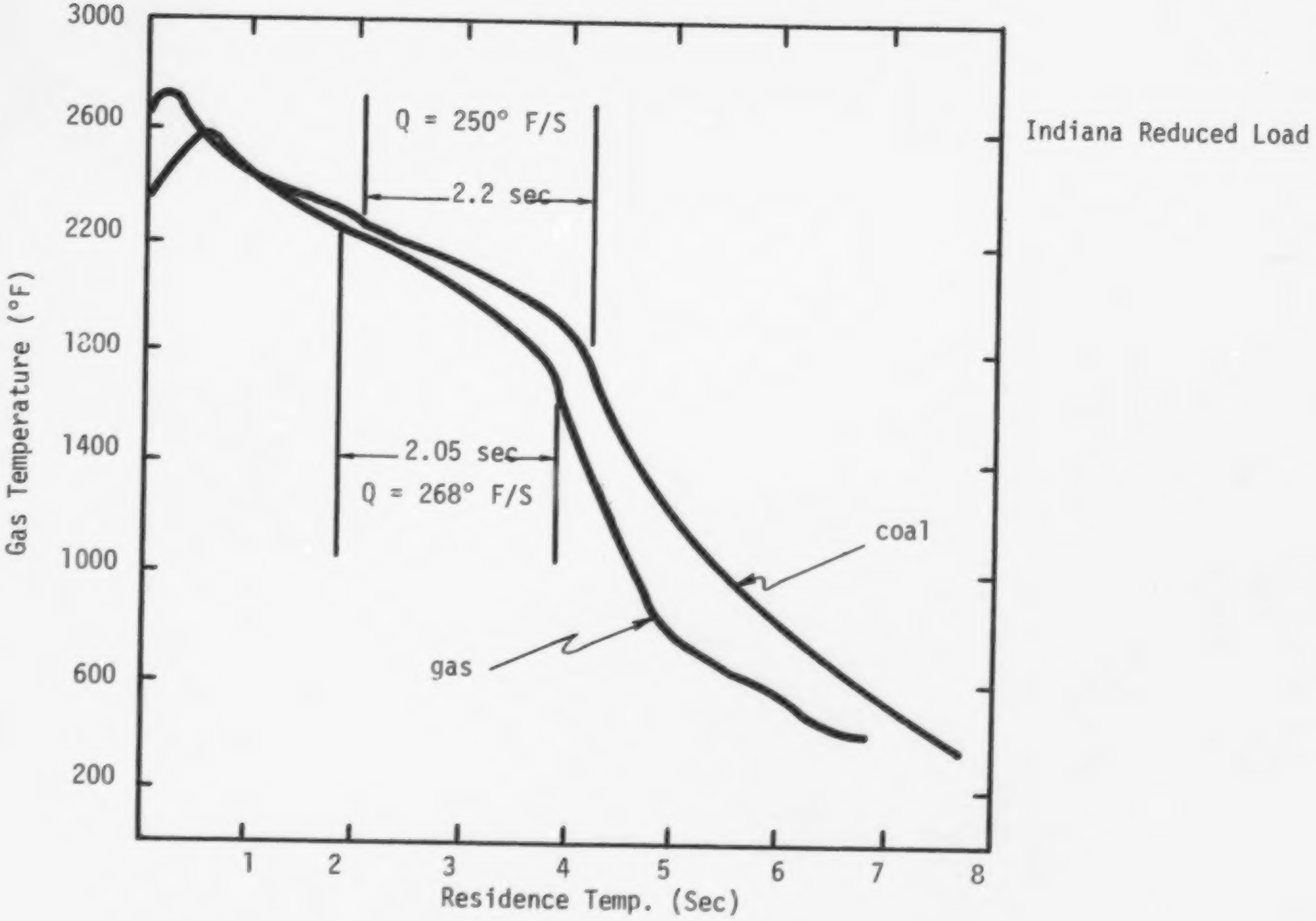

Figure 6-6. Thermal history comparison between coal and gas.

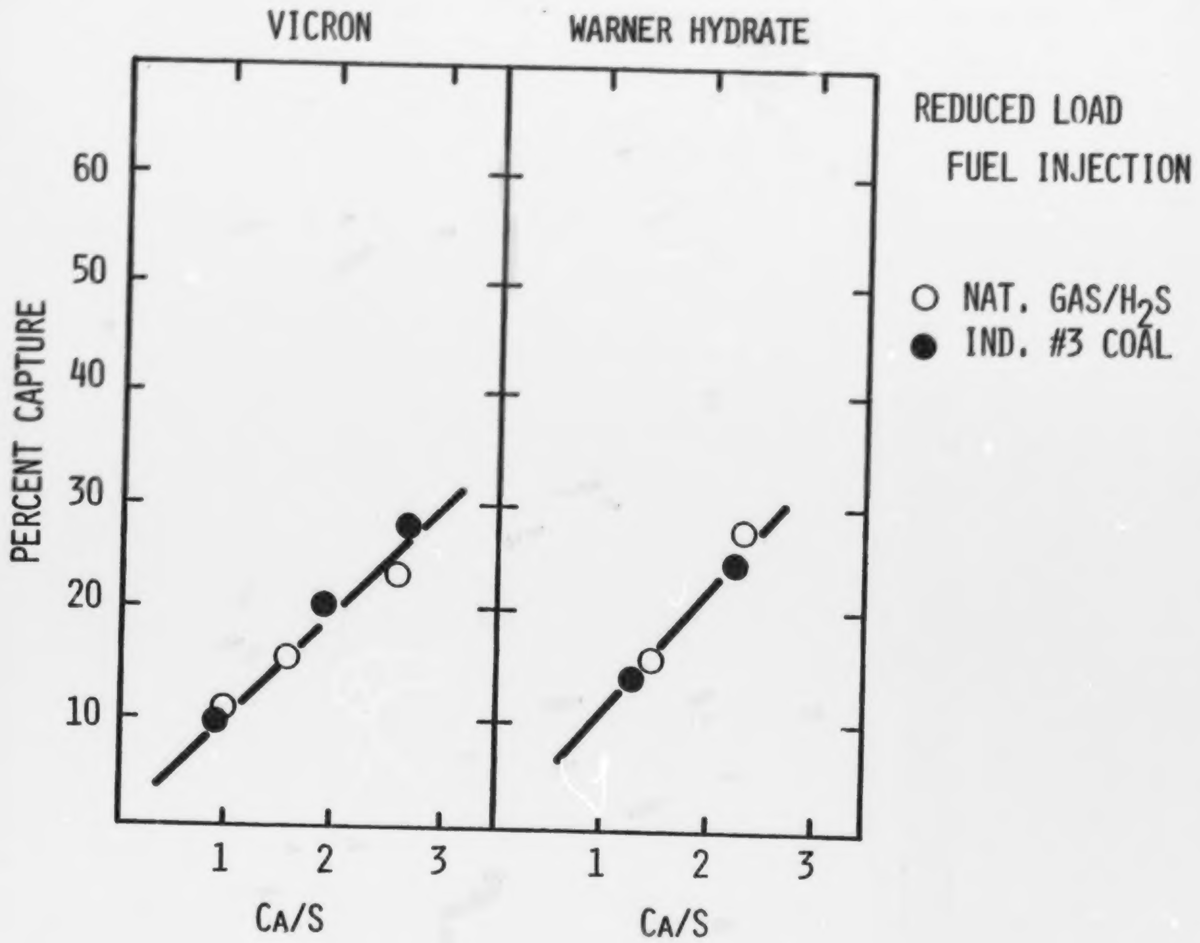

Figure 6-7. Reduced load fuel effect for burner injection.

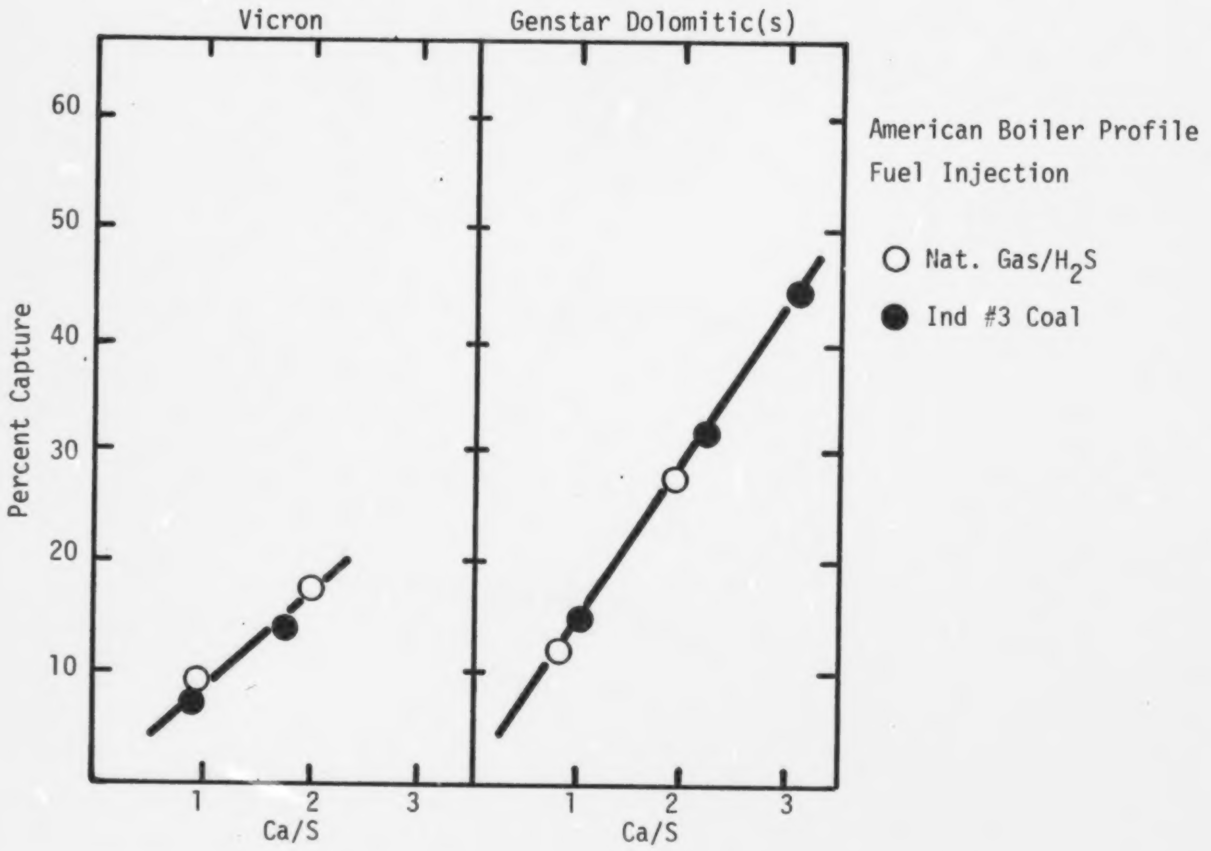

Figure 6-8. American Boiler profile fuel effect for burner injection.

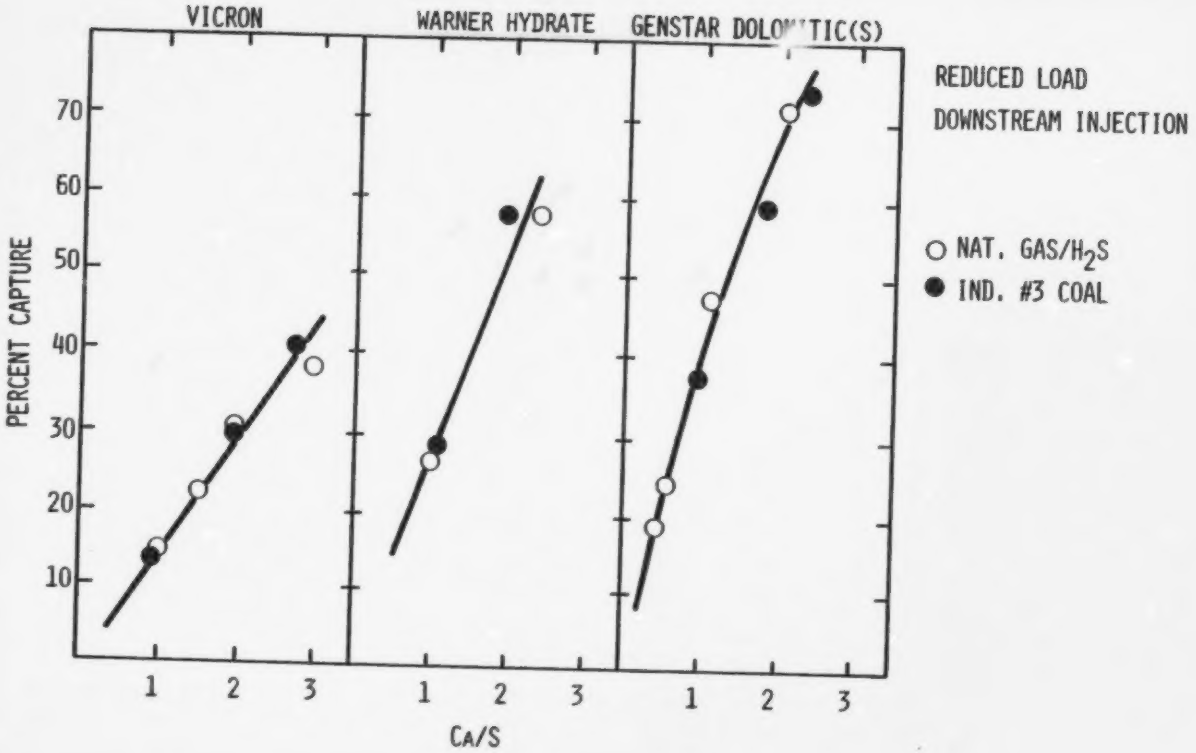

Figure 6-9. Reduced load mineral matter effect for downstream injection.

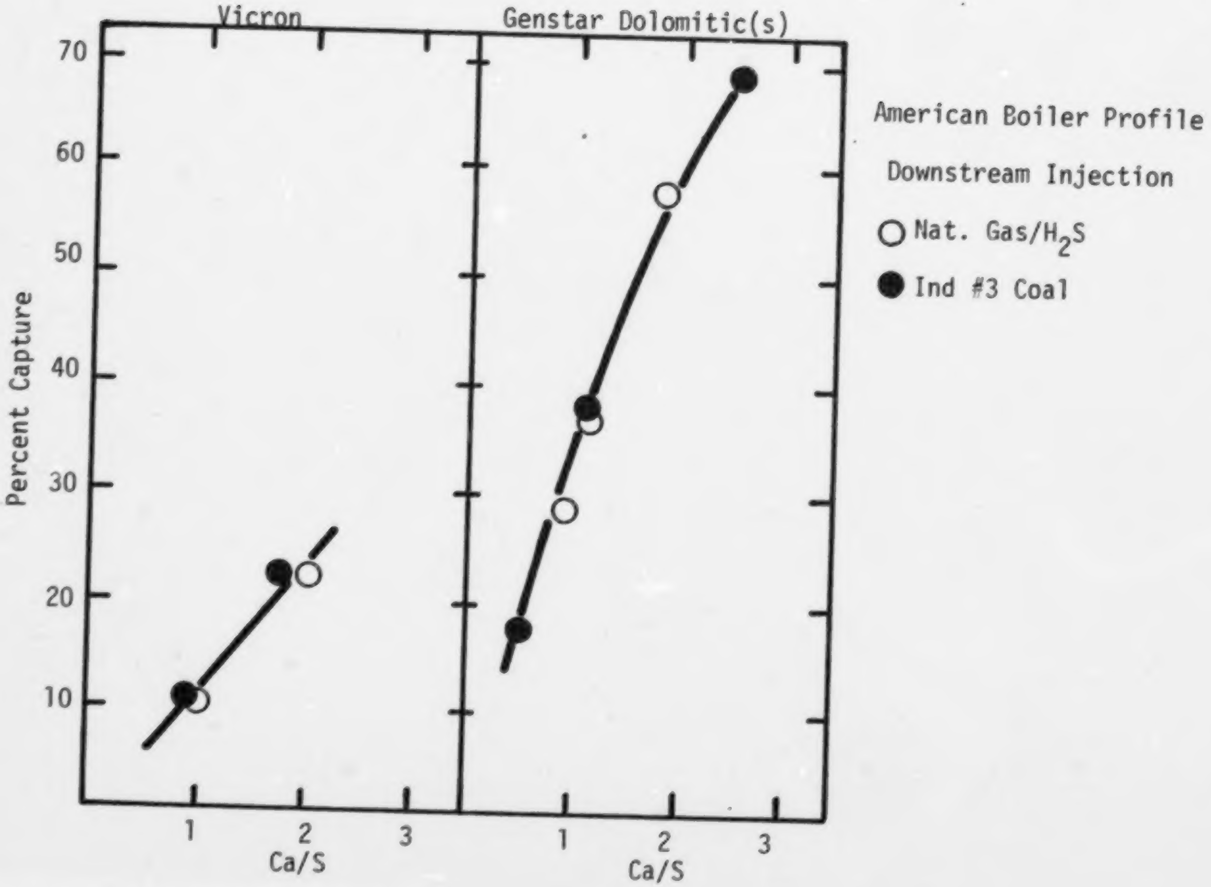

Figure 6-10. American Boiler profile mineral matter effect for downstream injection.

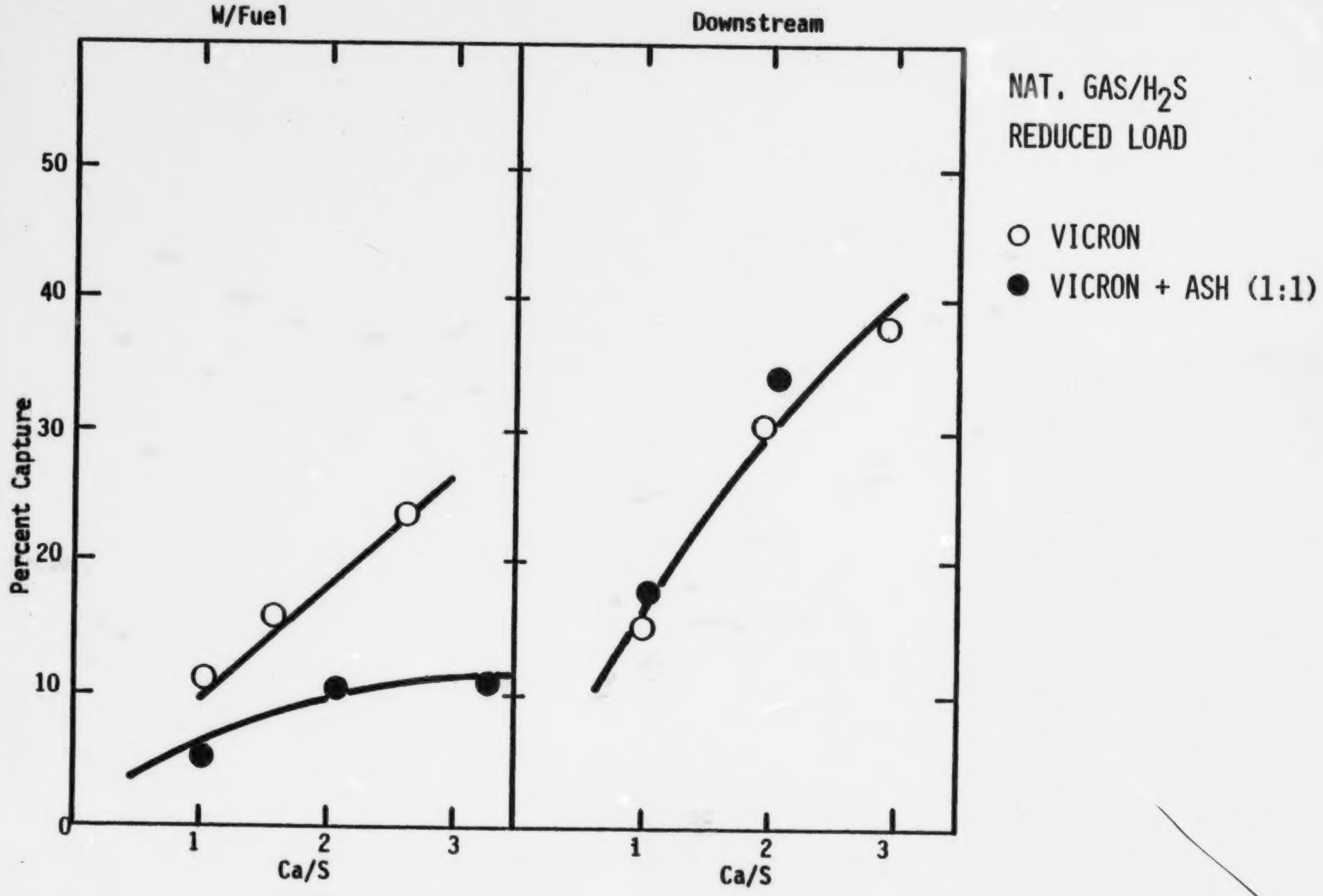

Figure 6-11. Influence of fly ash - premixed with sorbent.

injected at the fuel but not with downstream injection. Apparently, the interaction occurred only at temperatures somewhere above 2250°F.

The data in Figure 6-11 appeared to contradict the data shown previously in this chapter which indicated that regardless of injection location, the mineral matter in the coal had little or no effect on capture. One problem with the vicron/ash mixture experiment was that it did not completely simulate the experiments where sorbent was injected with coal. In the coal experiments, a fluidized sorbent stream was added through a "tee" fitting to the fluidized coal stream while in the mixture experiments, ash and sorbent were physically mixed and then fed from a hopper. Another difference was that in the coal experiments, the coal feedrate (and therefore the ash feedrate) was held constant as the sorbent feedrate was increased.

6.3 Mineral Interactions

6.3.1 Additive Screening

One of the central areas of study for this program was the identification of sorbent additives that could be used to increase or catalyze sulfur capture. Initially, Cr_2O_3 was identified as a promoter or catalyst during the new BSF characterization period because of capture differences in the old and new furnaces (see Chapter 4.0). This discovery led to other possible promoters of the sulfation reaction. Figure 6-12 gives some of the results from the additive screening tests. The additives tested were primarily from the transition metals region on the periodic table. Each additive was mixed with vicron such that the Ca/(Metal) molar ratio was held constant at 14.8. This ratio was chosen simply because it corresponded to the initial Cr_2O_3 concentration of 5.0 percent by weight. Of the additives tested, only Cr_2O_3 and MoO_3 showed significant increases in capture above the baseline data. All of the other additives were grouped into the shaded areas shown on the figure. One interesting note was that both Cr_2O_3 and MoO_3 produced better capture at the fuel than they did downstream.

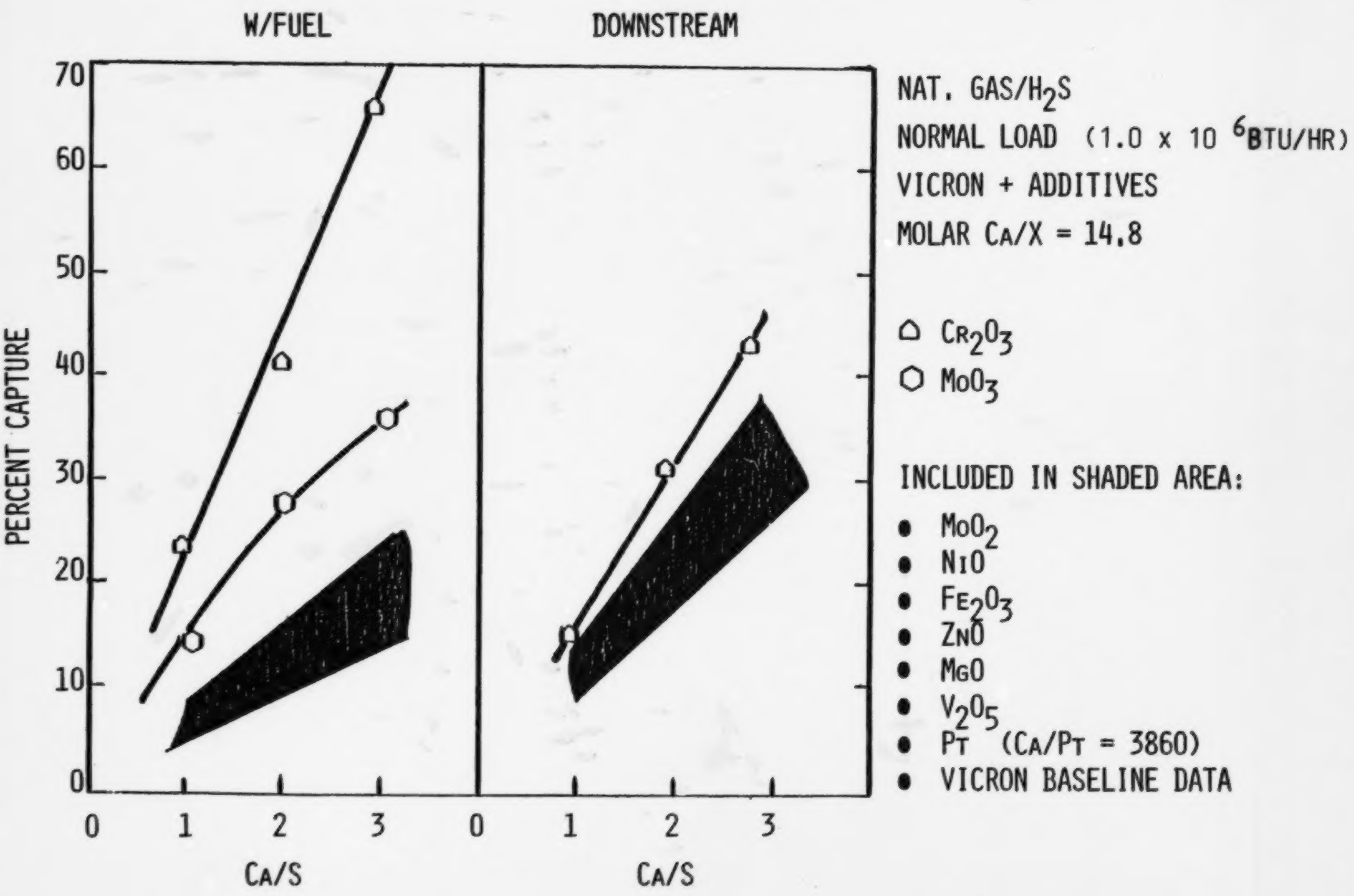

Figure 6-12. Transition metals additive screening.

Subsequently, Borgwardt (17) found that alkali metals compounds (lithium, sodium, potassium) gave positive results similar to those found with the chromium series materials. Figure 6-13 shows that mixing each of the alkali metal carbonates with Vicron resulted in increased SO_2 capture when the sorbent was injected with the fuel and downstream. In these experiments the ratio of metal ion to calcium was maintained equal to that for the 5% Cr_2O_3 addition. On this basis chromium proved to be the best promoter in terms of overall capture. With the reduced load profile, the capture with high temperature injection was equivalent to that with downstream, low temperature injection. Chromium appears to have the ability to compensate for the effect of thermal sintering of the sorbent.

In order to verify the additive results under different thermal conditions, the Cr_2O_3 and Na_2CO_3 were run with Vicron with the American Boiler profile as Figure 6-14 shows. For fuel injections, sodium did as well as the chromium which suggested that the mechanism for the sodium was temperature controlled. Downstream, at the cooler injection temperature, capture was only slightly better than the Vicron baseline.

All of the additives that had shown some increase in capture (Cr, Mo, Na, Li, K) had electronic configurations with one electron in an S orbital. On this basis, copper was tried as a potential promoter however, very little increase in capture was achieved.

The influence of additive concentration was investigated for two of the additives at reduced load. Figure 6-15 indicates that as additive concentration increased, capture also increased, but at a decreasing rate. For Cr_2O_3, the first percent had a dramatic effect while further increases in concentration produced only moderate increases in capture. A similar trend was seen with the Na_2CO_3 curve though it was not as sensitive to changes in concentration.

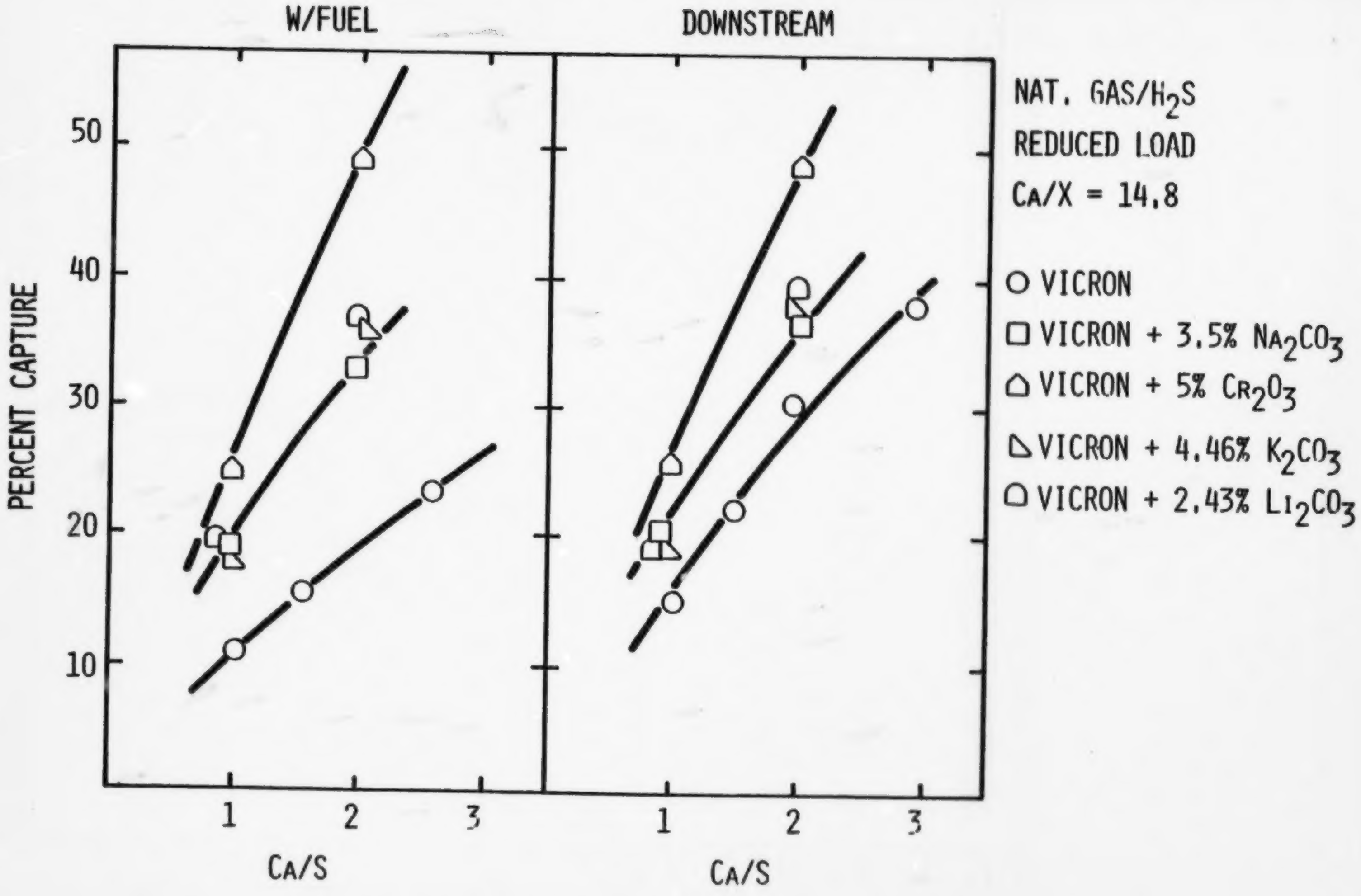

Figure 6-13. Alkali metal promoters.

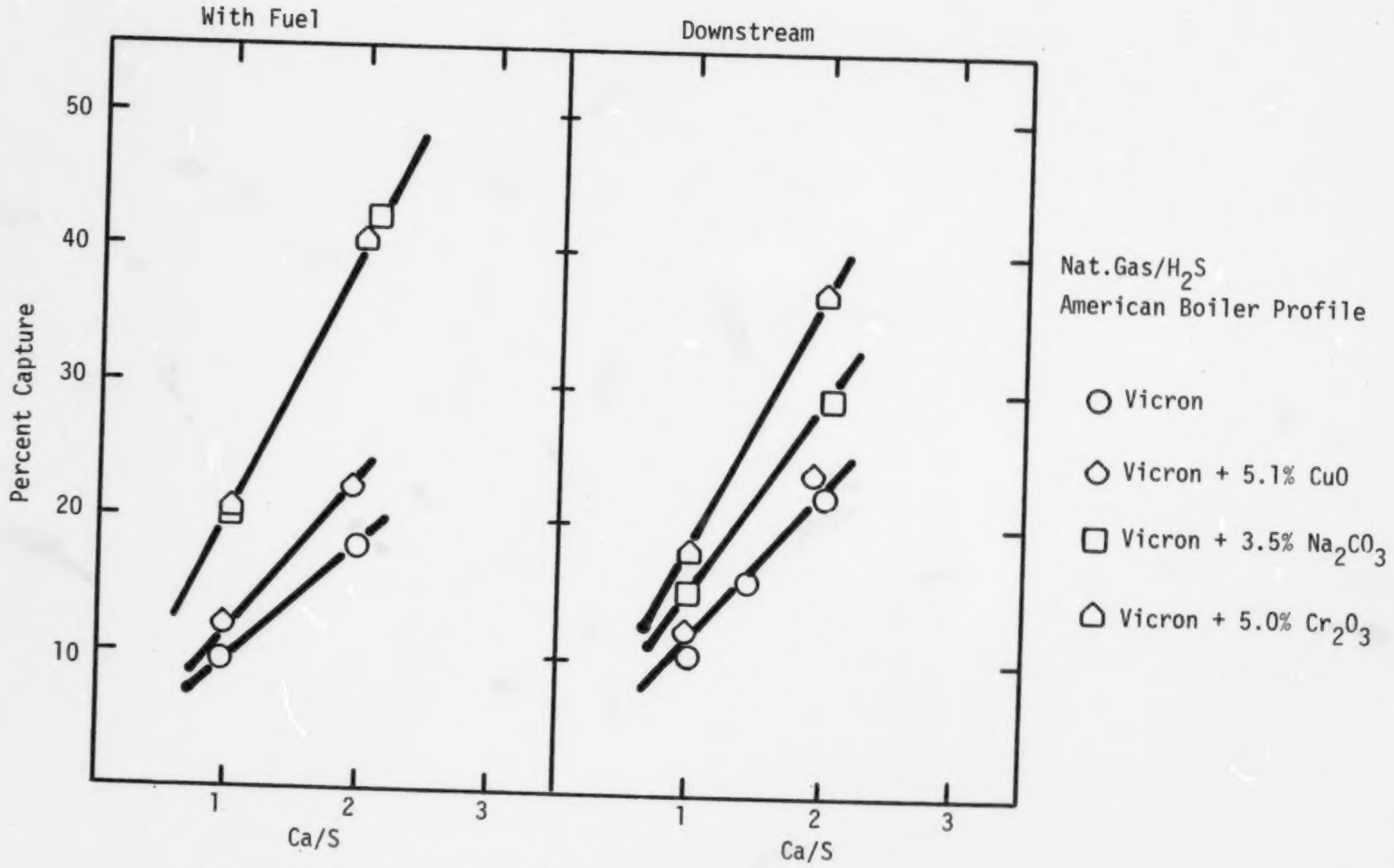

Figure 6-14. Additives with american boiler profile.

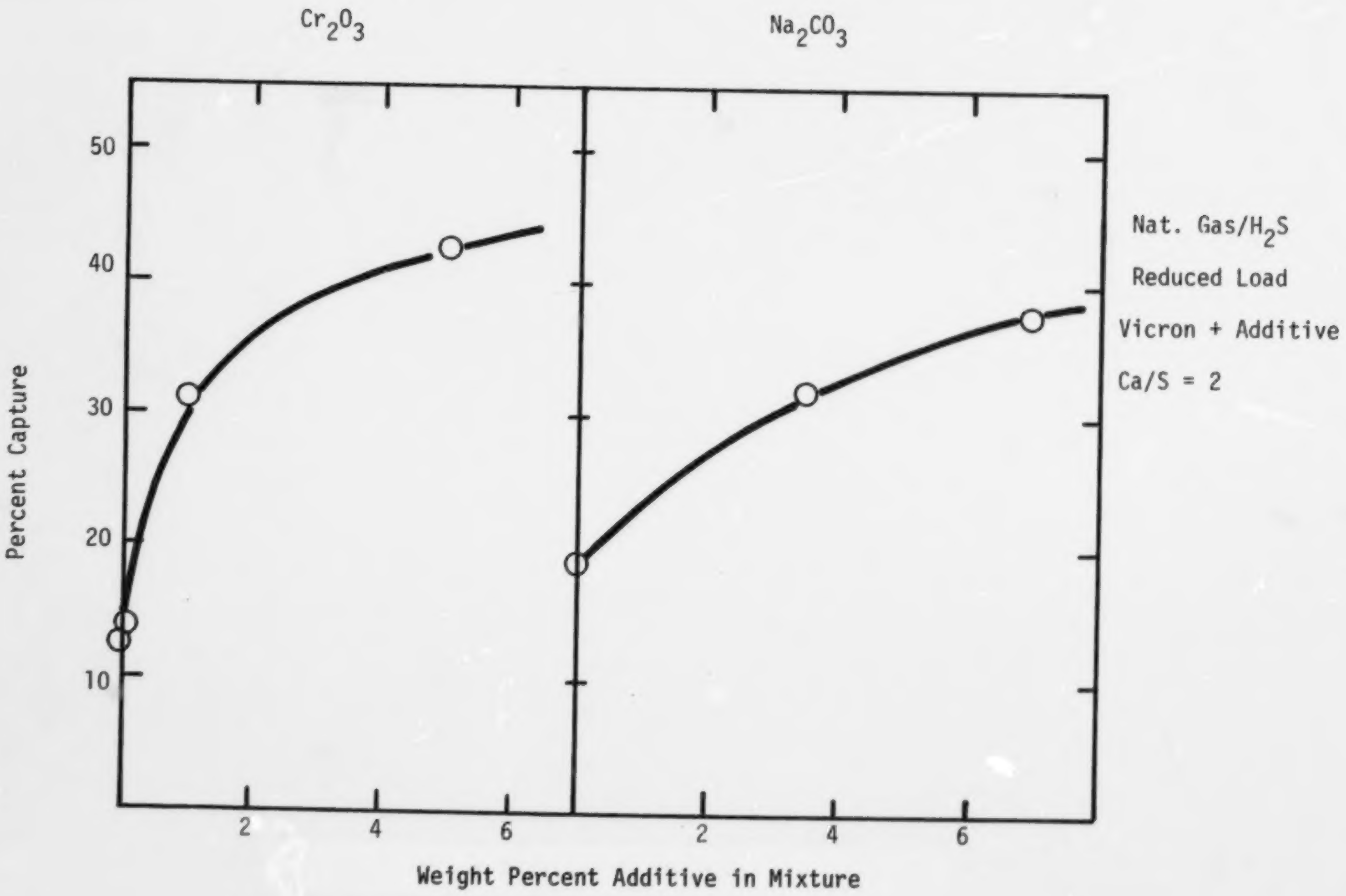

Figure 6-15. Influence of additive concentration.

6.3.2 Na and Cr Enhancement with Gas

The results of the additive screening studies indicated that the most promising additives were sodium and chromium, hence these two were studied in greater depth with a variety of sorbent and thermal parameters. These variables were tested in natural gas/H_2S flames initially and the results are presented in this subsection.

Sorbent Type

Figure 6-16 illustrates the influence of Cr_2O_3 addition with other types of sorbents. The open bars represent the capture measured with the sorbents alone and the shaded bars indicate the increase in capture that resulted from 5 percent (by weight) chromium addition. With all of the sorbents and with both burner zone and downstream sorbent injection, the capture increases with chromium promotion were significant. Even the performance of the Genstar pressure slaked dolomite was improved: 70 to 85 percent capture for the downstream sorbent injection and 35 to 70 percent capture for injection with the fuel. In general the enhancement above the baseline was greater when the promoted sorbents were injected into the high temperature region, although the absolute capture levels were generally higher for downstream injection.

Injection Location

The influence of injection location with Cr_2O_3 is illustrated by Figure 6-17 for two temperature profiles. In both cases, the burner injection results matched the downstream results even though the peak temperature experienced by the sorbent particles was 700 to 600°F hotter with burner injection. Similar results are shown in Figure 6-18 for sodium. For the reduced load, burner injection equaled downstream injection but for the American Boiler profile, burner injection produced higher capture than downstream injection.

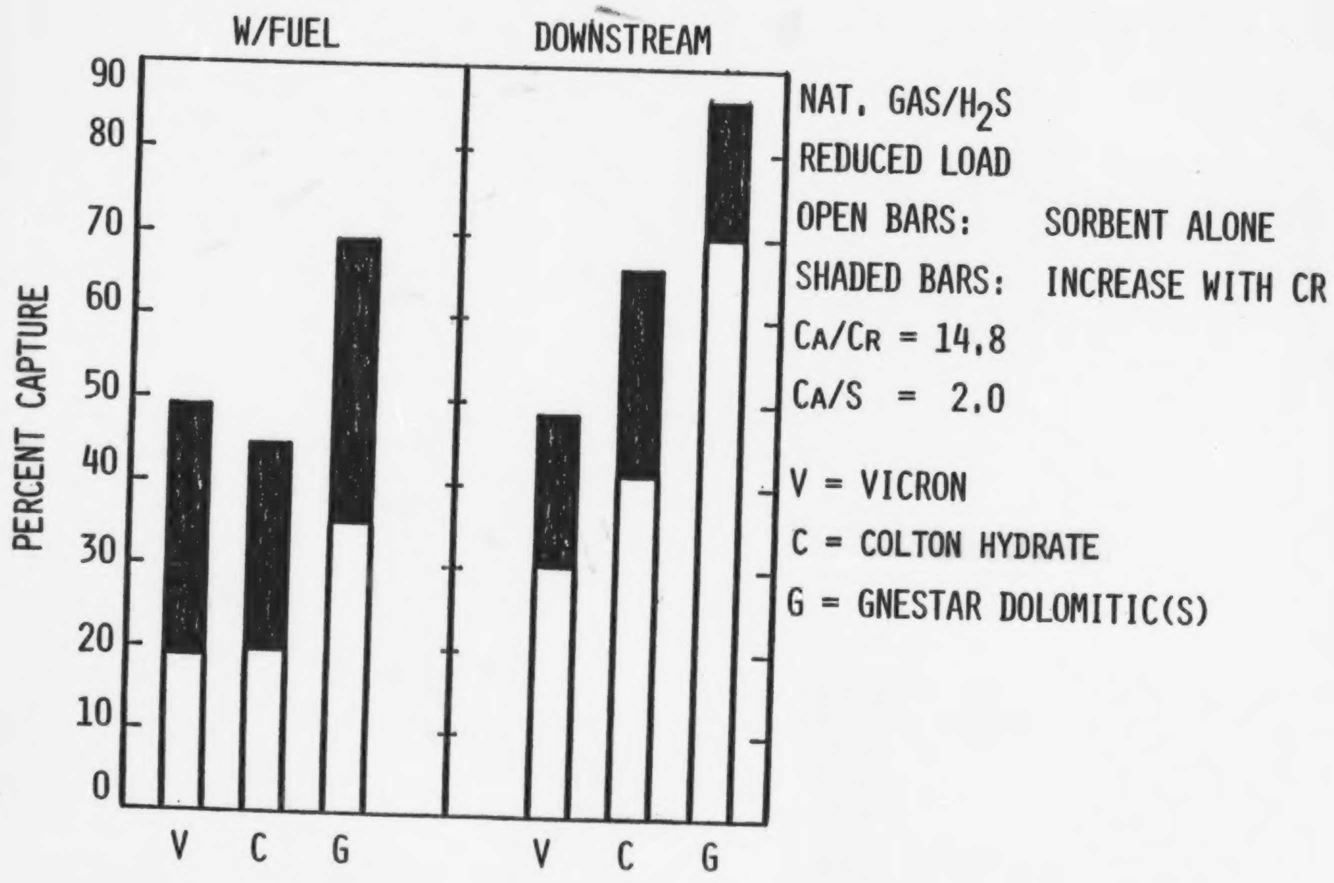

Figure 6-16. Chromium enhancement with different sorbent types.

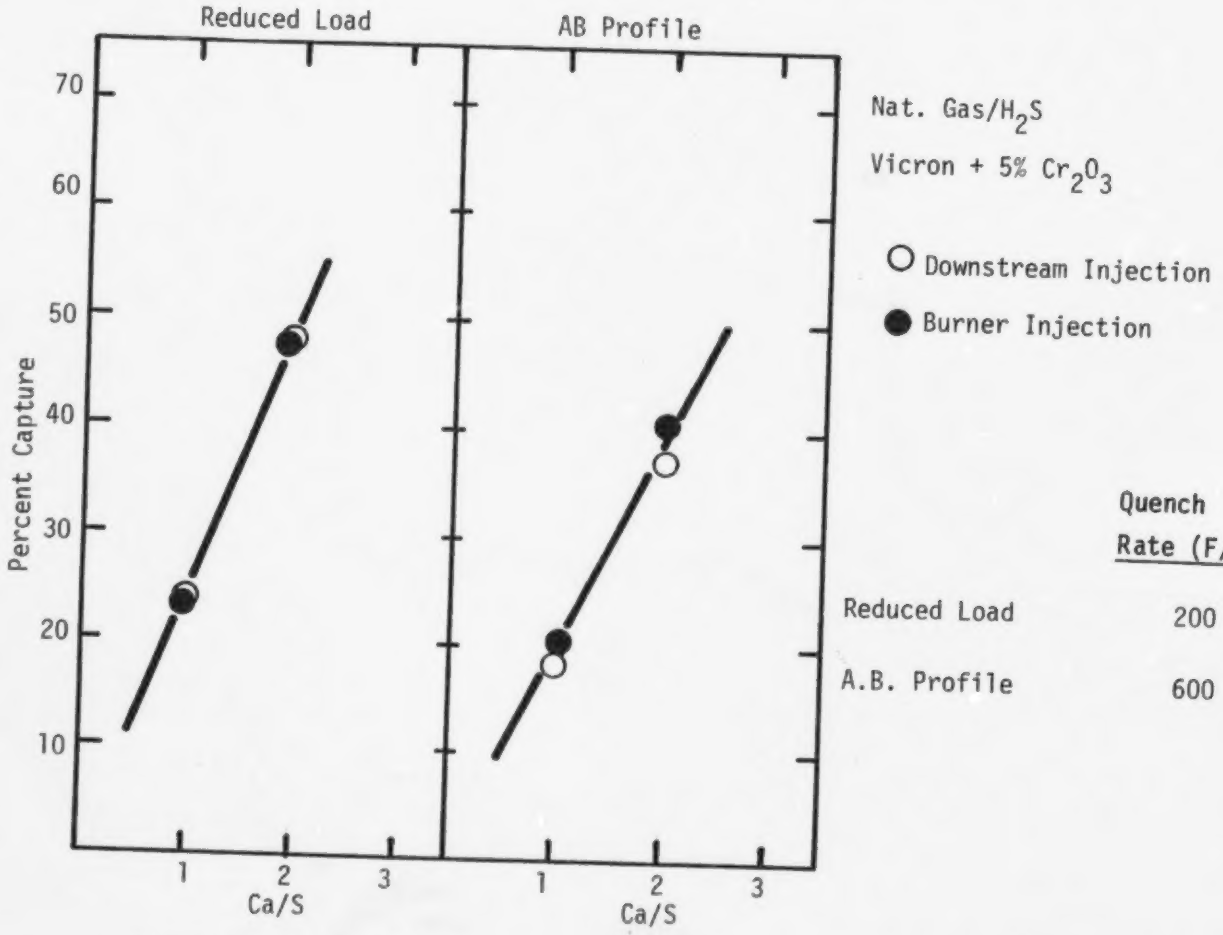

	Quench Rate (F/S)	Peak T. (°F)
Reduced Load	200	2600
A.B. Profile	600	2800

Figure 6-17. Influence of injection location with Cr_2O_3.

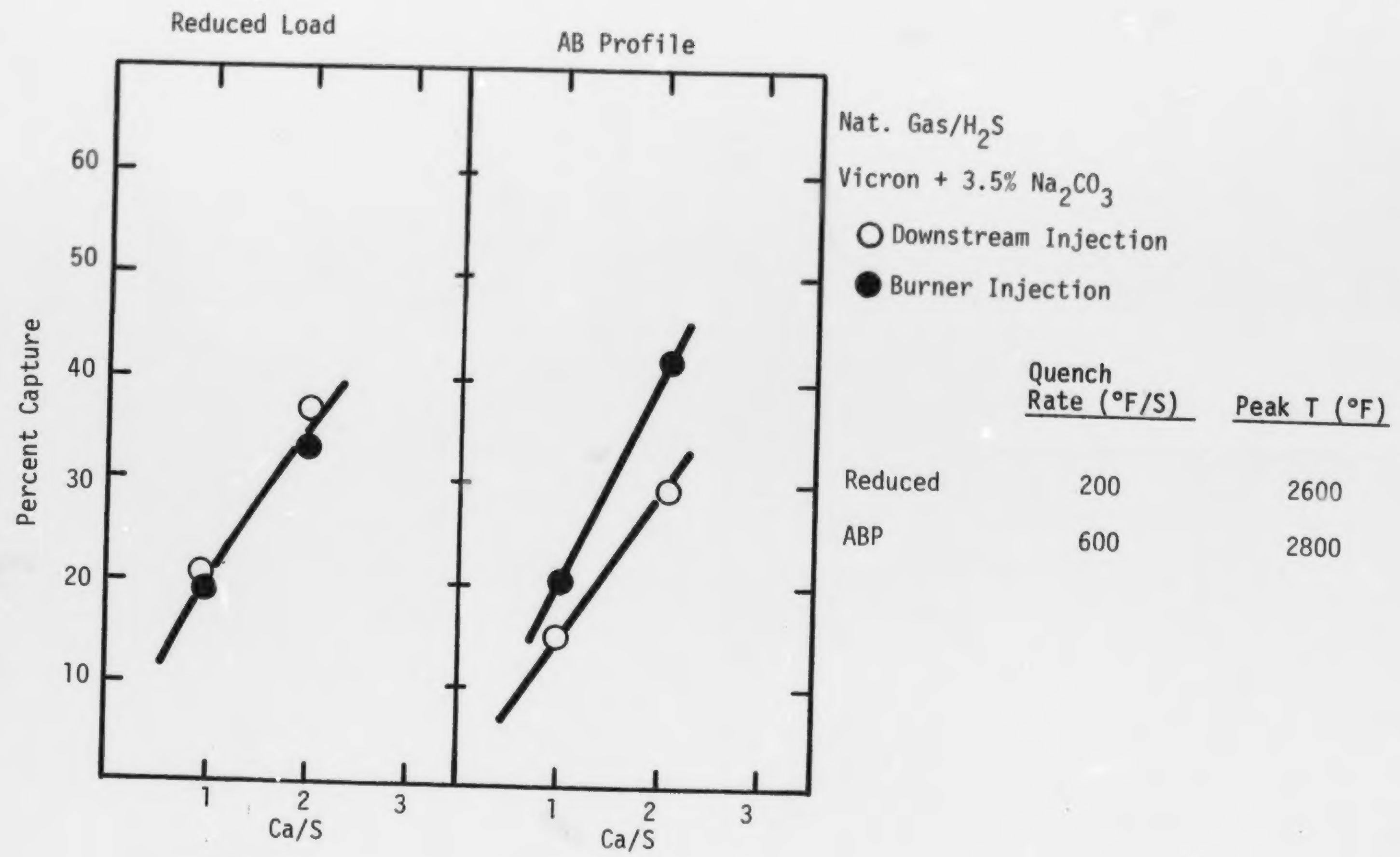

Figure 6-18. Influence of injection location with Na_2CO_3.

Thermal History

Figures 6-19 and 6-20 show the impact of thermal history on capture at two injection locations for Cr_2O_3 and Na_2CO_3, respectively. For the chromium studies, the reduced load captures were better than the American Boiler profile captures at both injection locations. The quench rate effect was isolated in the downstream tests since injection temperature was constant and the combination of peak temperature and quench rate was shown in the fuel injection tests. Apparently, there was a trade-off between the two factors with higher peak temperature tending to increase capture, and higher quench rate tending to decrease capture. For chromium, quench rate dominated since overall captures decreased with the American Boiler profile. For Na_2CO_3, the results were the same for downstream injection but for fuel injection, the hotter peak temperature compensated for the higher quench rate and capture at the two profiles was identical. These results indicate that sodium was more sensitive to injection temperature then the chromium.

6-19
6-20

The exact mechanism for the chromium and sodium enhancement is not clear at the present time; however, it appears likely that these materials promote capture by enhancing the product layer diffusion step since the model calculations indicate that product layer diffusion is the primary limitation to increased sulfation rates.

6.3.3 Na and Cr Enhancement with Coal

The next phase of this program focused on sodium and chromium enhancement with the parameters mentioned above in coal flames. The intent of these tests was to determine what effect coal mineral matter had on the enhancement seen with gas. Figure 6-21 shows the overall results of both additives injected with Indiana #3 coal. The most striking point in this figure is that sodium had no effect on capture whereas the chromium still promoted capture as it did with natural gas.

6-21

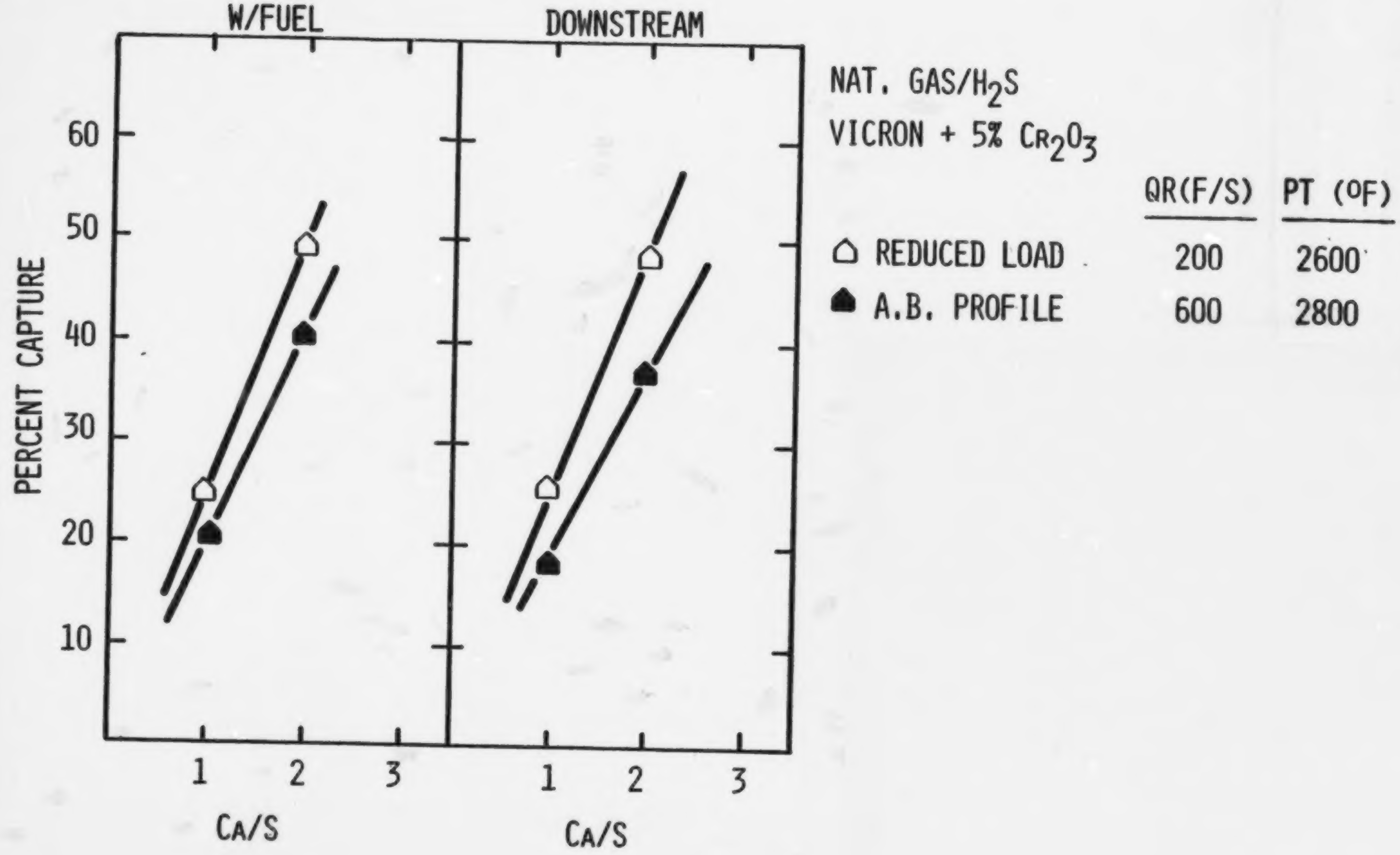

Figure 6-19. Impact of thermal history on enhancement with Cr_2O_3.

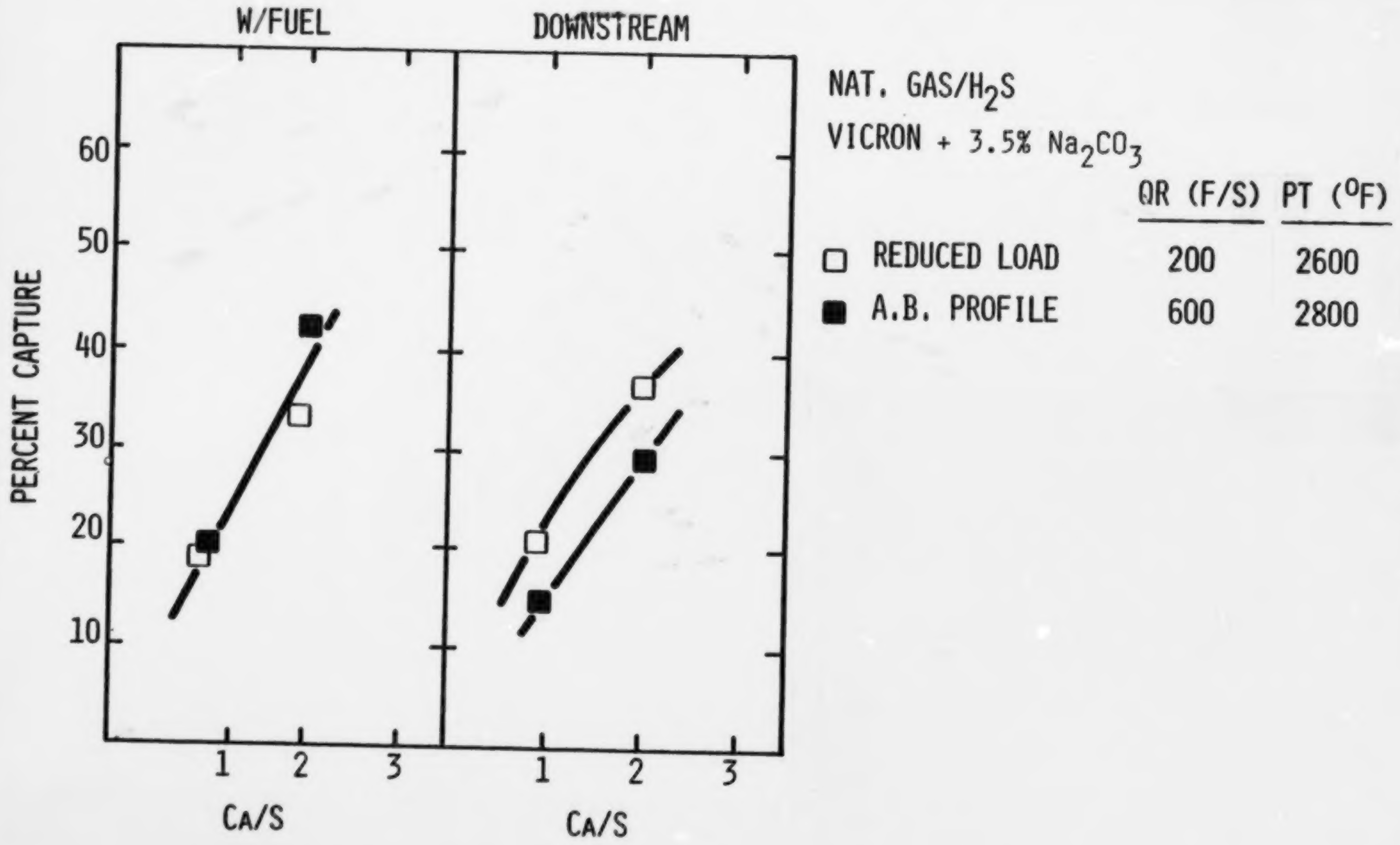

Figure 6-20. Impact of thermal history on enhancement with Na_2CO_3.

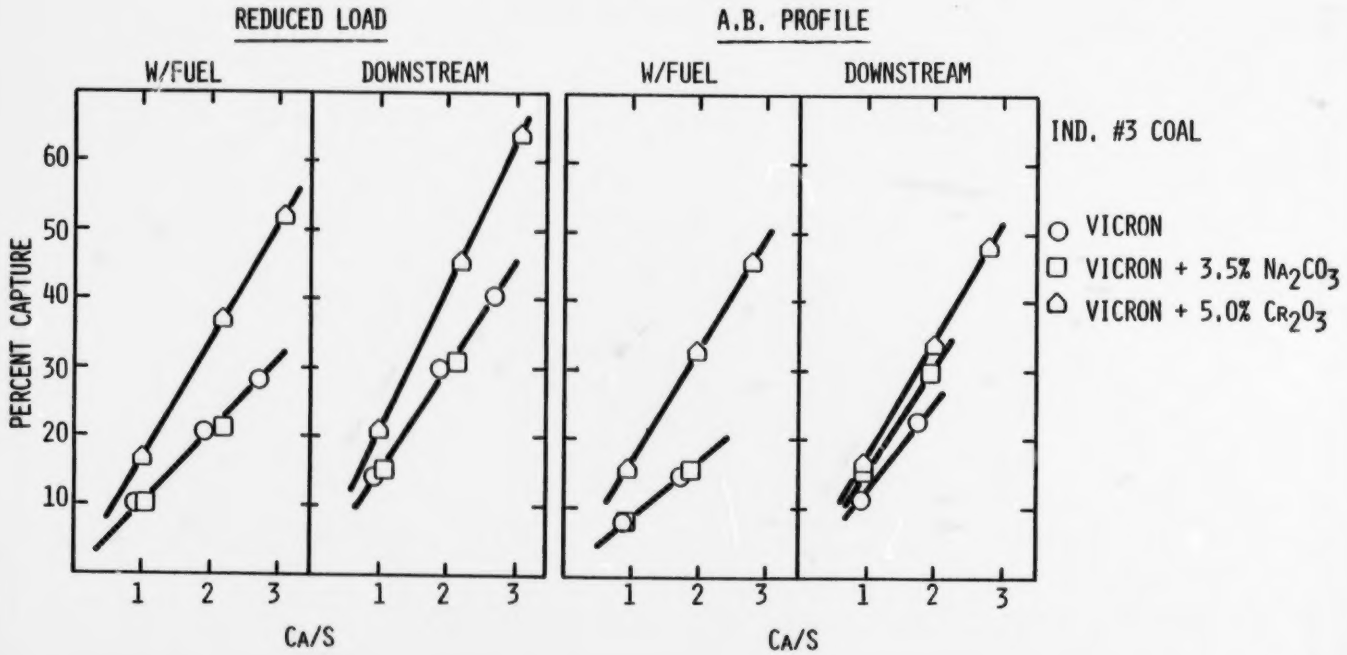

Figure 6-21. Enhancement with Cr and Na in coal flames.

Fuel Type Effects

Figure 6-22 compares coal and gas for chromium enhancement under a variety of conditions. In general, capture with gas was higher than capture with coal. Only downstream injection with the American Boiler profile gave similar capture between gas and coal. Figure 6-23 shows similar results for Na_2CO_3 enhancement with the two fuels. Again, capture with natural gas was significantly better in every case except for downstream injection with the American Boiler profile. With chromium, the difference between coal and gas was smaller than with sodium which indicated that mineral matter interacted with the sodium enhancement process to a greater extent. It is not clear why the downstream American Boiler profile results behaved differently than the other three cases.

Injection Location

The impact of injection location is shown in Figure 6-24 for both additives and both temperature profiles. The figure indicates that with sodium, downstream injection was strongly favored over burner injection. For chromium, downstream injection was slightly favored for the reduced load and there as no difference with the American Boiler profile. With sodium, the results look very much like the results for Vicron alone with coal since the sodium had essentially no effect on capture.

Thermal History

The effects of quench rate and thermal history for both additives are given in Figure 6-25. Overall, there were no dramatic changes in capture though the reduced load appears to have been favored slightly. Thermal history had less of an impact on enhancement with coal than it did with natural gas.

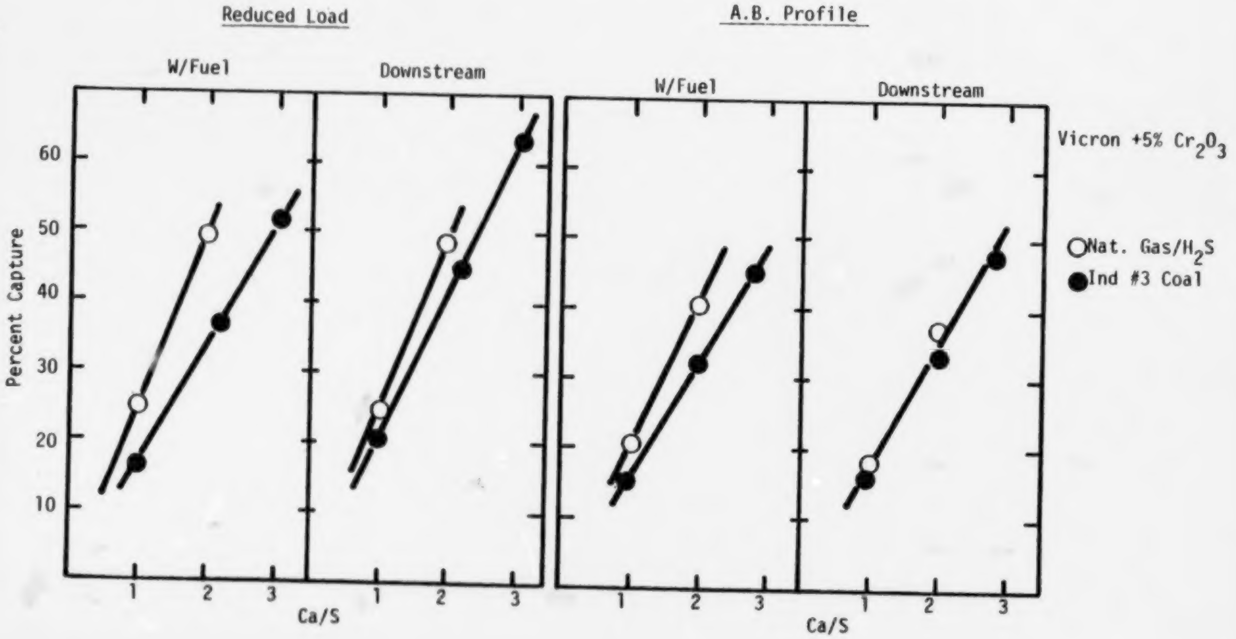

Figure 6-22. Impact of fuel type on enhancement with Cr_2O_3.

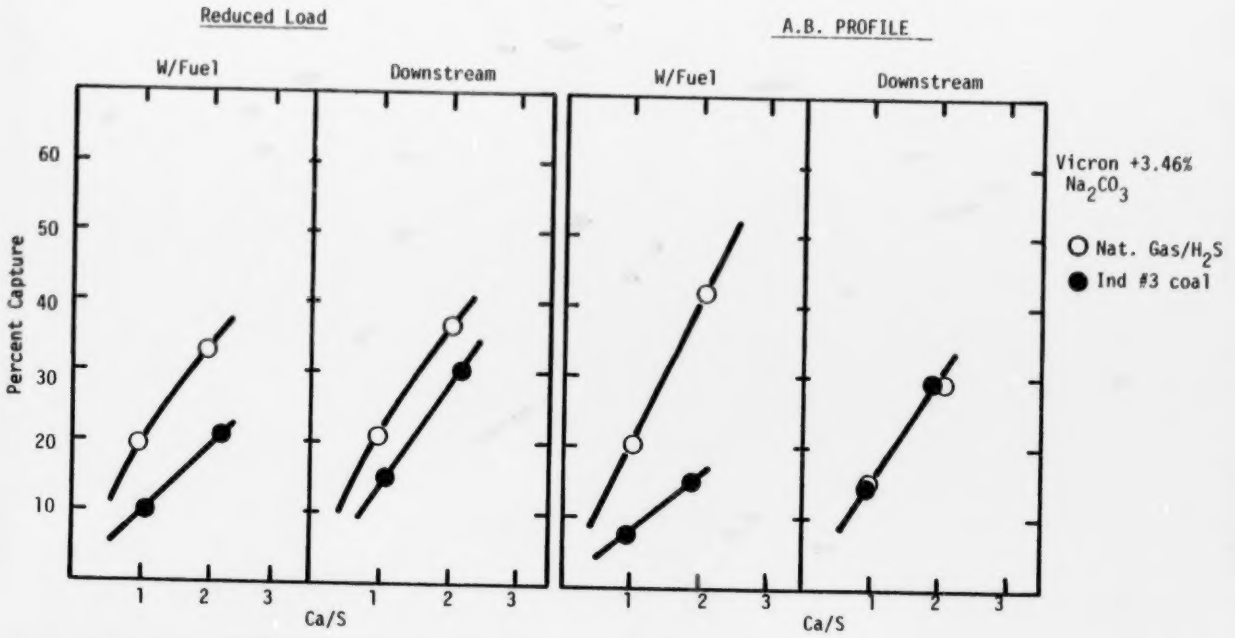

Figure 6-23. Impact of fuel type on enhancement with Na_2CO_3.

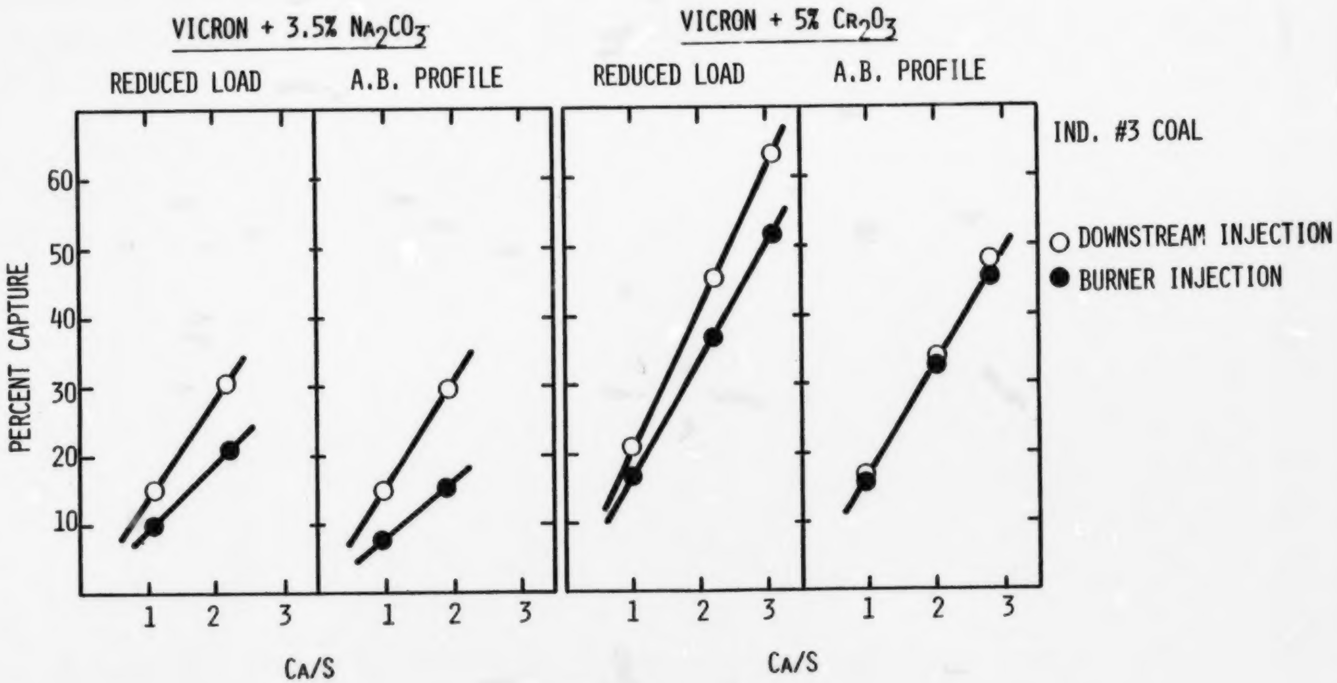

Figure 6-24. Impact of injection location on enhancement in coal flames.

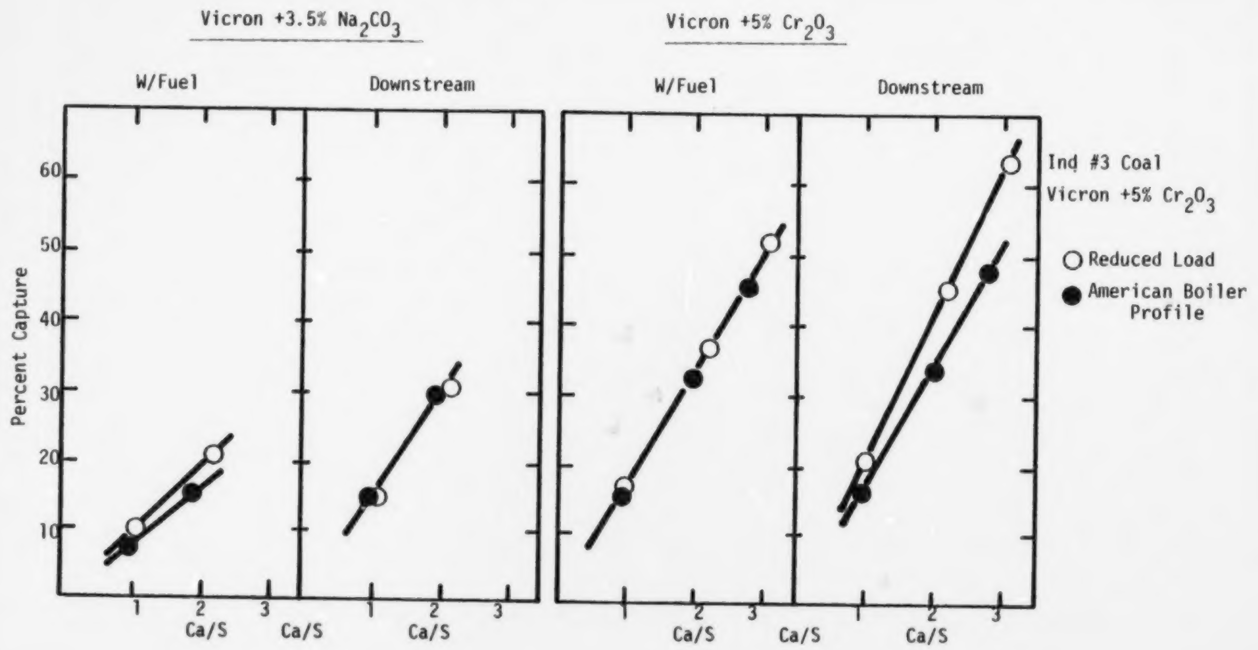

Figure 6-25. Impact of thermal history on enhancement in coal flames.

6.4 Mechanistic Parameters

As an attempt to elucidate some of the capture mechanisms, several concentrations and surface area tests were run. The influence of fuel sulfur concentration was studied by varying the amount of H_2S doped into the natural gas flames. SO_2 concentrations of 500, 1000, 1800, and 3000 ppm (dry 0% O_2) were tested with the Colton hydrate and the Genstar pressure slaked dolomitic lime (type S). The Ca/S ratio was held constant at 2.0 and the sorbent was injected at $2250^{o}F$ for all of the runs. These results are presented in Figure 6-26 along with model predictions. Both the data and the model showed an increase in sulfur capture with increasing SO_2 concentration. The curvature in the theoretical predictions, which is in agreement with the experimental results, is due to a trade-off between the zero order chemistry and the first order pore and product layer diffusion processes. At low SO_2 concentrations the product layer diffusion resistance (which is first order in SO_2) exceeds the chemical reaction resistance (zero order with respect to SO_2) for a larger fraction of the sulfation zone residence time; hence, the overall dependence on gas phase SO_2 concentration is much stronger than at high SO_2 concentrations where the chemical resistance is more limiting. The good agreement between the model predictions and the experimental data is typical of that observed with other sorbents and suggests that the model accurately represents the concentration dependence of the sulfation process.

Given the SO_2 concentration dependence shown in Figure 6-26, it was of interest to look at the importance of SO_2 concentration on capture with a vicron plus 5 percent Cr_2O_3 mixture. The same SO_2 concentrations used previously were again run for fuel and downstream injection of the mixture as shown in Figure 6-27. As concentration increased, there was a corresponding increase in capture almost identical in shape to the curves without chromium present. The mechanism for sulfur capture must depend on SO_2 concentration in the same way that the reactions without chromium.

Another reactant that was looked at briefly in terms of concentration dependence was oxygen. Figure 6-28 shows results for Vicron and Vicron plus 5 percent Cr_2O_3 injected at the burner. The oxygen was varied from the

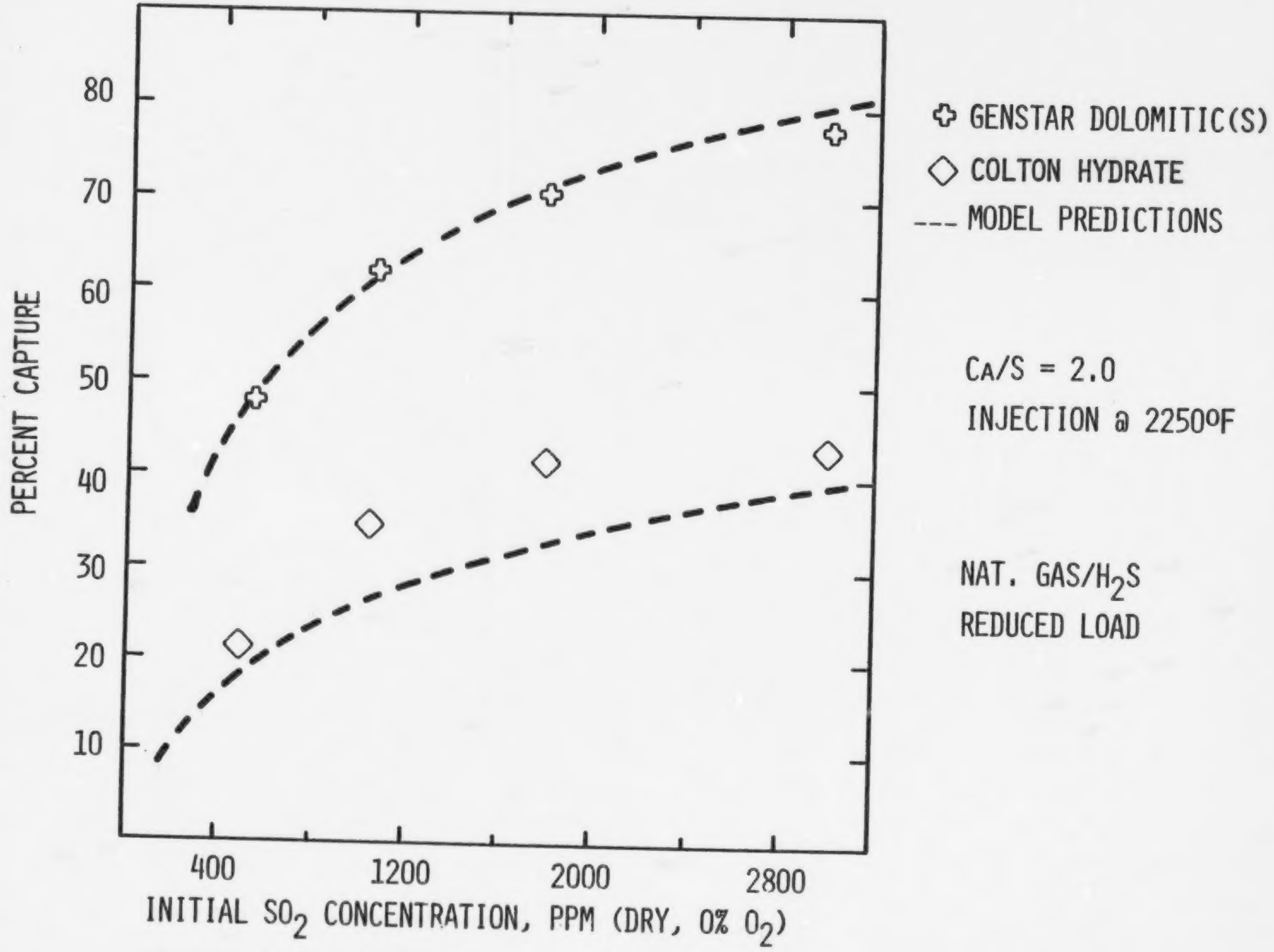

Figure 6-26. Influence of SO_2 partial pressure.

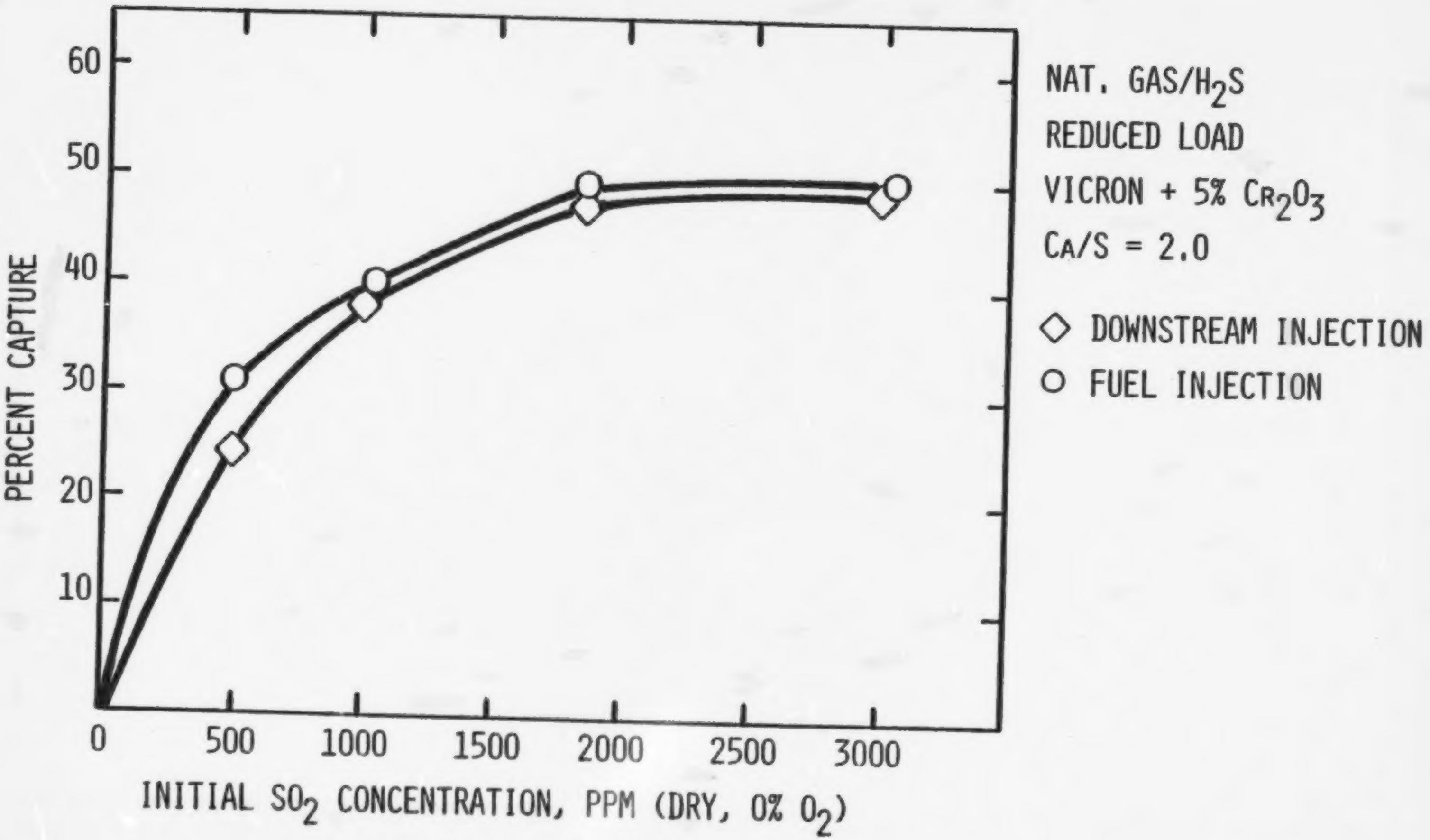

Figure 6-27. Influence of SO_2 partial pressure with Cr_2O_3.

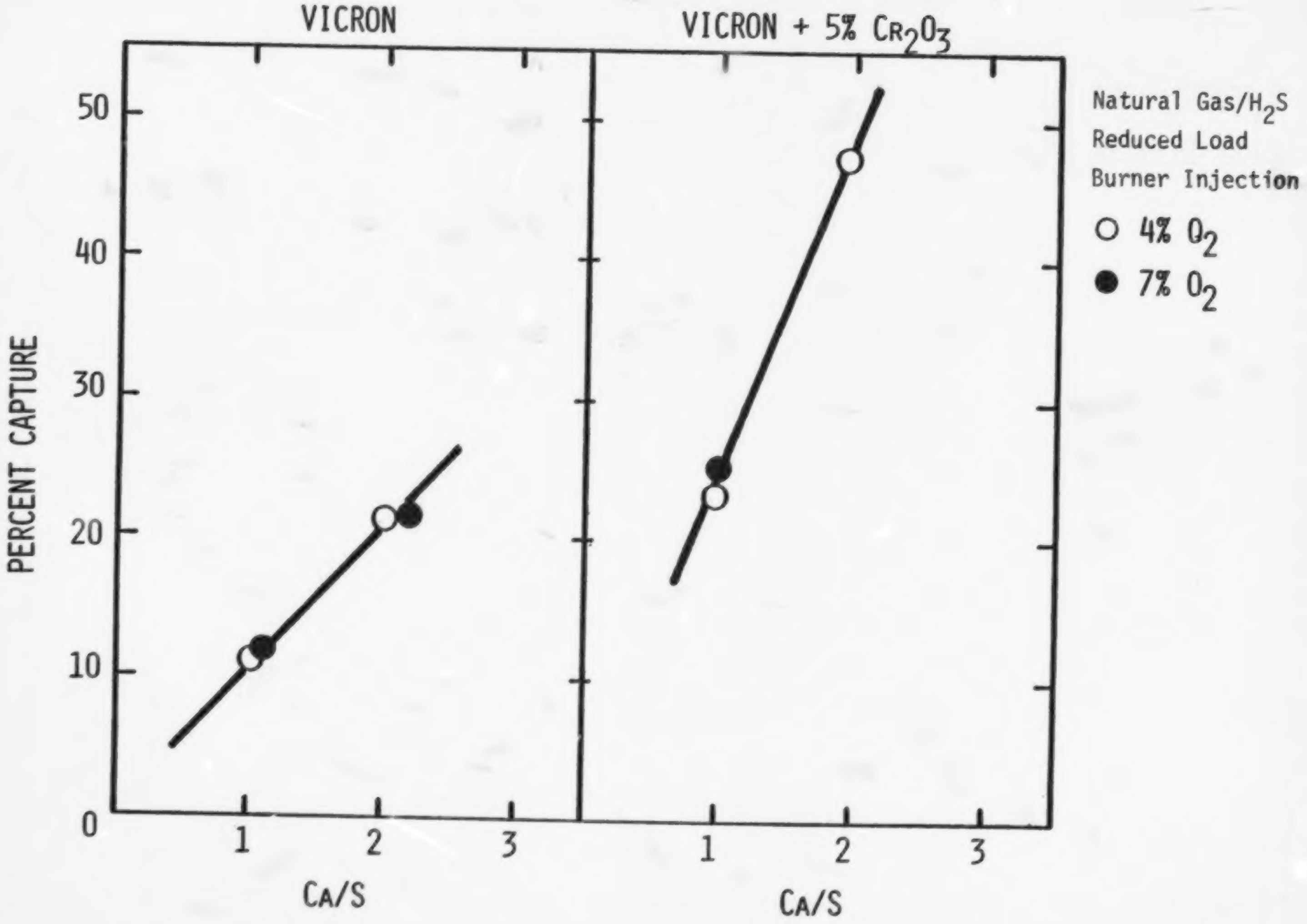

Figure 6-28. Dependence on O_2 concentration.

baseline 4 percent up to 7 percent and, as the figure indicates, there was no effect on capture. Evidently, the availability of oxygen is not a rate limiting step in the capture mechanism.

Figure 6-29 shows a detailed capture profile for Vicron plus 5 percent Cr_2O_3 compared with Vicron alone for injection at the burner. With chromium addition, the capture at one second and 2400°F had already equaled the Vicron capture at 4 seconds. At four seconds the capture with chromium was about three times higher than with Vicron alone. The "sulfation window" for CaO is generally thought to be from 2250-1700°F but with chromium present, some capture occurred even before the upper end of the window was reached. A similar zone capture profile is shown for downstream injection in Figure 6-30. The same type of results were generated with the downstream capture though not as dramatic as with the burner injection results. At any rate, the presence of chromium shifted the "sulfation window" into a higher temperature region.

Surface area measurements were made for Vicron alone and mixed with both additives for burner and downstream injection. Table 6-1 shows that Vicron had a measured specific surface area of 4.2 m^2/g for injection at the fuel and 12.4 m^2/g for downstream injection. Then numbers were fairly consistent with other independent measurements. With chromium however, surface area was dramatically decreased especially for downstream injection. This effect was first reported by Borgwardt (17) at an EPA laboratory at which point he suggested that the presence of chromium accelerated particle sintering (6.2). With the sodium additive, a slight decrease in surface area was seen for fuel injection and a slight increase was seen for downstream injection. Sodium added to the Vicron did not cause the dramatic decrease in surface area that was seen with chromium for downstream injection and yet, the capture was not as good (see Figure 6-14)

6.5 Summary

The results of the coal capture comparison data indicated that the best overall sorbents were the pressure slaked dolomitic materials which was the

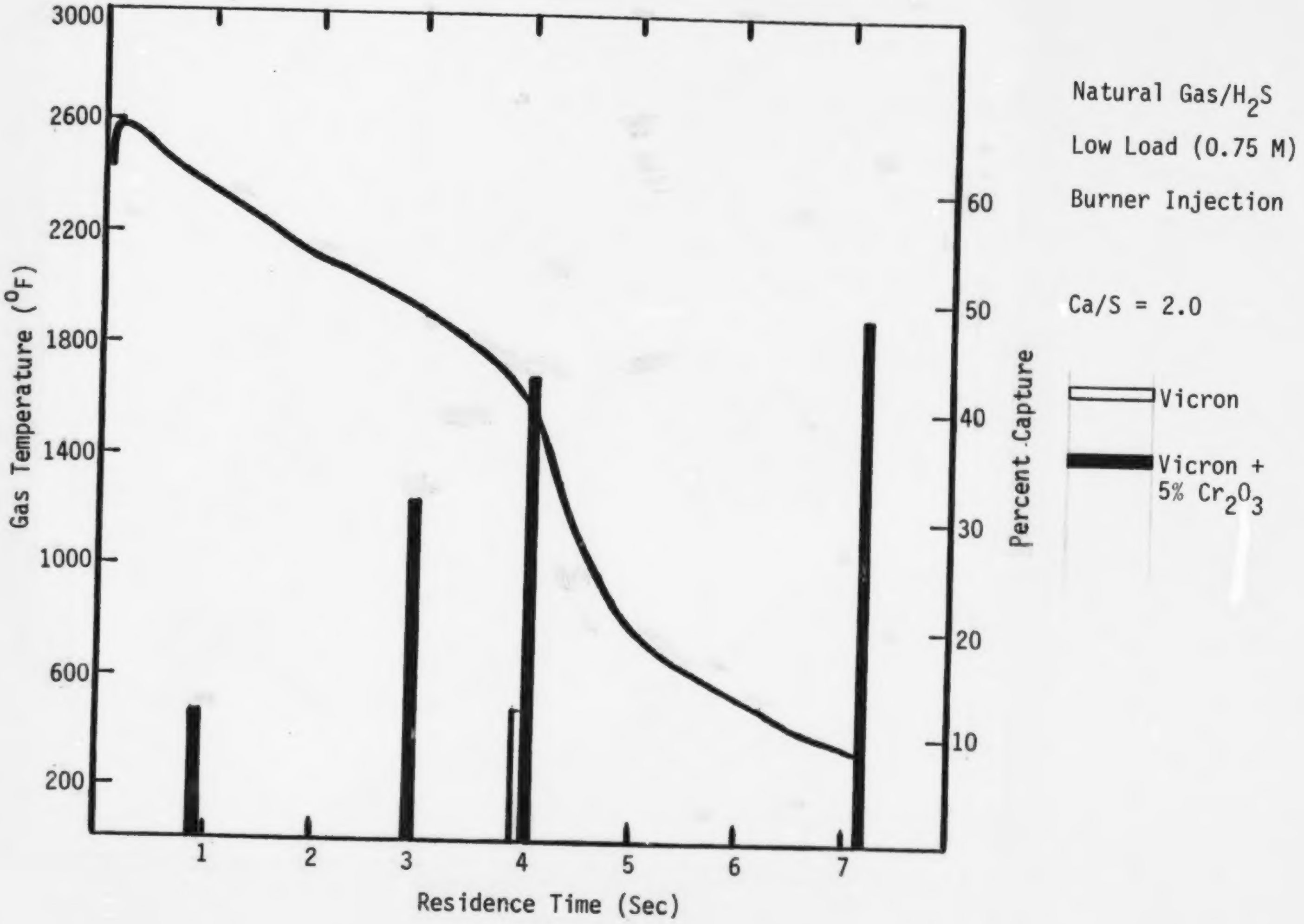

Figure 6-29. Zone capture for burner injection.

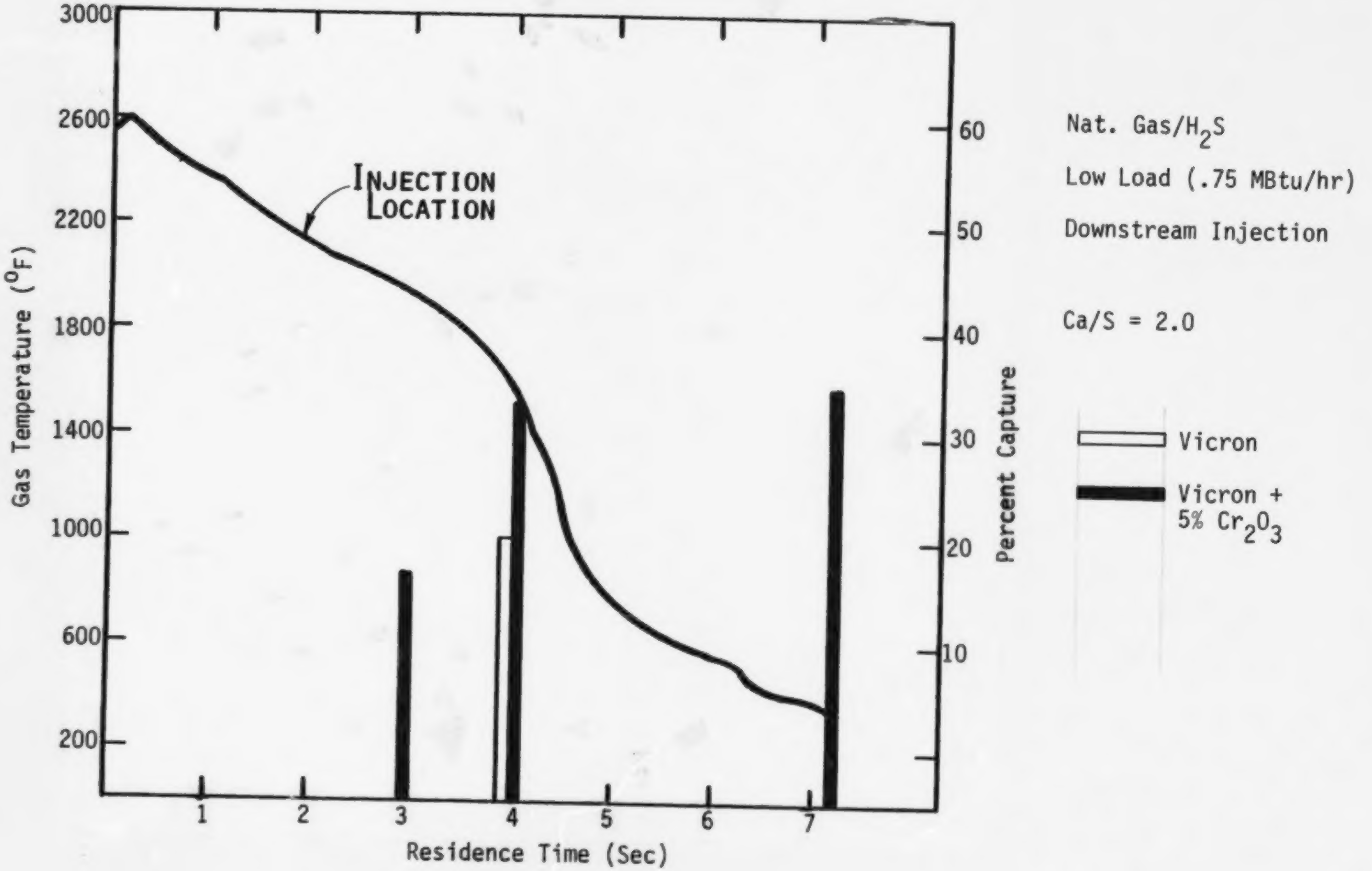

Figure 6-30. Zone capture for downstream injection.

TABLE 6-1. MEASURED SURFACE AREAS.

	VICRON	VICRON + 5% Cr_2O_3	VICRON + 3.5% Na_2CO_3
W/FUEL	4.2	3.2	3.4
DOWNSTREAM @ 2200°F	12.4	4.7	14.5

NATURAL GAS
A.B. PROFILE

same result produced in the gas capture comparison studies. Downstream injection gave better results than burner injection for a given sorbent and capture decreased with increasing quench rate in the sulfation zone. These trends were also very similar to those generated with gas capture. When a direct comparison between coal and gas was made, the capture results were very similar for any given sorbent type, injection location or thermal profile.

Mixing phenomenon was briefly touched upon with respect to sorbent and fly ash injection. For injection in the burner zone, it appeared that increasing sorbent/fly ash contacting decreased capture. For downstream injection, the fly ash had no effect on capture regardless of the amount of contacting. Certainly, more study in the area of mixing is required to fully understand the mechanisms involved.

The results of the additive screening studies suggested that Cr_2O_3 was the best capture promoter, followed by MoO_3 and Na_2CO_3 from the alkali metals group. Cr_2O_3 had the unusual property of promoting fuel injected sorbents to capture levels equal to or in excess of downstream injection. At high temperatures (~2800°F) the Na_2CO_3 was as effective as the Cr_2CO_3 which was promising since Na_2CO_3 is cheaper, more readily available, and less toxic than chromium. As concentration of both Na and Cr was increased in the sorbent mixtures, sulfur capture increased correspondingly.

Capture enhancement was shown to be independent of sorbent type. Even the highly reactive Genstar dolomitic was enhanced with Cr_2O_3 addition. With the additives, capture decreased with increasing quench rate just as the case without additives. With the chromium, capture was about the same with downstream injection as with burner injection. For sodium, higher captures could be achieved with burners injection depending on the peak temperature. It appeared that sodium was more sensitive to injection temperature than chromium since at high temperature, higher captures were achieved.

Using coal as the primary fuel reduced the effectiveness of both additives, and for Na_2CO_3, little or no enhancement was seen. The additive/

mineral matter interactions are not fully understood at the time and will require more work. Thermal parameters influenced additive enhancement in coal flames similar to gas flames. Downstream injection again proved more effective than burner injection and slightly better captures were generated with the low quench rate profile.

7.0 SULFUR CAPTURE MODEL

The computer model that was used for all of the predictions in this report is called the grain model and was developed by Geof Silcox of EER. The model was based on the work of Hartman and Coughlin (1976) and Hartman and Trinka (1980). They applied the grain model, the basic features of which are shown in Figure 7-1, to sulfation conditions typical of fluidized beds. The grain model as developed by Silcox is capable of predicting capture for pulverized sorbent addition in boiler. The model also accounts for the presence of MgO in dolomitic sorbents.

The SO_2 lime reaction was analyzed by considering that the gaseous reactant must undergo the following:

- Diffusion from the bulk gas to the particles surface.
- Pore diffusion to the particle's interior.
- Solid-state diffusion through the product layer.
- Reaction at the product-lime interface.

In considering the reaction,

$$CaO + 1/2O_2 + SO_2 = CaSO_4 \tag{7.1}$$

it was assumed that it was irreversible, that the sole product was $CaSO_4$, and that the overall rate of $CaSO_4$ formation could be modeled with a standard, two-parameter Arrhenius expression.

The following additional assumptions were made in the grain model analysis:

- The lime particles are fully calcined.
- The diffusion of reactant to the particle surface is not rate limiting.
- The reaction, $CaO + SO_2 + 1/2O_2 = CaSO_4$, is irreversible.
- The sole sulfation product is $CaSO_4$.

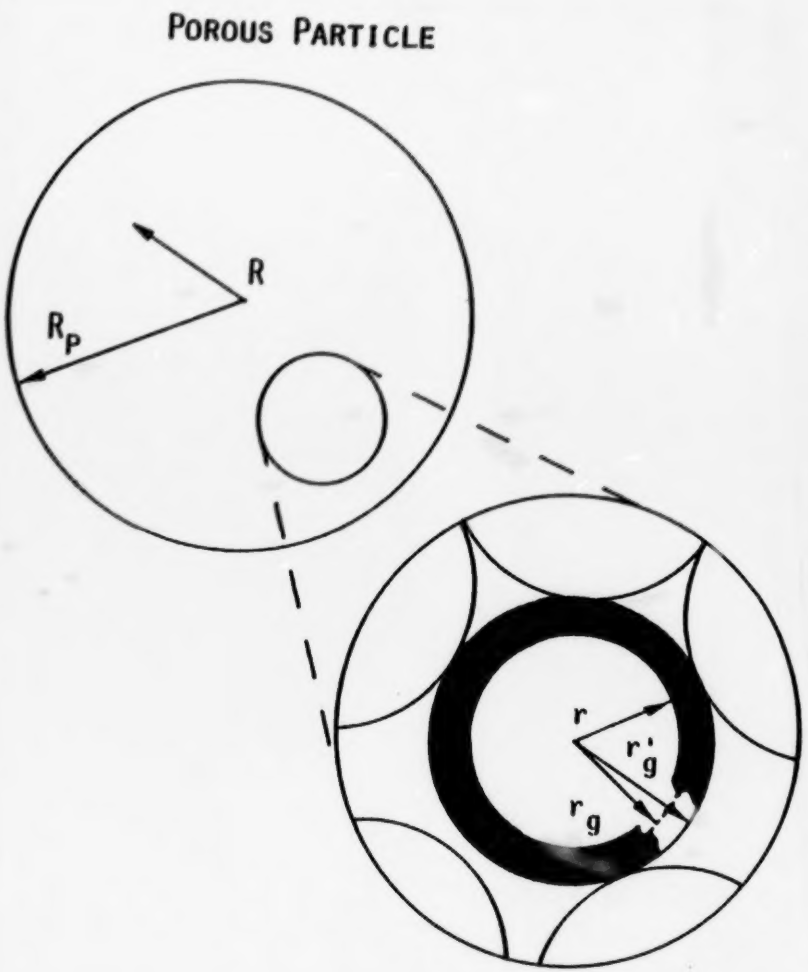
POROUS PARTICLE
R
R_P
r
r_g'
r_g

C_o = Bulk Gas Concentration

Enlarged View

r_g = Grain Radius

r = Radius of Unreacted Core

r_g' = Extended Grain Radius

Figure 7-1. The basic features of the grain model.

- The grains react by the shrinking core model.
- Excess oxygen is present and its concentration is constant.
- The lime particles are spherical and isothermal.
- The grains which constitute a particle are either pure CaO or else consist entirely of unreactive compounds. That is, there are no grains which are part impurity and part CaO.
- CaO and MgO grains have the same average size.
- Only CaO and MgO make significant contributions to a particle's surface area.

The governing equations for the grain model were obtained from material balances on the particle and the constituent grains. Starting with the particle, a balance on SO_2 in a spherical shell yielded (see Table 7-1 for nomenclature)

$$\frac{d^2C}{dR^2} + \frac{2}{R} + \frac{1}{D_{eff}} \frac{dD_{eff}}{dR} \frac{dC}{dR} - \frac{N}{D_{eff}} = 0 \tag{7.2}$$

In obtaining Eqn. 7.2 a steady-state approximation was made as justified by Luss (1968). The boundary conditions were written at the center of the particle and at the outer edge of the particle, R = Rp:

- At $R = 0$, $\frac{dC}{dR} = 0$ for all time. (7.3)

- At $R = R_p$, $C = C_0$ for all time.

The reaction rate term, N in Eqn. 7.2 has different forms depending on what value is chosen for the intrinsic order of the reaction with respect to SO_2. Models incorporating intrinsic orders of 0, 1/2, and 1 were developed by Silcox (1984). Only the zero order development will be discussed below.

In the zero order case, one must consider two subcases depending on whether or not diffusion of SO_2 through the product layer is rate limiting. The two forms of the rate term are given below:

TABLE 7-1 NOMENCLATURE FOR SULFATION CALCULATIONS

Symbol	Definition
A	Interfacial area available for reaction per unit volume of porous lime, $cm^2 cm^{-3}$
C	Concentration of SO_2 at some radius R, gmol cm^{-3}
Ce	Equilibrium concentration of SO_2, gmol cm^{-3}
C_o	Bulk gas concentration of reactant, gmol cm^{-3}
D_{eff}	The effective diffusivity of SO_2 in porous lime, $cm^2\ S^{-1}$
D_s	Product-layer-diffusion coefficient, $cm^2\ sec^{-1}$
K	Zero-order rate constant, gmol $cm^{-2}\ sec^{-1}$
M_{co}	Molecular weight of CaO
N	The rate at which reactant is consumed per unit volume of porous solid, gmol $cm^{-3}\ sec^{-1}$
r	Radius of the unreacted core of CaO, cm
r_g'	Extended grain radius, cm
r_g	Initial grain radius, cm
R	Radial distance inside the particle, cm
R_p	Particle radius, cm
t	Time, seconds
ρ_{co}	Density of CaO = 3.32 g cm^{-3}

- Kinetic control

$$N = K \cdot A$$

- Diffusion control

$$N = D_s \cdot \frac{dC_1}{dr_1} \cdot A \qquad (7.4)$$

where

$$D_s \cdot \frac{dc_1}{dr_1} = \frac{(C-Ce)Ds}{r(1-r/rg)} \qquad (7.5)$$

In addition to Eqn. 7.2 and 7.3, a material balance on CaO for a lime grain yielded the second and last governing equation:

- Kinetic control

$$\frac{dr}{dt} = \frac{M_{co}}{Co} K \qquad (7.6a)$$

- Diffusion control

$$\frac{dr}{dt} = - \frac{M_{co}}{Co} \cdot D_s \cdot \frac{dc_1}{dr_1} r$$

The initial condition for Eqn. 7.6 is that at $t = 0$, $r = r_g$ for all R.

Equation 7.2 was solved by writing it in finite difference form at evenly spaced positions within the particle. The resulting set of linear equations could not be solved directly due to the presence of two rate terms, i.e., Eqns. 7.4 and 7.5. An iterative solution was necessary.

The gases agreement between the grain model predictions and the data generated on the BSF indicates that the models predictive capabilities encompass temperature changes, concentration effects, sorbent composition, and Ca/S molar ratio.

8.0 CONCLUSIONS

The data presented in the previous chapters led to a number of conclusions. Some of these were expected since similar data had been seen on other facilities, while others were quite unexpected. The overall objective of this project was to study methods for optimizing sulfur capture and to investigate mineral matter interactions. In order to accomplish these goals, a new tower furnace was designed, constructed and tested.

8.1 Conclusions - Capture Optimization Studies

The capture optimization studies were broken into two main categories: sorbent screening studies and effects of thermal parameters. The results from the sorbent screening studies indicated that:

- The best overall captures were achieved with the pressure slaked dolomitic sorbents.
- In general, the dolomitic sorbents performed better than the calcitic sorbents and the hydroxides were superior to the carbonates.
- Pressure slaking improved capture with dolomitic materials and atmospheric slaking appeared to improve capture slightly with calcitic materials.
- Sulfur capture increased with increasing magnesium content. The magnesium in dolomitic sorbents did not react to form magnesium sulfate; increased sulfur capture was probably due to an enhancement of the product layer diffusion step.

Several of the sorbents tested in the sorbent screening studies were also tested under a variety of thermal conditions. The purpose of these tests was to determine what effect the various thermal parameters had on sulfur capture and if sorbents of different composition were influenced in the same manner. The major conclusions that were reached from these studies were:

- For downstream injection capture decreased with increasing quench rate in the sulfation zone independent of sorbent type.
- For burner injection, quench rate had little effect on capture. This was due to particle sintering which reduced particle surface area and consequently capture.
- Downstream injection consistently yielded higher captures than burner injection. Again, the effort was primarily due to increased particle surface areas generated under lower temperature conditions.
- The grain model can accurately predict captures for downstream injection with a variety of sorbent types and quench rates.

8.2 Conclusions - Mineral Matter Interaction Studies

Much of the information obtained in the optimization studies was applied to the studies on mineral matter interactions. Since all of the optimization testing was done with natural gas, one of the objectives of the mineral matter tests was to see if the same information applied to capture in coal flames. In addition, the additive studies were run under this series of tests.

Major conclusions that were reached from the coal studies were:

- Capture decreased with increasing quench rate in the sulfation zone.
- Downstream injection produced consistently higher captures than burner injection.
- The best captures with coal were achieved with the pressure slaked dolomitic sorbents. In general, the sorbent ranking was the same as in the gas studies.
- Under similar conditions, coal and gas gave similar captures.

All of the conclusions listed above indicated that coal and gas behaved similarly with respect to changes in sorbent composition or thermal history. A separate set of tests involving fly ash/sorbent injection indicated that:

- Premixing sorbent and fly ash reduced capture significantly for burner injection but had no effect for downstream injection.

The additive studies which were run with coal and gas comprised a large part of the overall test matrix. Initially, the additive screening was carried out with natural gas only to avoid any adverse mineral matter interactions that might occur. Selected additives were then run with coal and gas with different sorbents and thermal conditions. The results of the additive screening tests indicated that:

- Cr_2O_3 is the best promoter followed by Na_2CO_3 and MoO_3.
- At high temperatures (~2800°F) Na_2CO_3 could be as effective as Cr_2O_3.
- As additive concentration in the sorbent mixture increased, there was a corresponding increase in capture.

Having selected chromium and sodium as the two most promising additives, the coal and gas comparison studies showed:

- With Cr and Na, capture enhancement occurred independent of sorbent type.
- Capture decreased with increasing quench rate just as with coal and gas alone.
- Activation by additives favored high temperatures; Na was more sensitive to injection temperatures than Cr with gas.
- Similar captures were achieved with Cr for burner and downstream injection. Burner injection gave higher capture than downstream injection with Na.
- Surface area measurements indicated that Cr promoted particle sintering despite the high captures that were produced.
- With coal, the effectiveness of Cr was reduced as compared with gas, and Na became nearly ineffective.

- With coal and sorbent additives, downstream injection produced higher capture with decreasing quench rate.

Overall, the results of this study suggest that it is possible to achieve the EPA performance goal of 50 percent capture at a Ca/S ratio of 2.0 by at least two alternative methods: the use of high reactivity sorbents such as pressure slaked dolomites or the use of promoted limestones or hydroxides. Clearly, these two concepts can be combined to produce even higher capture levels though, economically, this may be unattractive. With coal, the use of additives did not look as promising as with gas. The additive/mineral matter interactions are not well understood at this point and should be investigated further.

9.0 REFERENCES

1. Gartrell, F. E., "Full Scale Desulfurization of Stack Gas by Dry Limestone Injection, TVA, EPA-650/2-73-019a, NTIS PB 228447, August 1973.

2. Coutant, R. W., R. E. Barrett, R. Simon, B. E. Campbell and E. H. Lougher, "Investigation of the Reactivity of Limestone and Dolomite for Capturing SO_2 from Flue Gas," Battelle Memorial Institute, APTD 0621: NTIS PB 196749, National Air Pollution Control Administration, Nov. 20, 1970

3. Attig, R. C. and P. Sedor, "Additive Injection for Sulfur Dioxide Control: A Pilot Plant Study," Babcock and Wilcox Co., APTD 1176: NTIS PB 226761, Department of Health, Education and Welfare, Mar. 27, 1970.

4. Wen, C. Y., and M. Ishida, Env. Sci. Tech., 7, 703 (1973).

5. Hyatt, E. P., E. B. Cutler, M. E. Wadsworth, J. Am. Ceramic Soc., 41, 70 (1958).

6. Borgwardt, R. H., Environ. Sci. Technol., 4, 59 (1970).

7. Borgwardt, R. H., A.I.Ch.E.J. (1984).

8. Ishihara, Yoshimi, "Kinetics of the Reaction of Calcined Limestone With Sulfur Dioxide in Combustion Gases," presented at the Dry Limestone Injection Process Symposium, Gilbertsville, Kentucky, June 22-26, 1970.

9. Ramachandrin, P. A. and J. M. Smith, A.I.Ch.E.J., 23, 353 (1977).

10. Bhatia, S. K. and D. D. Perlmutter, A.I.Ch.E.J., 27, 226 (1981).

11. Gartrell, F. E. "Full Scale Desulfurization of Stack Gas by Dry Limestone Injection." Volume I. EPA-650/2-73-019-A, NTIS PB 228447, August, 1973.

12. Hein, K. R. G., Glasser, W., "The Application of Dry Additives on Reducing SO_2 Emission for Brown Coal Fired Boilers." Paper presented at the Lignite Conference, San Antonio, Texas, June, 1981.

13. Zallen, D. M., Gershman, R., Heap, M. P., Nurick, W. H. "The Generalization of Low Emission Coal Burner Technology." Proceedings of the Third Stationary Source Combustion Symposium, Volume II, EPA-600/7-79-050b, NTIS PB 292540, 1979, p. 73.

14. Case, P. L., Ho, L., Clark, W. D., Kau, E., Pershing, D. W., Payne, R. and Heap, M. P. "Testing of Wall-Fired Furnaces to Reduce Emissions of NO_x and SO_x: Volume 1." EPA-600/7-85-026a, NTIS PB 85-224632, June, 1985.

9.0 REFERENCES (continued)

15. Case, P. L., L. Ho, M. P. Heap, R. Payne, D. W. Pershing, "Bench-Scale Studies of Limestone Injection for SO_2 Control," EPA-600/7-85-025, NTIS PB 85-224657, June, 1985.

16. Slaughter, D. M., et al., "Influence of Sorbent Composition on SO_2 Capture Efficiency in LIMB Applications," Presented at the 1984 Annual A.I.Ch.E. Meeting, San Francisco, CA, November 1984.

17. Borgwardt, R. H., Bruce, B. R., and J. Blake, "EPA Experimental Studies of the Mechanisms of Sulfur Capture by Limestone," In: Proceedings of First Joint Symposium on Dry SO_2 and Simultaneous SO_2/NO_x Control Technologies, Volume 1, EPA-600/9-85-020a, NTIS PB 85-232353, p. 6-1, July 1985.

18. Hartman, M. and Coughlin, R. W. "Reaction of Sulfur Dioxide with Limestone and the Grain Model, A.I.Ch.E. Journal, 22, 490 (1976).

19. Hartman, M. and Trinka, O. "Influence of Temperature on the Reactivity of Limestone Particles with Sulfur Dioxide," Chem. Engng. Sci., 35, 1189 (1980).

20. Luss, D. "On the Pseudo Steady State Approximation for Gas Solid Reactions," The Canadian Journal of Chem. Engng., 41, 154 (1968).

21. Silcox, G. D., Ph.D. Dissertation, Department of Chemical Engineering, University of Utah (1985).

APPENDIX A

Quality Assurance

A.0 QUALITY ASSURANCE

The collection and analysis of quality data has been the primary objective of this program. In order to ensure that the reported data is accurate, many quality assurance measures have been taken in all phases of the program. Most of the procedures and measurements used for data acquisition have been standardized by EPA or ASTM and those which have not are described in detail in this appendix.

A.1 Measurements Methods

A.1.1 Gas Species

Exhaust gas-phase species composition was measured using the BSF laboratory sampling systems. These systems were constructed in strict conformance with EPA performance specifications and their use helped ensure data quality. The species that were measured included: NO, NO_2, SO_2, CO, O_2, and CO_2, all of which were measured by continuous gas analyzers.

Table A-1 lists the specific instruments and full-scale ranges. The instrument ranges have been selected to exceed the maximum expected concentrations by a small margin. Table A-2 shows the expected and actual values for precision, accuracy, and completeness for the gas analyzers.

TA-1

TA-2

Gas phase measurements were made routinely at Port 10B and the exhaust port in the BSF (see Figure 2-1). Phase discrimination probes (see Figure 2-4) were used at both locations. The probes supplied two gas streams simultaneously. The main, particle-laden stream, which was used for continuous monitoring of O_2, CO, CO_2, NO_x, and the side, nearly particle-free stream, which was used for SO_2 measurement. The main stream-to-side stream flowrate ratio was approximately 5:1. A detailed schematic of the sample train is shown in Figures 2-5 and 2-6. The materials of the sample train were limited to glass, stainless steel, teflon, and a small amount of Kel-F (value seals). These materials have been demonstrated to be essentially non-reactive to the species being measured over the temperature range of the

TABLE A-1. BSF INSTRUMENTATION

Gas Measured	Type of Instrument	Manufacturer	Model No.	Range	Reference
NO, NO_x	Chemiluminescent	Thermo Electron Corp. (TECO)	10 AR	1000 RPM	Teco model 10 operating manual.
CO	Nondispersive Infrared (NDIR)	Anarad, Inc.	AR500R	500 ppm	Anarad AR 500 operating manual.
CO_2	Nondispersive Infrared (NDIR)	Anarad, Inc.	AR500R	25 percent	Anarad AR 500 operating manual.
O_2	Paramagnetic	Beckman	755	10 percent	Beckman 755 operating manual.
SO_2	UV Absorption	DuPont	400	5000 ppm	DuPont 400 operating manual.

TABLE A-2. EXPECTED AND ACTUAL VALUES FOR PRECISION, ACCURACY, AND COMPLETENESS FOR BSF INSTRUMENTATION.

Gas Measured	Precision (%)		Accuracy (%)		Completeness (%)	
	Actual	Goal	Actual	Goal	Actual	Goal
NO, NO_x (Chemilumenescent)	1.4	2	14.2	20	97	90
CO (NDIR)	0.4	2	–	20	97	90
CO_2 (NDIR)	0.3	2	6.7	20	97	90
O_2 (Paramagnetic)	0.5	2	11.2	20	97	90
SO_2 (UV Absorption)	0.2	2	8.1	20	97	90

system (32 to 200°F). All inflame measurements were taken at the centerline of the reactor unless a radial profile was taken at different intervals.

A.1.2 Solids Species

Solid samples were taken from the furnace in three ways: isokinetically with a surface area probe, isokinetically with an IFRF probe for solids loading, and non-isokinetically with a water-cooled "grab sample" probe. Detailed schematics of these three systems are shown in Chapter 2.0. All solids measurements were taken at the centerline of the flow stream.

A.1.3 Temperature Measurements

Gas-temperature measurements were made with a water-cooled stainless-steel suction pyrometer equipped with a ceramic tip. A suction pyrometer was used since bare thermocouples do not accurately measure gas temperatures. The gas measurements were always taken at the reactor centerline unless a radial profile was taken. A detailed schematic of the pyrometer system is illustrated in Figure 2-10. Furnace wall temperatures were measured using type S thermocouples embedded in a refractory plug. Wall temperatures were used only as a device to monitor the thermal condition of the furnace, not as an absolute temperature level. Temperatures in the convective section were measured using chromel/alumel (type K) thermocouples.

A.1.4 Other Measurements

Table A-3 shows a list of other measurements that were made routinely and the analytic procedure used. Table A-4 indicates what the precision, accuracy and completeness values were for these measurements. TA-3 TA-4

A.2 Calibration Procedures

Calibration procedures and frequency for each measurement system are listed in Table A-5. As shown in the table, standard calibration procedures were used for each system. Each system was calibrated at the frequency shown TA-5

TABLE A-3. OTHER MEASUREMENTS AND THE PROCEDURES USED.

Measurement	Method	Reference
Fuel Composition		
Carbon Hydrogen Nitrogen	Thermal conductivity of combusted sample	PE 240B operating manual
Ash	Sample conbusted	ASTM D3174
Moisture	Loss in weight	ASTM D3173
Sulfur	Infrared detection of SO_2 from combusted sample	LECO SC32 operating manual
Heating Valve	Calorimeter	ASTM D2015
Fuel Size	Sieves	ASTM D1917
Combustion Air Flowrate	Laminar Flow Elements	Meriam Laminar Flow Element Calibration Curves
Sorbent Feedrate	Manual calibration	K-tron Feeder Operating Manual
Coal Feedrate	Loss in ult calibration	K-tron Feeder Operating Manual
Gas Temperatures	Suction pyrometer	
Sorbent Surface Area	BET analysis	Quantasorb Surface Area Analyzer Operating Manual

TABLE A-4. ACCURACY PRECISION AND COMPLETENESS VALUES FOR BSF MEASUREMENTS

Gas Measured	Precision (%)		Accuracy (%)		Completeness (%)	
	Actual	Goal	Actual	Goal	Actual	Goal
Fuel Composition						
Carbon	.24	2	0.8	2	95	90
Hydrogen	1.38	5	0.6	5	95	90
Nitrogen	2.13	10	1.9	10	95	90
Ash	0.33	10	1.42	10	95	90
Moisture	2.55	10	8.71	10	95	90
Sulfur	2.36	10	0.55	10	95	90
Heating Valve	--	2	0.39	2	--	90
Fuel Size	2.0	2	2.0	3	90	90
Combustion Air Flowrate	0.11	5	2.7	5	100	100
Sorbent Feedrate	--	2	--	2	100	90
Coal Feedrate	2.3	5	4.1	5	100	100
Gas Temperatures	1.0	5	1.7	5	98	90
Sorbent Surface Area	--	5	--	5	95	90

TABLE A-5. CALIBRATION PROCEDURES

Measurement Parameter	Calibration Procedure	Calibration Frequency	Calibration Standard	Reference
Fuel Composition: Carbon Hydrogen Nitrogen Ash Moisture	Standard Samples	Daily	Known quantity of 100% acetanilide	Perkin Elmer 240B Operating Manual
Sulfur	Standard Sample	Daily	Certified sulfur	Leco SC 32 ASTM E 11
Fuel Flowrate/ Distribution	Weigh feed over time with independent balance	Monthly	Standard Weights	
Combustion Air Flowrate/Distribution	Compare with EPA Method 2 or dry gas meter	Biannually	EPA Method 2 or calibrated dry gas meter	Federal Register, Vol. 42, No. 160, August 18, 1977, pp 41754-41788
Sorbent Flowrate	Weigh feed over measured time with independent balance	Daily	Standard weights	
Exhaust Gas Composition $NO, NO_2, O_2, CO, CO_2, SO_2$	Compare to standard compressed gas	Daily	EPA Protocol 1 Gases or custom gas blends	EPA EMSL Protocol No. 1, June 1, 1978

in the table to ensure the accuracy of the measurements are traceable to the calibration standards.

Each of the continuous monitoring instruments was calibrated with three gases: a zero gas and two span gases at approximately 50 and 90 percent of span except in the case of SO_2 where the concentrations were chosen to match expected SO_2 levels during experimental runs. Table A-6 lists the span gases used to calibrate instruments. The daily procedure for instrument calibration is given below.

1) Turn on control room exhaust fan.

2) Switch 4-way valves on instrument sample panel to down (N_2) position.

   Adjust needle valves to get 2 s.c.f.h. flow to instruments. Turn DuPont 4-way valve counterclockwise to N_2, pressure gauge should read .8 psig.

3) Switch Beckman 755 to 10 percent range/scale.

4) Install pens in chart recorder according to proper color. With measurement switches off, adjust pens to zero position. Make sure pens are properly seated and turn on 6 measurement switches. Note in following procedures that the instrument zero and spans should match zero and span on the chart recorder.

5) Adjust instrument's zero knobs to make instruments read zero. Note: There is no front panel readout for the DuPont. Adjust course zero knob on DuPont so that DuPont record pen corresponds with zero on the chart paper.

6) O_2: Turn Beckman 755 4-way valve to the right (high span position). Adjust needle valve to 2 s.c.f.h. Adjust span knob to make front panel meter read 8.0% (or concentration of span gas). Switch back

TABLE A-6. CALIBRATION GASES

Gas	Concentration	Percent of Full-scale	Balance Gas	Grade
NO	500 ppm	50	Nitrogen	Certified Standard
NO	900 ppm	90	Nitrogen	Certified Standard
SO_2	2100 ppm	52	Air	Certified Standard
SO_2	520 ppm	13	Air	Certified Standard
CO	250 ppm	50	Nitrogen	Certified Standard
CO	450 ppm	90	Nitrogen	Certified Standard
CO_2	12.5%	50	Nitrogen	Certified Standard
CO_2	22.5%	90	Nitrogen	Certified Standard
O_2	5%	50	Nitrogen	Certified Standard
O_2	9%	90	Nitrogen	Certified Standard

to N_2 gas and reset zero. Switch range knob to 25% range/scale and turn 4-way valve up (sample position). Verify air flow.

7) Turn Anarad AR-500R 4-way valve to the span position, adjust needle valve to get 2 s.c.f.h. Adjust span knob to make front panel meter read 403 ppm (or concentration of span gas) re-check zero. Turn 4-way valve to up sample position.

8) CO/CO_2: Turn Anarad AR-600R r-way valve to the CO_2 span position (right). Adjust needle valve to get 2 s.c.f.h. Adjust CO_2 span knob to make front panel meter read 18.2% CO_2 (or concentration of span gas). Turn 4-way valve to the left (high CO span). Adjust needle valve to get 2 s.c.f.h. flow. Adjust CO span knob to make CO front panel meter read 8.9% or span concentration re-check zero. Turn 4-way valve to up sample position.

9) NO_x: Turn thermo-electron (TECO) 4-way valve to span position (right). Adjust needle valve to get 2.0 s.c.f.h. flow. Adjust "calibrate" knob to make front panel meter read 840 ppm (or concentration of span gas) re-check zero. Turn 4-way valve to up (sample) position.

10) Turn DuPont 4-way valve clockwise to the right high span (SO_2) position. Adjust flow to .9 psig. on "Range B", the DuPont analyzes SO_2 concentrations from 0-4000 ppm so set the span knob so that the DuPont recorder pen reads span gas concentration. Check low-span. Turn 4-way valve to sample position.

11) Sample gas can now be analyzed. When taking a sample the main bypass rotometer should read between 50-100 c.f.h. with the back pressure regulator set at 4 psi. DuPont bypass rotometer should read 5-10 s.c.f.h. and pressure should be .8 psig. The DuPont pressure may be changed by adjusting the sample or bypass flow rates.

A.3 Standard Systems Checks and Preventative Maintenance

At the beginning of each day of testing several routine system checks and maintenance tasks are performed to ensure that the systems are operating properly.

Initially, the sample system is cleaned, checked for leaks, and inspected for routine maintenance. A detailed description of these procedures is given below:

1) Filters: The two long Balston filter cartridges are the farthest most upstream filters and should be changed as needed, every eight hours of running time, or once a day. The two short filters, close all the valves on the main sample side of the 4-port manifold panel. This ensures that there is no air flow through the filter housing. Take filter housing apart and replace paper filter. When reassembling filter, make sure housing seats properly onto gaskets. Add a little vacuum grease now and then to keep gaskets pliable.

2) Cyclone Condensers: Each day drain the water collected in the two condensers. The Teflon tubing is long enough to allow the drain nuts to be removed without undoing the tubing. Remove one of the drain plugs and open a valve on the 4-port manifold panel to blow-out any left-over condensate. Replace plug and repeat with other condenser. Then fill bucket with ice-water to cover condensers. Keep a solution of ice-water in the bucket at all times when sampling. Failure to keep the condensers cold will result in water condensing in the sample and instrument lines.

3) Drierite Towers: Verify that the moisture capturing capability of the Drierite has not been exhausted (indicated by color change from blue to pink) if it has, change Drierite material.

4) Leak Test: Close main and heated sample valves on 4-port manifold panel. Close 4-way valves on instrument panel by turning them 45°

from vertical. Open Beckman 4-way valve to sample manifold position and open needle valve all the way. Screw back pressure regulator all the way. Open DuPont 4-way valve to sample position and open needle valve all the way. Close DuPont bypass valve (inside middle cabinet). Turn on sample pumps. Verify that there is no flow on the Beckman rotometer and that the back pressure regulator reads zero. There should also be no flow on the SO_2 sample rotometer. If there is flow through the Beckman rotometer, there is a leak in the main sample line. If there is flow through the DuPont rotometer there is a leak in the heated sample line. To trace leaks, turn off sample pumps, and open a main sample valve on the 4-port manifold panel to pressurize the main sample system. To pressurize the heated side, open a heated sample valve and its corresponding blowback valve. The main and heated systems may now be leak tested with bubble solution. When both sample systems are leak-tight, reset the back pressure to 4 psi and reset the DuPont bypass and instrument flow valves.

After the sampled system has been prepared and the instruments calibrated, an O_2 mass balance, or leak check, of the entire furnace system check is performed. With natural gas firing, the on-line computer calculates the expected exhaust oxygen concentration based on natural gas and air calibration curves. The computer calculated O_2 is also checked each day with a hand-held calculator. If all systems are operating properly, $)_2$ concentrations usually match within 0.2 percent (this depends somewhat on variation in the fuel composition). Oxygen concentrations higher than expected may indicate sample system leaks upstream of the sample manifold or leaks in the gas delivery system. O_2 concentrations lower than expected indicate leaks in the air delivery system.

A.4 Special Systems Checks

Throughout the course of this program, several independent or special checks were performed to ensure data quality.

In order to determine what amount of air pressure should be used on the suction pyrometer, a calibration curve was generated for pyrometer gauge pressure vs. gas temperature as shown in Figure A-1. The figure indicates that as gauge pressure was increased, the gas temperature also increased until it leveled out at about 20 psig. Consequently, all gas temperatures measurements were taken with the gauge pressure at 30 psig to ensure that the measurement was well into the flat part of the curve.

A radial temperature profile was made across the radiant furnace to determine if centerline temperatures were representative of the bulk furnace temperature. Figure A-2 shows the radial profiles for 2 ports and indicates that near the furnace walls, the temperatures dropped off but the peak was not quite at the centerline. Overall, the centerline measurement was fairly representative of the free stream temperature.

A comparison of the sorbent calibrations that were done with each sorbent was done to determine the feeder performance over time and a variable range of setpoints. Table A-7 shows a comparison for Vicron calibrations over a 3 month period. The data was extremely consistent over the whole range tested and over the course of the 3 months.

Several checks were made on the phase discrimination probes used in this program. The first involved testing a particular condition with two different probes; the regular BSF probes, and with another probe borrowed from the CTT at EER. The borrowed probe had been tested previously and had been shown to give accurate results. For this test, a standard capture experiment was set up and SO_2 levels were measured concurrently with a BSF probe and then the reference probe. The results were very consistent and are shown in Table A-8.

A second test that was carried out to check the operation of the phase discrimination probes is described below. Initially, sorbent was turned on for about 2 hours with the probes in place and no SO_2 flowing. The sample pump was turned on in order to draw samples through the probes. At the end

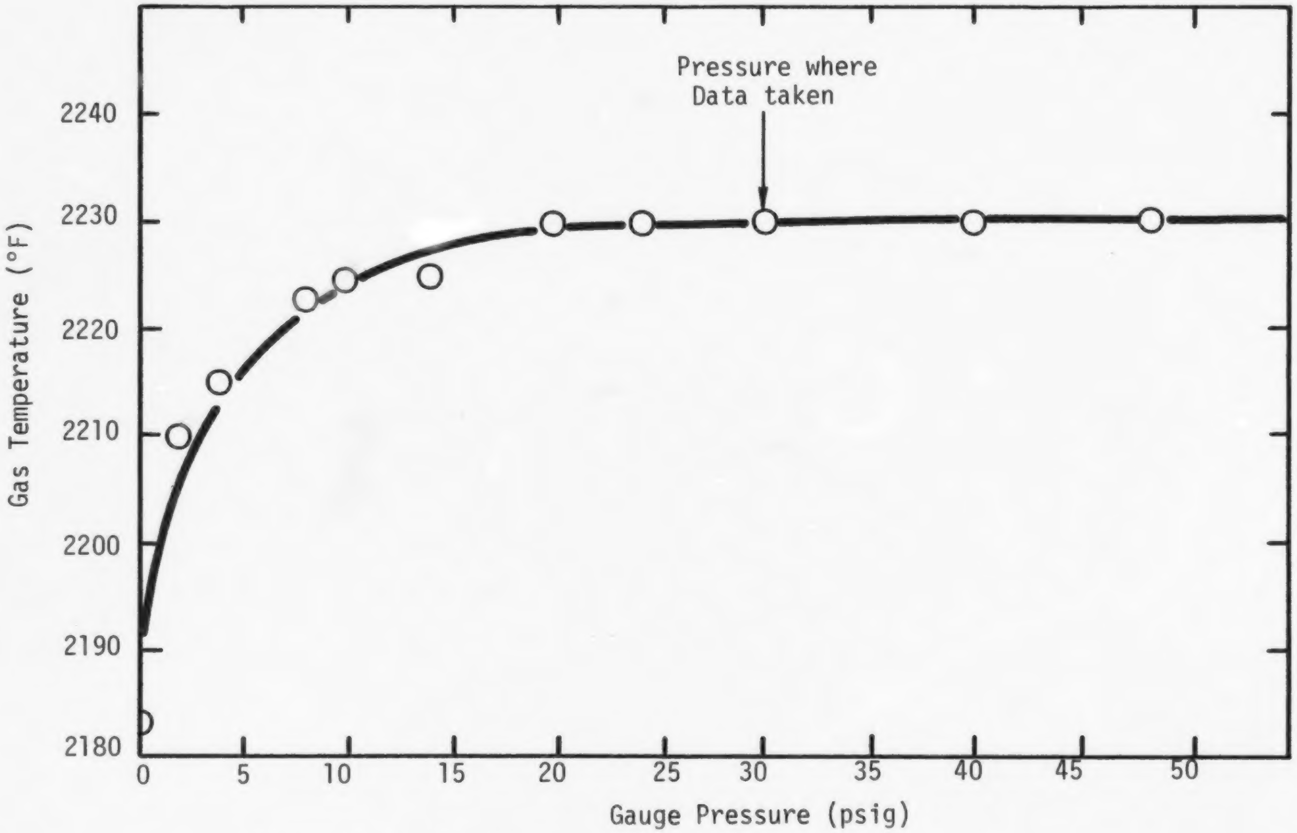

Figure A-1. Suction pyrometer quality control check.

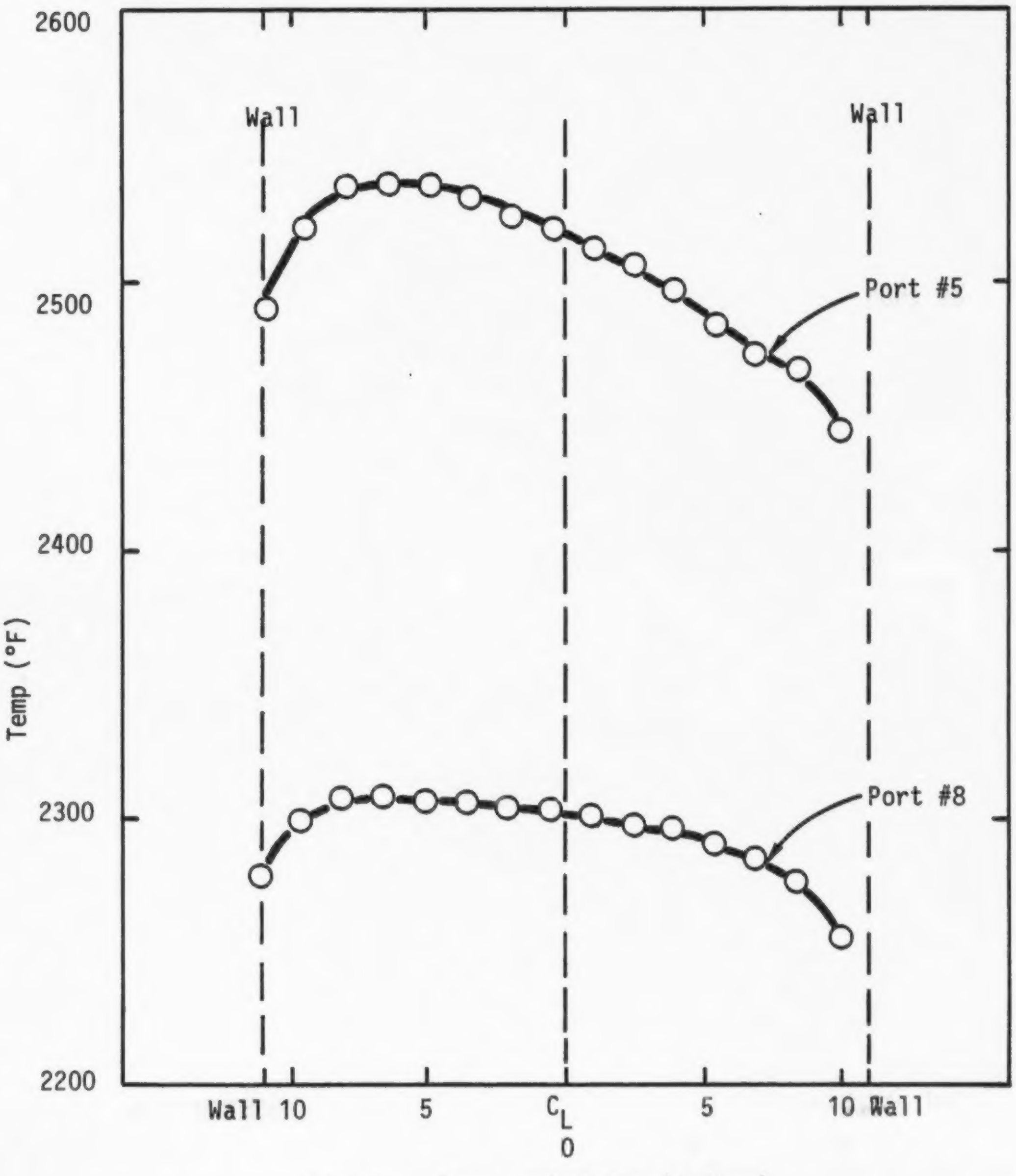

Figure A-2. Radial temperature profile.

TABLE A-7. VICRON SORBENT CALIBRATION

Date	Setpoint	Rate (g/min)	Rate per Setpoint (g/min)
5/8/84	11.5	48.4	4.21
	17.4	72.9	4.19
4/18/84	9.0	38.2	4.24
4/19/84	9.0	37.9	4.21
5/10/84	11.0	46.8	4.25
	16.0	67.5	4.22
7/6/84	12.0	50.9	4.24
	20.0	84.4	4.22

TABLE A-8. BSF PROBE DATA VS REFERENCE PROBE

Probe #	BSF probe (ppm SO_2)	Reference Probe (ppm SO_2)	% Error
8	987	975	1.2
10A	1001	983	1.8
Exhaust	809	817	- 1.0

of this period, it was assumed that the probes were laden with as much unreacted sorbent as could possibly occur under normal testing. The dirty probes were pulled out of the ports, SO_2 was turned on and the sorbent turned off. SO_2 measurements were taken with "clean" probes and then immediately replaced with the dirty probes. The SO_2 levels did not change with the dirty probes, thus indicating that SO_2 capture was not occurring within the probes or sample lines even after sorbent had been run for a significant period of time.

A radial SO_2 capture profile was done for a low capture condition as shown in Figure A-3. The figure shows that from the centerline to the furnace wall, capture did not change for the two ports tested. This data suggested that pulling samples from the centerline was representative since the SO_2 appeared to be well mixed across the furnace.

A.5 Data Reduction and Reporting

After raw data has been collected from various experiments, a fair amount of data reduction is required before results can be reported in their final form. Equations used to calculate results for each of the measurements are discussed below. Many of the results are obtained directly from the measurements and thus will not require calculations.

1. Fuel and Particulate Analysis for Carbon, Hydrogen, Nitrogen

The data consist of millivolt responses form the analyzer. These millivolt responses are converted to micrograms using a graphical calibration curve generated with three standards. Weight percent is then calculated for each element, knowing the total sample weight as follows:

$$\text{element weight \%} = \frac{\text{element weight}}{\text{sample weight}} \times 100$$

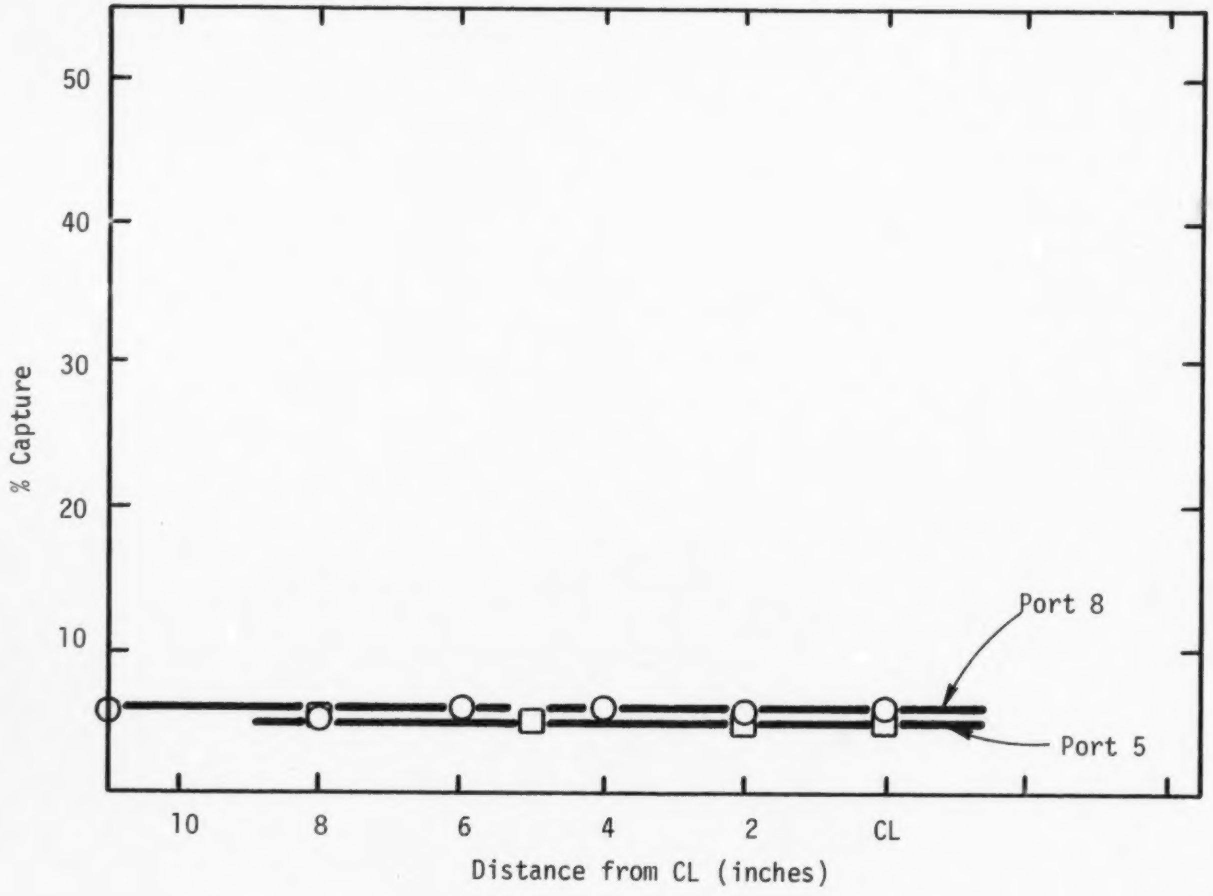

Figure A-3. SO_2 radial capture profile.

2. Fuel Size Distribution

Analytical data consist of weights of each size fraction which are converted to percent weight less than each size fraction from the equation:

$$\text{fraction weight \%} = \frac{\text{fraction weight}}{\text{total weight}} \times 100$$

Results are presented graphically plotting cumulative weight percent against particle size.

3. Fuel Flow Rate/Distribution

Fuel flow rate is obtained directly from the weigh feeder and is averaged over each test period.

4. Combustion Air Flow Rate/Distribution

Combustion air flow rate is read directly from rotameters or is calculated from pressure drop measured across laminar flow elements based on the equation:

$$Q = K(P)^{1/2}$$

where Q is the flow rate, K is a calibration factor determined for each flow element, P is the pressure drop measured across the element and T is the absolute temperature.

5. Combustion Air, Furnace Gas and Exhaust Gas Temperatures

Temperatures are measured by thermocouples and provide results in units of degrees centigrade which can then be converted to other temperature scales, as required.

6. Exhaust Gas Composition: NO, NO_2, O_2, CO, CO_2, DO_2

The above gas compositions are measured as chart divisions on a strip chart recorder. The measured divisions are converted to concentration (ppm or %) based on calculations with certified gases. Results are corrected to 0 percent oxygen concentration based on the measured oxygen concentrations.

7. Sorbent Flow Rate

Sorbent feed rate is determined by the set point of a volumetric feeder and the feeder calibration curve (mass vs. feeder setpoint). The feeder is calibrated daily with each sorbent.

8. Sorbent Size Distribution

Sorbent size distribution is plotted directly as size against cumulative weight percent by a Micromeritics Sedigraph Analyzer. Figure A-4 shows an example of a sorbent size distribution.

9. Sorbent Surface Area

Sorbent surface area is measured by a BET Quantasorb Analyzer. This analyzer measures the quantity of nitrogen condensed on the sample surface by thermal conductivity based on calibration standards. This quantity of nitrogen is converted to surface area based on a monolayer of nitrogen condensed on the sample and the known volume of nitrogen molecules following the instrument manufacturer's instructions.

A.6 Basic SO_2 Capture Experiments

The procedure for a typical SO_2 capture experiment as been standardized and is described in detail below.

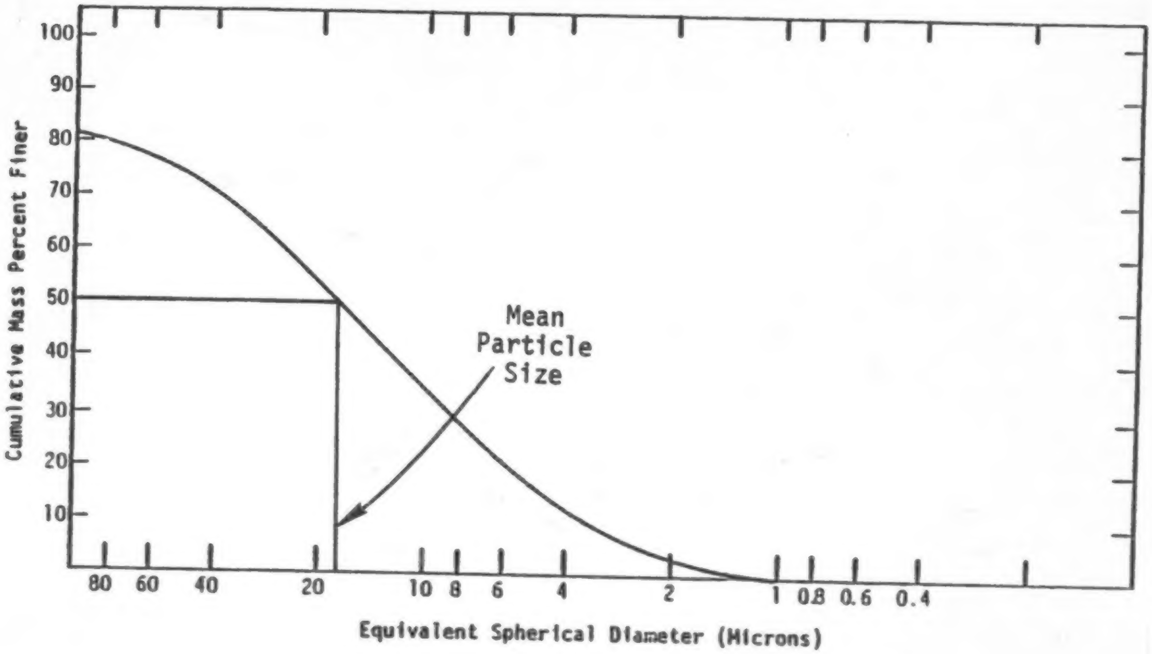

Figure A-4. Example of sorbent particle size distribution.

For a natural gas experiment, the baseline conditions are checked initially which includes correct air and fuel flow rates, exhaust O_2, CO, CO_2, NO_x, furnace temperatures, as well as burner and overall stoichiometries. After these considerations produce stable traces, the H_2S flow rate is adjusted to give the desired SO_2 concentration in the flue gas. SO_2 concentrations are checked for at least two ports two different times to ensure that SO_2 concentration does not change in the flue gas throughout the furnace.

After the SO_2 level is verified, the sorbent injection system is started and SO_2 is measured until steady. At this point, measurements are taken at all ports desired in succession. The sorbent is then turned off and the SO_2 level is allowed to return to the baseline condition. The maximum time that the sorbent is on during any single experiment is 20 minutes. For coal, the procedure is identical except that the coal produces its own SO_2 and the H_2S system is not used.